Numerical ocean model study of the Agulhas Bank and the Cool Ridge

Nicolette Chang

Thesis Presented for the Degree of

DOCTOR OF PHILOSOPHY

Department of Oceanography

UNIVERSITY OF CAPE TOWN

October 2008

Abstract

The oceanic structure and circulation of the Agulhas Bank, the very wide continental shelf area off South Africa, has been explored in this thesis. The Agulhas Bank is a complex ocean region influenced by shelf processes as well as a nearby western boundary current, the Agulhas Current on its eastern margin and the Benguela Upwelling system on its western margin. In addition, a cold water feature, known as the cool ridge, has been observed on the Eastern Agulhas Bank. A consistent dynamical description is not available but it is commonly observed as a south-westerly flow of cold water in the upper water column, roughly following the 100m isobath and extending seawards off the coast. The formation of the cool ridge has also been investigated in this thesis by means of a numerical ocean model.

Previous studies on the Agulhas Bank have been limited temporally and / or spatially. Thus, the Agulhas Bank as a whole has been inadequately sampled to provide a comprehensive representation. In order to remedy these deficiencies, the Regional Ocean Modeling System (ROMS) was used to study the Agulhas Bank dynamics. A large-scale model of the surrounding oceans, the SAfE (South African Experiment) configuration of the ROMS model, was used to force a one-way embedded finer-resolution model over the Agulhas Bank. This produced, 8 years of model data at an approximate horizontal resolution of 8km and 32 vertical terrain-following levels. Two main experiments were performed to understand the nature of the Agulhas Bank. Firstly, the "Reference Experiment" derived a seasonal ocean climatology of the Agulhas Bank. Secondly, the "No Agulhas Experiment" was carried out in an approach in which the Agulhas Current was removed from the shelf edge. A comparison of these two experiments yielded the influence of the Agulhas Current on the Agulhas Bank.

The ROMS model was able to reproduce the main observed seasonal structure and circulation of the Agulhas Bank as well as the cool ridge. The Agulhas Bank showed marked seasonality, with its two-layer structure being significantly influenced by the Agulhas Current. The direct influence of the Agulhas Current on the Bank occurs on the Outer Agulhas Bank by the Agulhas Current itself or an Agulhas Current filament. Ekman veering by the interaction of the Agulhas Current with the bottom topography on the slope of the eastern Agulhas Bank advect cool water vertically onto the Bank. This strengthens the thermocline from below, in contrast to surface warming by solar insolation in summer and the Agulhas

Current in winter. Cold waters, upwelled over the shelf edge, indirectly affect the greater Agulhas Bank by their advection by the predominantly westward mean currents. The most significant influence of the cold shelf-upwelled waters are in bringing cold waters to shallower depths over most of the Agulhas Bank. This may influence the waters that upwell at the coast, which on the eastern Agulhas Bank (without the Agulhas Current) are trapped under a thick warm surface layer.

The cool ridge in the model was found to have seasonal variability. It was subsurface in the mean and largest in vertical and horizontal extent in summer. In the model, the cool ridge is primarily forced by the Agulhas Current. Ekman veering of the bottom water on the outer eastern Agulhas Bank and Agulhas Bight, causes the vertical advection of cold waters up the slope of the shelf edge. On the Outer Agulhas Bank, these cold waters serve to force up the thermocline. In a vertical cross-section, this appears as doming over the shelf edge. These cold waters are responsible for the observed ridging in the thermocline and isotherms as observed in previous measurements. Obtaining a mean for the cool ridge is complicated as it is a dynamic structure, its location and manifestation changing depending on the position and speed of the Agulhas Current. Furthermore, influence by winds and other shelf processes may alter its structure. However, a tentative description is: the cool ridge is the doming of the thermocline over cool waters that have been vertically advected by Ekman veering along the shelf edge.

Declaration

I hereby declare that this thesis is my own original work. The ideas and experiments are largely my own but I acknowledge guidance from my supervisors, Prof. Frank Shillington and Dr. Pierrick Penven.

The model configuration, SAfE and the Matlab programme for calculating the heat equation advection terms were provided by Dr. Pierrick Penven.

No part of this research has been submitted in the past, or is being submitted, for a degree at any other University.

Acknowledgements

I would like to express my gratitude to my supervisors: Dr. Pierrick Penven and Prof. Frank Shillington. Their guidance and patience have been instrumental in helping me throughout this degree. Dr. Penven has provided expert advice and has been an inspiration to me. I am thankful for the encouragement and advice Prof. Shillington has given me: firstly, in helping me choose oceanography and supporting me in my career.

I am grateful to various people from the Department of Oceanography, UCT who have supported me through the duration of this thesis. The following people stand out. Rachmat Harris provided administrative support and friendship as well as occasionally feeding me. For valuable discussions: Jennifer Veitch and Frank Colberg.

I am appreciative of the financial assistance received from the UCT/CSIR Scholarship and the Department of Oceanography. I would like to thank the facilitators of this. I am also thankful to Dr. Pedro Monteiro and the CSIR for support while finishing this thesis.

I would also like to acknowledge the following, without which I would never have survived this process: Winnie the Pooh, Jellytots, google, chocolate, Stargate, microwave popcorn, cupcakes and picnics on the beach.

I would like to express my gratitude to my family and friends who have encouraged me, tolerated my moods and hiding, all while believing I could finish this thesis. Special thanks to my sister, Genevieve, for all your help and giving me a push when I needed it. Lastly, I wish to thank my parents who helped make all of this possible.

Contents

List of Figures

List of Abbreviations

Abbreviation	Details
AB	Agulhas Bank
AC	Agulhas Current
ARR	Agulhas Retroflection Region
bbl	bottom boundary layer
CAB	Central Agulhas Bank
CR	Cool Ridge
EAB	East Agulhas Bank
EKE	Eddy Kinetic Energy
SAfE	South African Experiment
SSH	Sea Surface Height
SST	Sea Surface Temperature
WAB	West Agulhas Bank

Chapter 1

Introduction

Southern Africa is bordered by the warm, fast-flowing western boundary current of the Indian Ocean, the Agulhas Current (AC), to the east and the cold eastern boundary system of the Atlantic Ocean, the Benguela Upwelling System, to the west. To the south of South Africa, the continental shelf, the Agulhas Bank (AB), extends offshore in a triangular shape. The AB is approximately 800km in length along the coast and at its apex the shelf is 250km wide (Hutchings, 1994). Due to its position and shape, it serves as a mixing region between these two contrasting regimes resulting in a complex oceanic region. This region is economically important to South Africa, for example, for shipping and fisheries where it is the spawning ground for the Cape anchovy.

The AC drives warm water onto the AB at the surface through fluctuations of the AC and its eddies and plumes (Lutjeharms et al., 1989; Schumann and van Heerden, 1988). In addition, subsurface cooler water enters the eastern AB (EAB) shelf through frictional effects (Hutchings, 1994) or dynamic upwelling under the AC (Probyn et al., 1994; Chapman and Largier, 1989). On the western AB (WAB), AC water is found on the surface particularly in summer but rarely in winter (Largier et al., 1992). In the Benguela Upwelling System, cold Atlantic Central Water enters onto the WAB through wind stress / upward tilt of isotherms (Chapman and Largier, 1989; Shannon and Nelson, 1996). These waters will be brought closer to the surface through coastal upwelling. The AB is thus a mixing region of warm and cold water stirred by two distinct current regimes.

Of particular importance to the AB is the stratification which plays an important role in the biology of the AB (Probyn et al., 1994; Hutchings, 1994). In shallow oceanic regions, such as the continental shelf, solar insolation plays a key role in the heating of the upper water column as well as the oceanic forcing of the adjacent AC flowing along the slope of the

EAB. Direct wind forcing also plays a role, particularly in the destabilisation of the water column, through vertical mixing, in winter.

A ridge of cold water, in this thesis refered to as the cool ridge (CR), is a feature of the East and Central Agulhas Bank, it has been observed to extend south-westwards off the South African coast from approximately 24°S, in a layer lying at shallow depths (Swart and Largier, 1987; Boyd and Shillington, 1994; Roberts, 2005). The cool water at shallower depths appears to coincide with the surface chlorophyll maximum on the AB (Demarcq et al., 2003) and therefore has an impact on the marine biology. The origin, behaviour and fate of this feature is undefined and therefore its implications on the AB structure and circulation is uncertain. The CR appears to be a predominantly subsurface feature (Boyd and Shillington, 1994) and a consistent 3-dimensional understanding is required. This can be provided by a numerical ocean model.

Numerical ocean models provide a temporally and spatially high resolution of data output which is dynamically consistent and available at relatively cheap computational power. This contrasts to *in situ* studies which are performed over a fixed time period thus providing only a synoptic view of the physical oceanic conditions and limited spatial coverage. Satellite studies, although temporally more consistent can usually only reveal surface expressions of features.

In South Africa, research into the Benguela Upwelling System has benefited from the application of the ROMS (Regional Ocean Modeling System) model to this region (Penven et al., 2001b). With the improvement of the modelling of the AC to the south of Africa, better information can be obtained from the study of the adjacent coastal ocean region, the AB.

This thesis aims to clarify and elucidate the dominant physical processes of the AB, such as the generation of the CR. For the AB, the sources of warm water are relatively well understood: warming of the surface layer by the sun, interactions by the warm AC and its associated mesoscale features. In contrast, the underlying cold water on the AB warrants additional investigation due to its importance as a bottom layer, specifically the process by which the cool water reaches and spreads on the AB. The specific objectives and research questions are posed in Section 1.7.

1.1 Geographic Setting

The Agulhas Bank is the southern extension of the continental shelf off South Africa (Figure 1.1). It is roughly triangular in shape and considered to span approximately 800km between 18°E and 29°E and at its southern tip, 250km offshore (34.8–36.9°S), covering approximately 116 000km^2 (Hutchings, 1994).

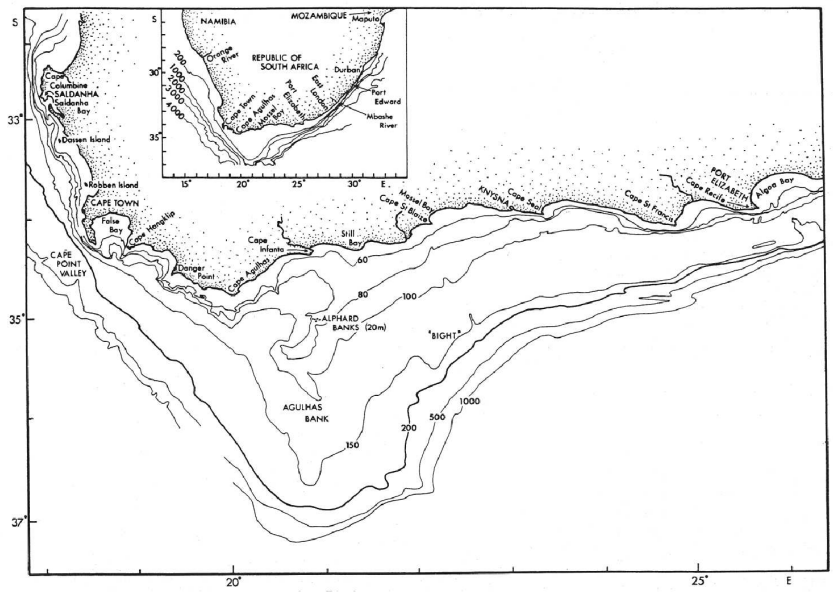

Figure 1.1: Bathymetry of the Agulhas Bank (Boyd and Shillington, 1994).

The eastern and southern boundaries have a well-defined shelf break while the western boundary is "less steep and more irregular" (Dingle and Scrutton, 1974 cited in Schumann and Beekman, 1984, pg. 191). On the AB, from the coast to 50m, the shelf drops steeply before deepening gradually to the shelf break, located at approximately the 200m isobath (Hutchings, 1994). In contrast to the smooth, gentle slope offshore from Cape Agulhas (20°E) to Cape Hangklip (18°50' E), the mid-shelf region around Cape Point displays narrowing and a convergence of isobaths (Largier et al., 1992). Other bathymetric features of the Bank include the Alphard Banks (approximately 20–21°E, 35°S) in the west and an eastward-facing bight on the eastern shelf (22–24°E), known as the Agulhas Bight. The Agulhas Bight is described as "an upper-slope embayment in the Agulhas Bight, ... defined on the landward side by the concave pattern of closely spaced isobaths in the 200–1000 m depth range" (Ben-Avraham et al., 1997, pg. 87). The coastline along the south coast of South Africa is marked by southeast facing bays with protruding capes (Schumann et al., 1988).

The AB is considered to be divided up into several subregions depending on the hydrographic characteristics. Shannon (1966, as cited in Largier and Swart, 1987; Swart and Largier, 1987; Schumann and Beekman, 1984), noted the difference in hydrographic structure between the west and east AB, divided by a meridional line located between Cape Agulhas (20°E) and Cape Infanta (21°E). Swart and Largier (1987) suggested that stratification on the AB, separated by the CR, distinguishes the two regions. *In situ* temperature data (Schumann and Beekman, 1984) appear to confirm this division located south of Cape Infanta–Cape Agulhas which is also observable in sea surface temperature satellite data. On the EAB, stratification is enhanced by advection of warm waters of the Agulhas Current above the thermocline and cold waters from shelf-edge upwelling below the thermocline (Swart and Largier, 1987). In the west, away from the AC, less advection of these waters occur which results in the weakening of the thermocline but may be strengthened by shear-edge eddies and plumes from the south (Swart and Largier, 1987).

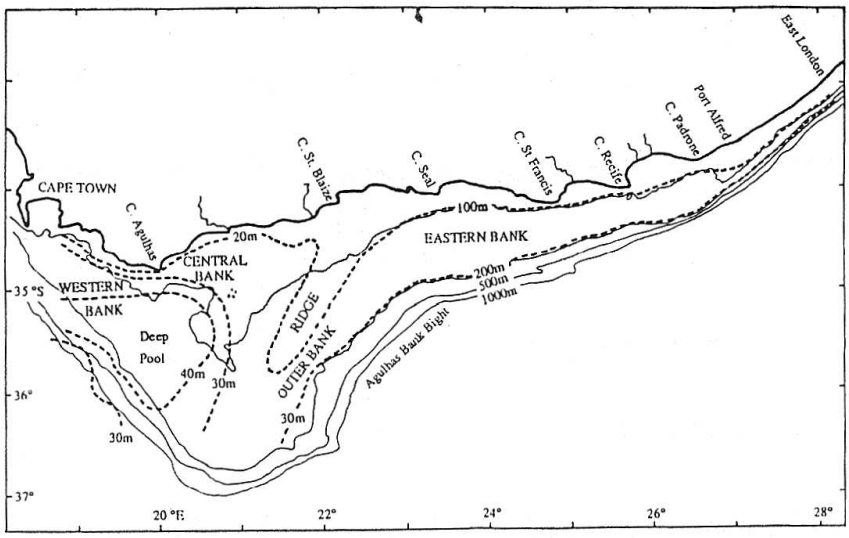

Figure 1.2: Representation of subdivisions of the Agulhas Bank (Probyn et al., 1994).

Considering thermal structures and circulation from hydrographic studies, the AB can be divided into three main subregions: Western Agulhas Bank (WAB) dominated by wind-driven upwelling and linked to the Benguela; central Agulhas Bank (CAB); and Eastern Agulhas Bank (EAB) which is dominated by the Agulhas Current. The CAB could be regarded as a shelf region, dominated by tides, wind stress and solar insolation as opposed to forcing from the open ocean (Schumann and Beekman, 1984). In addition the region inshore, along the coast, is considered to be influenced by local conditions such as the winds and bathymetry.

These regions are summarised in Figure 1.2 which displays the approximate sectors that the Bank can be divided into.

1.2 Meteorological Setting

The meteorology of the AB region is not well described. Of importance to the AB is the wind variability, which drives coastal upwelling along the WAB and the south coast. Few wind data are available and where examined are unsuitably located. For example, wind speeds are underestimated as measurements are taken at stations inland thus excluding effects such as orographic steering (Schumann and Martin, 1991). Meteorology for the south coast of South Africa and the AB has been studied by Hunter (1987), Schumann and Martin (1991), Schumann (1992), and Jury (1994) who provides a review for the EAB. Hunter (1987) presents a more comprehensive study of the meteorology of the region using many sources of observations; his emphasis was on the synoptic scale variability, in contrast to the other studies which concentrate on only the wind field (Schumann and Martin, 1991; Schumann, 1992). For this section, a basic overview of the large scale circulation (climatology) relevant to the AB is provided, but the focus will be on wind variability on the AB. Sea surface temperature variability on the AB has been linked to wind stress in a model sensitivity study (Blanke et al., 2002), for example, the wind contribution to interannual SST on the AB is as high as 90%. However, the effects of the AC were not fully represented in this model, non-local variations in the AC (Natal Pulses for example) were absent in this model (Penven, 2000).

Atmospheric circulation over Southern Africa is subject to tropical, subtropical and temperate control, as summarised in Figure 1.3. Over South Africa the dominant feature is subtropical control, part of the 30°S high pressure belt, specifically the South Indian Anticyclone, the continental high and the South Atlantic Anticyclone (Tyson and Preston-Whyte, 2000). The South Indian and South Atlantic Anticyclones vary in position throughout the year, undergoing both latitudinal and longitudinal shift. The southeasterly flow associated with the South Atlantic Anticyclone is steered along the coast and is important as these winds are responsible for coastal upwelling in the southern Benguela (Shannon and Nelson, 1996). The winds on the AB are dominated by the mid-latitude westerlies (Hardman-Mountford et al., 2003). Upwelling-inducing easterlies on the south coast are associated with two systems: the continental high ridging to the south or by the presence of a transient cell (Schumann and Martin, 1991; Jury, 1994).

In winter the anticyclones move 5–6° northward. This allows the westerly belt to extend northwards. Low pressure systems that form in this westerly belt are thus able to influence the southern Benguela and the coastline of the AB (Shillington, 1998; Hardman-Mountford et al., 2003). These low pressure systems induce strong northwesterly to southwesterly winds along the coast.

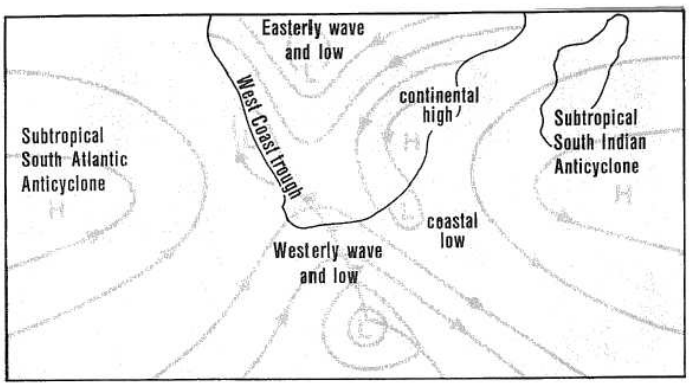

Figure 1.3: Surface atmospheric circulation features (Tyson and Preston-Whyte, 2000).

There is a limited correlation between air pressure and the winds along the South African coast (Schumann, 1989). This is due to air pressure being measured from the synoptic system but the winds were subject to changes on a local, smaller scale by factors such as topography.

In general, south of Africa strong westerly winds dominate throughout the year (Shannon and Nelson, 1996). Maximum westerly wind stress occurs in winter whilst the weakest winds are found in summer (Figure 1.4). On the west coast, the strongest longshore winds lies south of 25°S, from late spring to early autumn these strong winds also cover Cape Columbine and Cape Peninsula (Shannon and Nelson, 1996)

SOM (Self Organising Map) analysis of QuikSCaT winds from 1999 to 2000 over the Benguela showed the wind field to be divided into 6 discrete regimes (Risien et al., 2004). The southernmost regime, from 35 to 33°S, showed the highest synoptic winds stress variability due to the passage of frontal systems and the movement of anticyclones. Mid-October to mid-May is associated with strong southeasterly wind stress. Whilst weak westerly to northwesterly was found from mid-May to July 2000.

Along the coastline of the AB, the winds flow parallel to the coastline due to the interior escarpment, coastal mountains and horizontal thermal gradients (Schumann and Martin, 1991). The strongest monthly-mean southeasterly winds at Cape Town occur in summer from November to January, with the southeasterly contributing more than 70% of the summer

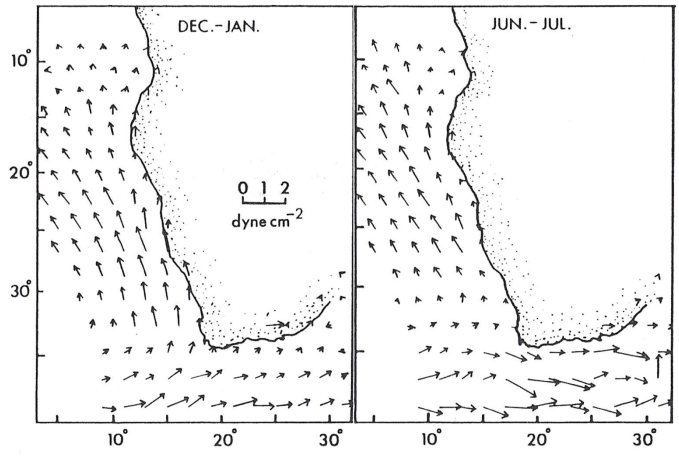

Figure 1.4: Surface winds for December-January and June-July (Shannon and Nelson, 1996).

winds from November to March. These winds reach a minimum in magnitude and frequency in June. NW winds dominate in winter and are stronger in magnitude.

At stations along the EAB, throughout the year, westerly-component winds were predominant at sites such as Port Elizabeth and Cape St Francis (Hunter, 1987). In summer, easterly-component winds at the coast have the highest frequency in summer (20%) as compared to summer westerlies (15%) (Jury, 1994) with exception of Port Elizabeth which was found to be dominated by westerlies in all seasons (Schumann and Martin, 1991). Maximum speeds for easterly winds are found in October and November (Schumann and Martin, 1991). In winter, westerly-component winds dominate.

Wind speeds are stronger to the east of the AB except for the region between 22 and 23°E where the coastal region has comparatively lighter winds (Jury, 1994). Offshore over the AB, the winds are less directionally polarised and wind speed are greater than at the coast (Jury, 1994). Furthermore, stronger winds are found along the capes due to "reduced friction over the sea and topographic acceleration by land" (Schumann and Martin, 1991).

In summary, upwelling on the west coast is associated with southeasterly winds whilst on the south coast, easterly-component winds may induce-upwelling. These winds are more frequent in summer and associated cooler surface temperatures are expected in this season.

1.3 Regional Oceanic Setting

This section summarises the large-scale oceanic region south of Africa surrounding the AB. The main character and features of this region can be summarised in the following figure (Figure 1.5):

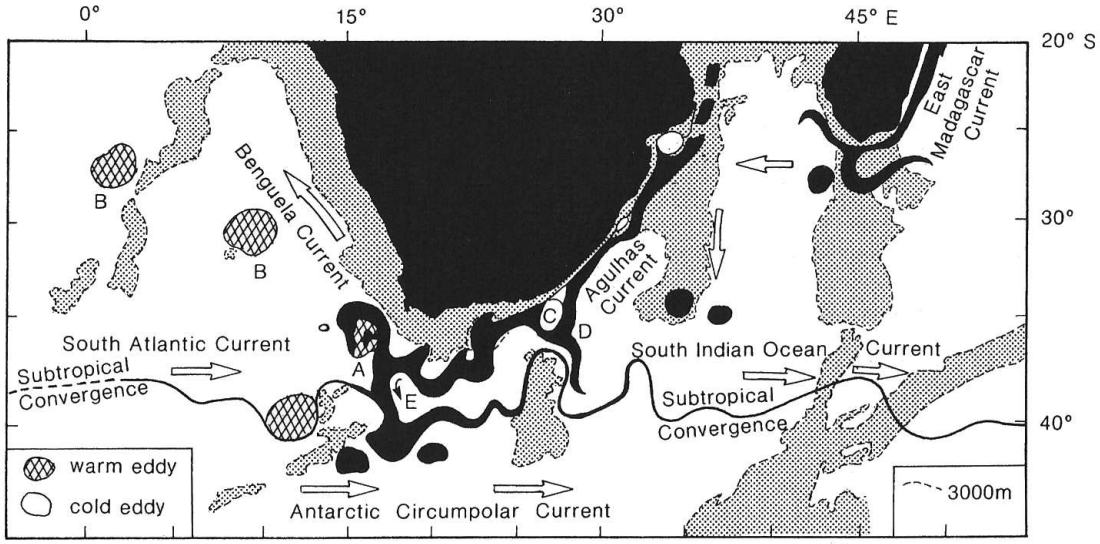

Figure 1.5: Main large-scale features of the southern Agulhas Current region (Lutjeharms, 1996 modified from Van Ballegooyen et al., 1991). A – shed Agulhas ring, B – Agulhas rings, C – cyclonic eddy forming part of Natal Pulse, D – upstream retroflection at the Agulhas Plateau due to C, E – Agulhas retroflection.

The AC dominates this region and can be summarised as: "the major, most energetic western boundary current in the Southern Hemisphere" (Valentine et al., 1993). The retroflection of the AC and the Agulhas Return Current are located downstream of this region. The importance of the region lies in the interocean exchange which occurs here (de Ruijter et al., 1999). For example, Agulhas rings which carry heat and salt into the Atlantic and have large-scale consequences. This region is characterised by high variability as seen in the eddy kinetic energy (EKE) distribution (Penven et al., 2006c). On the west coast of Southern Africa, the Benguela Current System dominates. It is characterised by relatively slow equatorward flow and cold waters from wind-driven coastal upwelling. Transient features of mesoscale lengths are associated with the AC. These include: Agulhas rings shed by the Current, Natal pulses, plumes and eddies.

1.3.1 The Agulhas Current System

Located off Southeast Africa, the southwestward-flowing AC (Figure 1.5) is the western branch of the South Indian subtropical gyre (de Ruijter et al., 1999). The AC can be divided into two sections: the northern and southern AC regions. In the northern part (approximately between 26 and 34°S), the AC is at its most intense in velocity (peak monthly velocity of around 2.6m.s^{-1}) and flows close to the coast at the shelf edge following the narrow continental shelf (Lutjeharms, 2006). The AC tends to be stable in this region, meandering by up to only 15km on either side (Grundlingh, 1983; Lutjeharms, 1996). The width of the AC is approximately 90km as observed by steeply sloping isotherms (Grundlingh, 1980). In the southern Agulhas region, close to Cape Padrone (between 33.5 and 34°S), the shelf widens to form the AB. There, the AC diverges from the coast and is generally unstable with the occurrence of meandering and the formation of shear edge eddies and associated plumes inshore of the current (Lutjeharms et al., 1989).

At around the southern tip of the AB, the AC leaves the shelf and at approximately 20°E, the current retroflects in a loop and flows eastward adjacent to the Subtropical Convergence, as the Agulhas Return Current (Grundlingh, 1983). In this region, AC water may escape to the South Atlantic. This usually occurs in the forms of rings and eddies (Lutjeharms, 1996) but also occurs in a northward branch of the AC known as an Agulhas filament (Lutjeharms and Cooper, 1996). These filaments are found on the edge of the WAB. This interocean leakage is important as it plays a role in the exchange of heat and salt between the Indian and Atlantic Ocean which has global climate implications as well as influencing the local hydrographic character (Lutjeharms, 1996).

The source waters of the AC are considered to be derived from east of Madagascar, through the Mozambique Channel and through the recirculation associated with the South-west Indian Ocean subgyre (Lutjeharms, 1996). These sources contribute the following transports: 25Sv, 5Sv and 35Sv, respectively (Stramma and Lutjeharms, 1997). Average transport for the AC was measured by a moored-array to be 69.7Sv off 31°S (Bryden et al., 2005).

Surface waters of the AC are derived from Tropical Thermocline Water originating from the tropical zone of the Indian Ocean (Valentine et al., 1993), 16.0 to 26.0°C with salinties greater 35.5psu. Two central waters are found in the AC region: Southeast Atlantic Ocean (6.0–16.0°C, 34.5–35.5psu) and Southwest Indian Ocean (8.0–15.0°C and 34.6–35.5psu). Although the TS characteristics are similar, the waters are distinguishable by their nutrient

profiles (Chapman and Largier, 1989).

1.3.2 The Benguela Upwelling System

The Benguela Upwelling System forms the eastern arm of the South Atlantic gyre (Shannon and Nelson, 1996) and bounds the AB to the west. The Benguela is characterised by typical coastal upwelling found on the eastern boundary's of the world's ocean: wind-driven divergence at the coast induces replenishment of cold, nutrient rich water from depth creating a region of high productivity (Hill et al., 1998). The northern boundary extends up to the Angola-Benguela front found between 14 and 17°S (Shannon and Nelson, 1996) whilst the southern boundary is the Agulhas Retroflection region - although upwelling can extend past Cape Town and extend eastwards along the south coast to Cape Agulhas (Shillington, 1998).

Associated with the Benguela is an equatorward jet that transports up to 25Sv with surface velocities in the order of 30cm.s^{-1} (Shannon and Nelson, 1996). Surface flow is balanced by a mean poleward undercurrent with an average speed of 5km.day^{-1} (Shillington, 1998).

Features of the AC may interact with this region. Water from the Indian Ocean is introduced into the Benguela by the eddy-shedding process occurring at the Agulhas Retroflection region, additional Indian Ocean water may enter through the branching of the AC at the continental shelf (Garzoli and Gordon, 1996). Furthermore, Subantarctic Surface water may be entrained via the eddy-shedding process from the Antarctic Circumpolar Current into the Benguela Current or via the flow of the South Atlantic Current through exchanges across the subtropical front (Garzoli and Gordon, 1996).

The water in the Benguela is mainly of Atlantic origin. Results from Garzoli and Gordon (1996), attributed 50% to South Atlantic water, 25% to Indian Ocean water, and 25% to a mixture of Agulhas and tropical Atlantic water. Indian Ocean waters are transported into this region by Agulhas Current. Water on the shelf brought to the surface in upwelling, Benguela thermocline water, ranges from 34.5–35.5psu and 6–16°C (Shannon and Nelson, 1996). Deeper water, underlying this later is Antarctic Intermediate Water (AAIW) at 34.2–34.5psu and potential temperatures of 4–5°C its average core depth varies, 700–800 m in the South-east Atlantic. AAIW found in the Benguela have various origins, differing both in salinity and oxygenation, including: the Indian Ocean, the South Atlantic Current and the tropical Atlantic (Shannon and Nelson, 1996).

1.4 Hydrographic Setting of the Agulhas Bank

The AB is a complex region due to its position between the two regimes of the AC and Benguela Current. The AB displays fluctuations on daily, seasonal (Schumann and Beekman, 1984) and possibly longer time scales (Schumann et al., 1995).

The distinct seasonality in the water column temperature is a feature of the AB (Shannon, 1966; Bang, 1970; Schumann and Beekman, 1984; Eagle and Orren, 1985; Walker, 1986). In summer, the water column is stable and highly stratified, forming a two-layer system (Eagle and Orren, 1985). The thermocline may lie in the upper 50m (Schumann and Beekman, 1984). The surface layer is warmed by solar insolation and by plumes of warm, saline AC water (Swart and Largier, 1987). Average summer SST are 20–23°C and significant variability on the AB was observed for the EAB, Cape Peninsula and inner WAB (Demarcq et al., 2003). Monthly standard deviation for summer and autumn months on the EAB were between 1.5 and 2°C and attributed to the AC whilst around the Cape Peninsula in February / March exceeded 2°C (Demarcq et al., 2003). The bottom waters are cold and show seasonal changes with summer and autumn being the coldest around 11°C (Eagle and Orren, 1985). The main contributor of cold bottom waters are thought to be shelf-edge upwelling between the AC and the eastern edge of the AB (Schumann and van Heerden, 1988; Schumann, 1986; Walker, 1986; Schumann, 1987).

In winter, the water column over the AB is uniform and well-mixed from the destabilising effects of increased wind shear and negative heat fluxes most noticeable in the west (Largier and Swart, 1987). Mean winter SST are 15–19°C (Demarcq et al., 2003). With the thermocline as deep as 80–90m on the WAB and CAB (Hutchings, 1994).

In a review of the research performed on the AB, Hutchings (1994) produced a graphical summary of the main features of the AB (Figure 1.6). Figure 1.6 shows the AC flowing along the shelf edge of the EAB. At the southern tip of the AB, the AC either moves around the edge or moves southwards. Inshore of the AC, eddies are noted. At several regions along the east coast, upwelling driven by the divergence of the AC with the shelf-edge is indicated. Shelf-edge upwelling along the EAB and WAB are also shown. Wind-driven upwelling is another important process found along the WAB and along the coastline and capes of the south coast. The approximate position and extent of the CR mid-AB is also displayed.

Circulation over the AB is localised and related to the dominant forcing. An idea of the general circulation at 30m over the AB is provided in Figure 1.7 based on ADCP data (Boyd

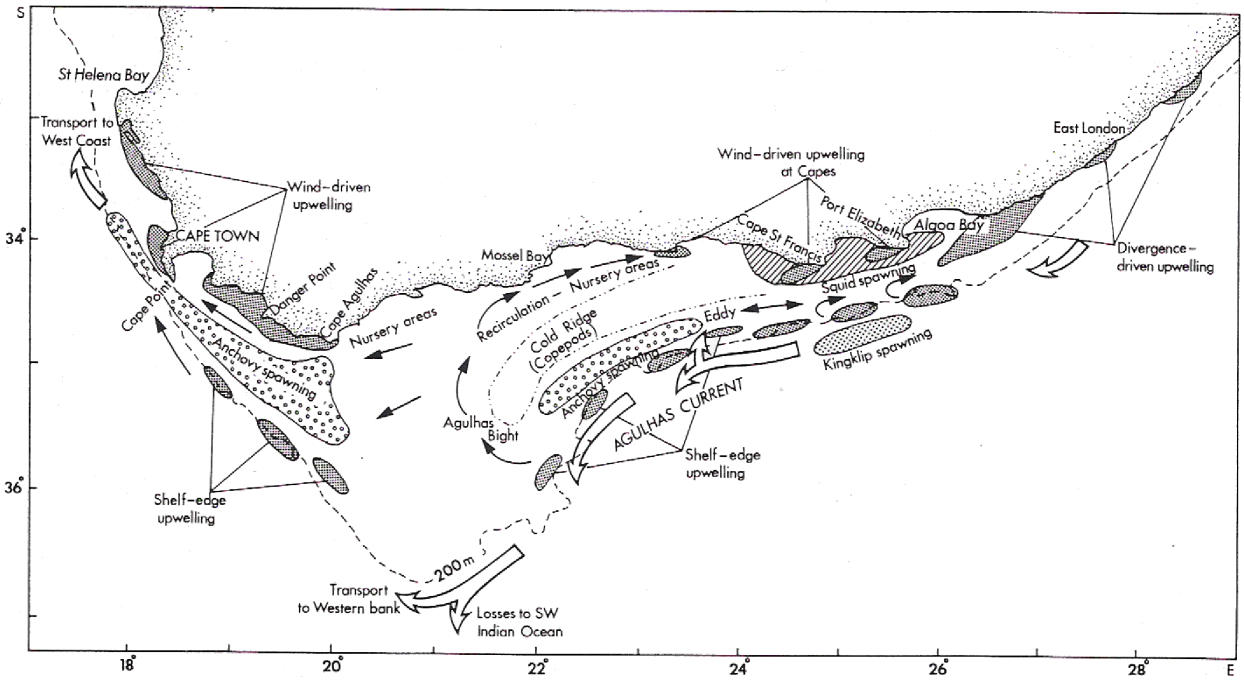

Figure 1.6: Major physical processes affecting the Agulhas Bank including biological processes (Hutchings, 1994).

et al., 1992). The outer AB is directly forced by the AC whilst the inner-shelf (along the coast) is more wind-driven. This leaves the central AB as a transitional region with weak and differing currents (Boyd and Shillington, 1994). This pattern can be observed in the thermal structure over the WAB, where three hydrographically independent subregions can be identified in spring and summer: the coastal or inner shelf region mostly driven by wind processes; the shelf-edge or outer shelf region driven by oceanic processes; and a shelf or mid-shelf region intermediate to the two other regions (Largier et al., 1992).

As seen from the dominant processes map provided by Hutchings (1994) and the circulation patterns by Boyd et al. (1992), two important process types are apparent: those related to oceanic influence (particularly the AC) and those driven by the wind at the coast (related to coastal upwelling). The following section therefore considers the structure and circulation of the AB in a process-related manner: the Inner-AB (or coastal wind-driven upwelling zone); the Outer-AB (driven by oceanic influence, the AC or associated eddies and plumes) and Mid-AB, the transitional region in between. The terms EAB, WAB and CAB will still refer to the geographic locations as shown in Figure 1.2.

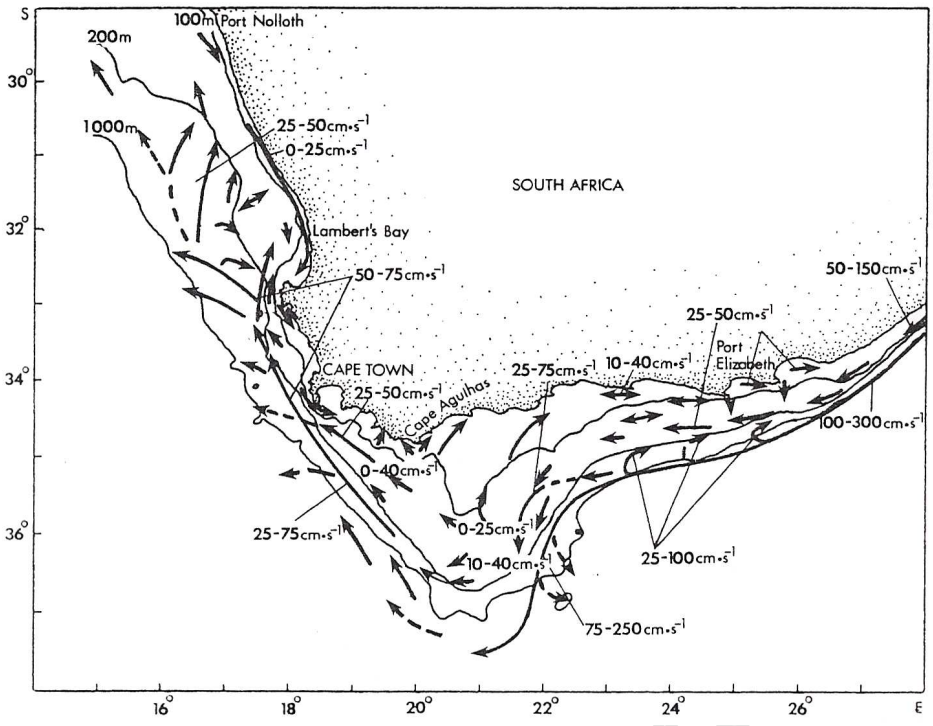

Figure 1.7: Schematic flow field of near-surface currents based on ADCP data collected between November 1989 and January 1992. Velocity ranges reflect typical values, not extremes (from Boyd et al., 1992).

1.4.1 The Inner-Agulhas Bank: Influence of Wind-driven Upwelling

Although upwelling occurs along most of the coastline of the AB, the two regimes on either side of Cape Agulhas are often considered separately (Shannon, 1985). Upwelling west of and including Cape Agulhas is considered part of the southern Benguela, and responds to southeasterly windstress (as well as easterly) (Largier et al., 1992). The upwelling cell at Cape Agulhas is subject to sporadic upwelling rather than being a permanent cell (Lutjeharms and Meeuwis, 1987). Upwelling east of Cape Agulhas, on the other hand, is induced by easterly winds along the coastline and capes (Schumann et al., 1982). Pockets of upwelled waters are also observed as a response to the passage of coastal trapped waves along the coast (Bang, 1970).

The AB coastline features many crenulated bays (Figure 1.8). On the WAB, the major features of the coastline are the Cape Peninsula and False Bay (Shillington, 1998). The WAB has small southwestward facing bays such as Walker Bay (Lutjeharms and Stockton, 1991). Coastal upwelling associated with the Benguela Upwelling System extends around the Cape Peninsula and onto the coastal WAB up to Cape Agulhas (Shillington, 1998).

East of Cape Agulhas, along the south coast and along the many headlands, coastal

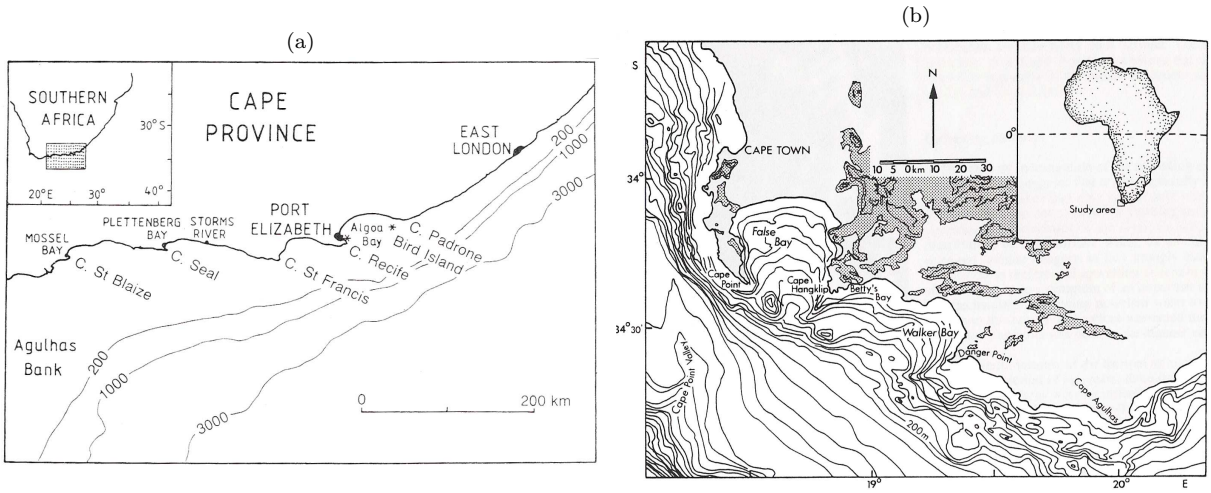

Figure 1.8: Capes and bays along the (a) EAB (Schumann and van Heerden, 1988) and (b) WAB (Lutjeharms and Stockton, 1991).

upwelling occurs in response to easterly winds and is confined to the area close to the coast (Schumann et al., 1982; Beckley, 1988). Cold mean temperatures were correlated with the increase in frequency of easterly winds in January and February (Schumann et al., 1995). Upwelling is associated with the shoaling of isotherms at the coast, although the thermocline may not reach the surface in some upwelling events (Schumann et al., 1982). Throughout the upwelling season, isotherms remain tilted towards the coast. Since the Ekman layer is also shallow through the season, the onset of easterly winds induces rapid drops in surface temperature (Schumann et al., 1995). Upwelling can be induced by low wind speeds but with further increase in wind speed there is no consistent drop in temperature (Schumann et al., 1995), this suggests it is possible for weak winds to upwell cold bottom waters due to the shallow mixed layer.

The drop in temperature with easterly winds is quickly reversed with the onset of opposing (westerly) winds (Schumann et al., 1982). Upwelling events on the south coast tend to be of a short duration with few events lasting more than 4 days due to the variable nature of the winds (Schumann, 1999). Westerly winds are also reported to correlate with a decrease in surface temperature through mixing with cooler waters below (Schumann et al., 1995).

In contrast to the southern coastline, the dynamics within large bays react differently to winds and are reflected in the temperature profiles (Schumann et al., 1995). Upwelling occurs on the southern side of the cape in response to easterly winds, the westward coastal jet develops and thus upwelling starts at the cape and progresses westward (Schumann et al., 1982). Within the bay, the bathymetry is shallow such that water moves westward along the

north coastline of the bay instead of offshore in response to easterly winds. Convergence of water within the bay then causes downwelling (Schumann et al., 1982).

Upwelling in response to easterly winds is a simplified explanation for the coast east of Cape Agulhas. For example, Schumann et al. (1982) found situations where easterly winds blew but with no corresponding upwelling of cold water observed at the surface. Thus, other factors such as wind strength and duration as well as the ocean state need to be considered.

West of Cape Agulhas, upwelling responds to southeasterly winds that are predominant in summer and autumn (Largier et al., 1992). In cases of strong southeasterly winds, the thermocline may breach the surface resulting in the expression of a front. Following the weakening of upwelling winds, warm water may move inshore but subsurface isotherms remain tilted toward the coast throughout the upwelling season (Boyd et al., 1985). In spring and when winds are insufficient to cause the thermocline to breach the surface, the constant uptilt of isotherms is found and is associated with subsurface upwelling (Largier et al., 1992). Upwelling along the Cape Peninsula has a larger response to south to southeasterly winds than Walker Bay on the WAB (Boyd et al., 1985).

Coastal currents on the AB are mostly barotropic and directly forced by the winds which are mainly easterly or westerly (Boyd et al., 1992). Currents from the coast up to the 100m isobath are variable in direction but mostly align with the bathymetry (Boyd and Oberholster, 1994). Although the flow may vary, eastward flow dominates the coastal region (Schumann, 1992). Coastal trapped waves passing along the coast results in the reversal of flow (from eastwards to westwards) as well as high sea level variability (Schumann and Brink, 1990 cited in Boyd and Shillington, 1994).

1.4.2 The Outer-Agulhas Bank: Oceanic Influence

The main character of the outershelf is that it is directly influenced by the deeper ocean, particularly the AC as on the EAB.

The AB east of 24°E is subject to the influences of the AC (Boyd et al., 1992) as well as coastal upwelling due to the the narrow shelf in this region, this includes Algoa Bay (Beckley, 1988). Algoa Bay will therefore be discussed in relation to oceanic forcing.

The warm AC flows along the shelf edge with speeds between 1.5 and 3.0m.s^{-1} (Boyd and Shillington, 1994). Between Mossel Bay and Cape St Francis, current flow is highly variable due to counter currents found along the 200m isobath, thus yielding weak average currents (Boyd and Oberholster, 1994). Strong west-east flow may be observed at the shelf

edge inshore of the AC due to an inshore plume or return tongue (Boyd et al., 1992). These shear-edge features on the landward border of the AC are always present (Lutjeharms et al., 1989) and affect the AB where they are concentrated offshore the 200m isobath between Port Elizabeth and Mossel Bay. Features first appear around East London and appear to increase in magnitude downstream from average 82km to 120km at the Agulhas Bight (Lutjeharms, 1981).

Loss of biota may occur at the shelf edge on the EAB but the plumes and boundary features on the EAB may serve to reintroduce biota back onto the Bank (Boyd et al., 1992). Between the AC and the 100m isobath, currents are reportedly westward (Boyd and Oberholster, 1994; Boyd et al., 1992; Boyd and Shillington, 1994). Bottom flow on the EAB is southwestwards and driven by inertial currents (Chapman and Largier, 1989).

The vertical thermal structure of the outer EAB is subject to shoaling of the thermocline due to both bathymetry and the effect of the AC (Schumann, 1986; Walker, 1986; Schumann, 1987; Schumann and van Heerden, 1988; Lutjeharms et al., 2000). Where the shelf is wide, uplift of the isotherms is followed by a dip mid-shelf and shoaling onshore (Swart and Largier, 1987). Boyd et al. (1985) report that this uplift is found particularly in late summer and autumn, suggesting seasonality to the AC. Influx of bottom water onto the shelf is limited on the WAB as the water column is deeper (Boyd et al., 1985).

The possible cause of shelf-edge upwelling is summarised by Schumann et al. (1988, pg. 580): "Ekman veering in the bottom boundary layer (Schumann, 1987), topographically controlled changes in the current structure (Gill and Schumann, 1979), and upwelling associated with a widening shelf (Blanton et al., 1981)". Furthermore, Swart and Largier (1987) suggested that the mechanism of shelf-edge upwelling, is either a result of sidewall friction of a feature between shelf and slope or possibly wind stress causing cross-current Ekman transport. Doming of the isotherms at the shelf edge onto the AB may also result from eddies and associated reverse plumes (Swart and Largier, 1987).

Between East London and Port Elizabeth, at the Port Alfred upwelling cell, the shelf widens causing cold water to upwell inshore of the AC (Lutjeharms et al., 2000). This upwelling is generally subsurface. Further action by winds exposes these cold waters to the surface (Lutjeharms et al., 2000). These cold upwelled waters may then spread through Algoa Bay (Schumann et al., 1982; Walker, 1986; Schumann et al., 1988).

Algoa Bay appears to gain cool water by upwelling at Cape Padrone which extends along

the northern shore of Algoa Bay followed by wind-mixing in the shallow bay (Schumann et al., 1988). The presence of cool waters in the southwest corner of Algoa Bay (Goschen and Schumann, 1995) may suggest another mechanism, such as from uplift of isotherm from the AC and its eddies. Another proposed mechanism is by shelf-edge upwelling, in which 10°C water may be found at shallow depths of 20m in Algoa Bay (Beckley, 1988). A decrease in temperature by as much as 9°C was observed at Cape Recife, particularly in summer and autumn with increased easterly winds (Beckley, 1983) suggesting relatively cold water is available close to the surface.

All the waters east of 21°E within the 6–14°C range belong to a single water mass (Nelson, 1985 in Chapman and Largier, 1989). The basal waters of the AB below 100m are usually less than 10°C and attributed to Indian Ocean Central Water introduced by shelf-edge upwelling (Chapman and Largier, 1989; Swart and Largier, 1987). Surface water is fed by plumes consisting of Subtropical Surface Water. In autumn, surface water on the AB is Subtropical Surface Water but with a lower salinity, due to mixing with less saline bottom water during the previous season (Swart and Largier, 1987).

Around the Agulhas Bight, south of Mossel Bay, the AC may follow the "bending of the AB" resulting in some penetration of the AC onto the shelf edge (Schumann and Beekman, 1984; Lutjeharms et al., 1989; Boyd et al., 1992). South of the Agulhas Bight, the AC travels in a south-southwesterly direction to above the 500m isobath. This region reflects similar flow patterns to that of the AC (Lutjeharms et al., 1989). Boyd et al. (1992) observed this phenomenon and the flow was found with weakened velocities after the intrusion had occurred. The extent of the intrusion may possibly be restricted by the presence of the CR (Lutjeharms et al., 1989).

On the WAB, warm shelf edge water of AC origin is found moving in a northwesterly direction. This feature is suggested to be either a filament of the AC and therefore has a deep structure controlled by topography (even exceeding 500m), or a shallow layer of warm water driven by the wind (up to 60m depths) (Largier et al., 1992; Lutjeharms and Cooper, 1996). A large volume of cool water is observed at depth in this WAB shelf-edge region, suggesting that this has been entrained/upwelled onto the AB due to the Ekman layer at the bottom due to the northwestward flow (Largier et al., 1992). Flow on the WAB is generally northwestward in summer (Boyd et al., 1992; Shannon and Nelson, 1996). This may represent the average flow in the region as the limited drifter data show that flow on the WAB shelf

edge varies in direction and may even be poleward (Lutjeharms et al., 2007); this variable flow (in magnitude and direction) is driven by eddies and filaments from the AC. The average flow on the WAB (Figure 1.7) tends to align with the bathymetry and as it moves past the Cape Peninsula, converges to form part of the baroclinicly-dominated Benguela System. Along the Cape Peninsula offshore the 200m isobath, this convergent flow is directed into the "Good Hope Jet". The Good Hope Jet is a strong equatorward jet of average speed 58cm.s^{-1} (Shannon and Nelson, 1996). This flow is also be associated with equatorward winds with an onshore component (Boyd and Nelson, 1998).

Upwelling along the west coast and WAB, particularly at certain sites such as at canyons introduces South Atlantic Central Water onto the AB (Chapman and Largier, 1989). Cold water (less than 10°C) is upwelled episodically to depths of 140m and is observed at the surface above 60m during the summer and is constantly present at the 100m isobath (Boyd et al., 1985). The path of this bottom water moves up parallel to the slope onto the shelf and then flows southeasterly approximately along the isobaths (Chapman and Largier, 1989). Most of the cold bottom water on the WAB is contained inshore of the CR (Largier and Swart, 1987) and in the deep pool indicated by Probyn et al. (1994) in Figure 1.2. On the WAB, there is strong stratification and a deep thermocline as an extension of the deep pool (Largier et al., 1992). Temperatures here are consistent with oceanic water (Largier et al., 1992).

1.4.3 The Mid-Agulhas Bank: Transitional region

The Central Agulhas Bank (CAB) is associated with weak, highly variable flow (Boyd and Oberholster, 1994; Boyd et al., 1992). Schumann and Beekman (1984) describe this region to be transitional, with the region south of Cape Agulhas showing divergent flow. Frontal structures in the region of Cape Infanta suggest the onshore extent to which the eddies reach (Schumann and Beekman, 1984), and thus the offshore extent of the CAB.

Away from the influence of the AC, the CAB shows strong seasonal variability, with a seasonal SST change of up to 5°C between summer and winter (Demarcq et al., 2003). SST variability was highest in summer from December to April for this region (Demarcq et al., 2003). Off Cape Infanta (20°50'E) the water column is well mixed from winter-to-spring, whilst the summer-to-autumn has a stratified water column, formed by surface warming and the introduction of a cold water mass along the bottom, or possibly the thickening of this

layer (Eagle and Orren, 1985). This bottom water is distinct from the surface water mass and the winter-mixed water, due to its lower salinity and higher concentration of nutrients. It exhibited variability over the 5-year study, thus suggesting the bottom water is advected onto the AB from oceanic sources. Interestingly, colder water was found further inshore than offshore (around the 100m isobath) but Eagle and Orren (1985) could not clearly distinguish the pathway or origin of this colder water.

Between Mossel Bay and Cape Agulhas, cyclonic motion was observed and ascribed to be associated with "a subsurface band of cool water", the cool ridge (Boyd et al., 1992, pg. 193). Flow offshore of this isobath tends to follow the bathymetry, from east to west, firstly flowing in a southwesterly direction before later veering northwesterly. This northwesterly flow is described to continue northwards to eventually form the Good Hope Jet, off the Cape Peninsula.

1.5 The Cool Ridge

The cool ridge (CR) is a cool-water feature, resembling a tongue, flanked by warmer Agulhas Bank waters located on the eastern and central Bank (Figure 1.9). Observational data show that in the vertical, the feature presents as a ridge, with the doming of isotherms or the thermocline, hence the terminology of "cool ridge" or "cold ridge". According to Probyn et al. (1994), the cold ridge is distinguishable from shelf break upwelling in the intensity of thermoclines. The width and size of the feature has not been described explicitly nor has its variability been quantified.

Reports indicate that the CR is generally subsurface (Hutchings, 1994; Boyd and Shillington, 1994) although it has been observed at the surface in satellite SST images (Walker, 1986; Roberts, 2005). The CR starts at the coastline between Mossel Bay and Cape St. Francis and extends in a south-westerly direction aligned with the 100m isobath (Hutchings, 1994).

The forcing of the CR is not completely understood. The two main hypotheses are that the feature is oceanically forced (Boyd and Shillington, 1994) or wind-forced as in coastal upwelling (Roberts, 2005).

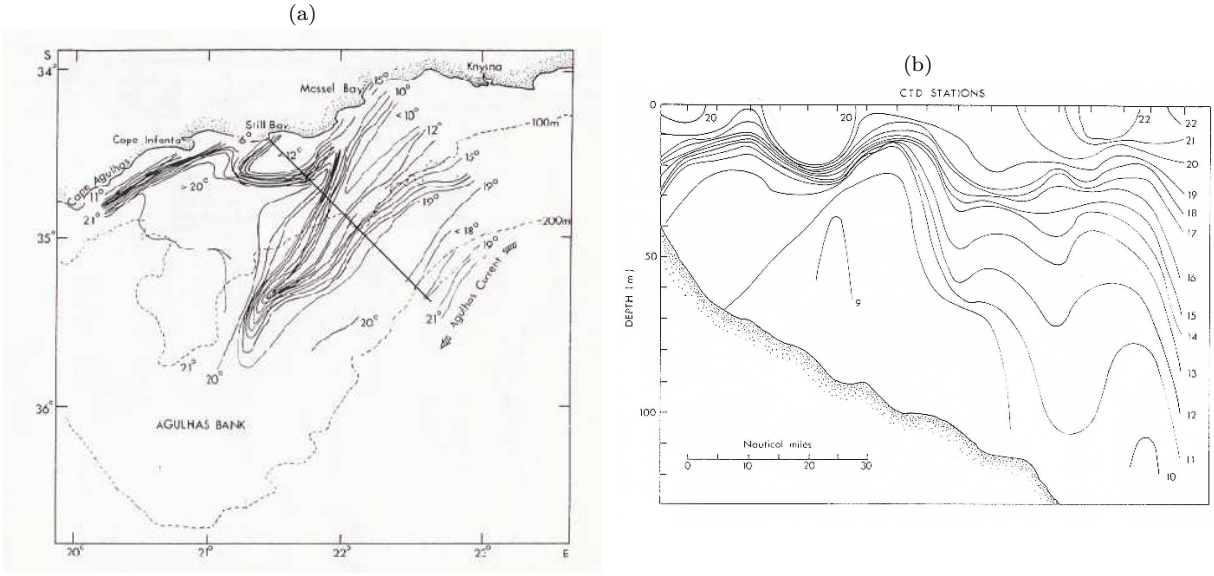

Figure 1.9: (a) Horizontal temperature map at 20m for 3–12 March 1986. Line indicates approximate position of the vertical section. (b) Vertical temperature off Still Bay 5 March 1986. Adapted from Swart and Largier (1987).

The persistence of the CR for approximately 6 months starting October 1985 has suggested to Swart and Largier (1987) that the ridge is subject to oceanic forcing. They found the CR to be most prevalent between summer and autumn. Boyd and Shillington (1994), identified the CR as occurring in the regions over the AB where the 17°C isotherm (representative of the top of the thermocline) was present in the upper 30m of the water column. Using temperature data from November of each year from 1988 to 1991, they followed the progression of the CR. The CR was observed to vary between years and was not apparent in 1990 (Boyd and Shillington, 1994). This absence coincided with warm-core features on the AB and suggested that the presence of warm-core features over the AB influences this cool feature. Water upwelled at the capes on the EAB was determined not to combine with the region of upwelling over the WAB upwelling but "rather feeds the CR offshore of the body of warmer mixed water" (pp 118). The data do not indicate the origin of the cool water on the EAB and CAB (Boyd and Shillington, 1994).

Lutjeharms and Meyer (2008) attributes the CR to being the path of cold basal water along the EAB. The basal waters originate at the Port Alfred Upwelling cell (not by shear edge features or by shelf-edge upwelling along the length of the EAB) and move parallel to isobaths on the AB. However, these conclusions are obtained by putting together data, in the form of "snapshots", from a combination of various sources over inconsistent time periods, rather than a long-term consistent dataset.

Roberts (2005) suggested that the CR originates from coastal upwelling forming a plume along the coast which is then advected southwest by westward shelf currents. Using satellite imagery, the CR was observed "mainly during summer upwelling, between November and April" (pg. 47). In certain situations of intense coastal upwelling, the CR was not apparent, this suggests that advective forces in the offshore direction are needed to form the CR (Roberts, 2005). The following paragraphs summarises the observations and theories on the formation of the CR.

Walker (1986) observed the CR in satellite imagery off Cape St. Francis lying roughly over the 100m isobath in April 1984 and to a lesser extent off Port Elizabeth and Still Bay. The feature is described as an upwelling tongue advected offshore and westwards by strong easterly winds. For that period the wind over the region was stronger than the climatological mean and an increased frequency in easterly winds was noted. The author suggests this anomalous wind also contributed to the seaward movement of the AC which added cold water onto the AB by dynamic upwelling.

In his review of the meteorology of the EAB, Jury (1994) suggests that the CR is forced by the winds over the AB. Wind velocity over the AB increases with distance away from the coast which results in cyclonic shear along the 100m isobath and an associated increased uplift of the thermocline.

The cold waters of the CR are associated with increased productivity. Roberts (2005) noted a copepod maximum in conjunction with the CR. This increased productivity is displayed in Demarcq et al. (2003), where a monthly climatology of satellite-derived chlorophyll calculated from data ranging from September 1997 to April 2002 shows chlorophyll to be highest in a tongue on the EAB extending toward the CAB. This tongue is present over most months of the year but highest from April to June. This pattern was not apparent in the SST images. This is reiterated by Demarcq et al. (2007), where maximum chlorophyll-a concentration associated with the CR was found from April to June.

The CR may also play an important role in the productivity of the central bank and through its exchanges with the western bank, feed the productivity of the western Bank (Swart and Largier, 1987). The CR plays an important role in the biology of the AB yet its forcing and behaviour are not understood. Available literature on the AB provides an inconsistent description of the CR due to the various sources and differing time periods over which each of the studies were undertaken.

1.6 Modelling the Southern African oceanic region

Around southern Africa, several numerical circulation models have been used to study the large and regional scale features, but modelling of the coastal ocean prior to 2000 were limited (Penven et al., 2001a). In a review by Shillington et al. (2006), numerical ocean modelling for the Benguela region is discussed. Early models for the coast off southern Africa favoured the west coast such as that of van Foreest and Brundrit (1982). Regional scale modelling of the southewestern southern African was performed using NORWECOM, an adaptation of the Princeton Ocean model (POM) (Skogen, 1999 in Shillington et al., 2006). This model had a coarse resolution of 20km and was unable to accurately resolve mesoscale features on the west coast and western Agulhas Bank (Penven et al., 2001b). On a basin scale, several models have been applied to the oceanic region around southern Africa. Shillington et al. (2006) list the following examples: SPEM was applied to the South Atlantic by Barnier et al. (1998); MOM2 to the South Atlantic by Biastoch and Krauss (1999); FRAM to the region south of Southern Africa up to Antarctica (Lutjeharms and Webb, 1995); and POCM to the Agulhas region by Matano and Beier (2003). These model configurations were designed to resolve large scale features and thus the grid spacing was too coarse for coastal applications.

As part of the VIBES project (VIability of exploited pelagic fish resources in the Benguela Ecosysytems in relation to the environment and Spatial aspects), increased resolution was required in order to model the environment of pelagic fish populations to understand their recruitment, spawning and transport processes (Penven et al., 2001a). The Regional Ocean Modelling System (ROMS) was chosen for this task. This was setup and fully described by Penven (2000) and is known as PLUME. PLUME consisted of a pie-shaped grid in the southern Benguela enclosing the southwest corner of the continent, extending from 40°S to 28°S and from 10°E to 24°E. Topography was derived from the ETOPO2 dataset (Smith and Sandwell, 1997) and surface forcings extracted from the COADS dataset (Da Silva et al., 1994). The boundaries to the open ocean were forced by the seasonal climatology from the Agulhas as Primitive Equations (AGAPE) basin-scale ocean model (Biastoch and Krauss, 1999). Grid resolution of this model consisted of 18km offshore increasing to 9km inshore.

Penven et al. (2001a), commented that the model output from PLUME and observed ocean structures showed a "generally reasonable agreement" (pg. 674). In Lutjeharms et al. (2003), a study of cyclonic eddies inshore of the AC discussed the model results in comparison

to hydrographic and satellite data. Sea surface temperature variations were said to be realistic and surface conditions concurred with observed structures, although the location of the AC at certain periods was noted to be unstable.

ROMS has been successfully applied to many coastal regions. In particular, eastern boundary regions such as the California Current System (Marchesiello et al., 2003), Peru Current System (Penven et al., 2005) and Benguela Current System (Penven, 2000). Speich et al. (2006) used ROMS at a resolution of 1/6° to investigate the behaviour of the AC and its sensitivity to the topography. The model represented the AC acceptably with a volume transport of 75Sv at 30°E. Mesoscale features were also resolved with eddy-shedding and meanders present in the model. The model showed that the steepness of the topography constrained the AC such that by smoothing the slope the AC preferred to leak directly into the South Atlantic. The formation of Agulhas Rings was also not favoured. When the AB is replaced by a narrow zonal shelf the AC follows the shelf with increased leakage into the South Atlantic.

Modelling using ROMS had benefited from embedding. Embedding or nesting involves a hierarchy of models which are able to interact with each other; in 1-way embedding, typically, results from a coarser-resolution grid are used to provide the lateral boundary conditions to a finer-resolution grid (Penven et al., 2006b; Blayo and Debreu, 1999). Where features at the coast or on the shelf a high resolution need be resolved, 1-way embedding has provided the procedure to couple the larger-scale offshore features with these smaller spatial scale features. This was done for the ROMS model configuration applied to the California upwelling system by Penven et al. (2006b). This procedure allows for higher resolution locally with limited computational power, which can be applied to the modelling of the AB at reasonably-high resolution.

1.7 Summary and Objectives

The vertical doming of cold water in a horizontal tongue extending from the coast southwestwards over the AB can be extracted from the various literature to describe the CR in general. Its forcing is uncertain. Its persistence over long periods of time (Swart and Largier, 1987) or absence even when winds are upwelling-favourable (Boyd and Shillington, 1994) suggest oceanic forcing. On the other hand, its observed attachment to the coast and its intensification coinciding with increased easterly wind stress in certain cases (Roberts, 2005) suggests the influence of wind-forced coastal upwelling. In the monthly satellite climatology by Demarcq et al. (2003), the CR is apparent in the chlorophyll but not in the SST. Chlorophyll-a is an integrated variable which supports the notion that the CR is partly subsurface. A consistent description or seasonal behaviour of this feature is not presently available.

The ROMS model with nested child provides increased temporal and spatial resolution to study the AB and the CR, since no consistent long term data exist for the analysis of this feature (Roberts, 2005). Its subsurface nature means that satellites may not be helpful although chlorophyll, in the right conditions, may provide a better method to track the feature than SST. In order to study the process by which the CR forms, a consistent and extensive modelling dataset is required.

The most important consequence for the CR is that on the biology of the AB. Productivity will be increased when cool nutrient-rich waters are brought closer to the surface. Therefore in this thesis, the process which brings isotherms closer to the surface, in the form of doming in the vertical, that will in turn influence productivity on the AB will be regarded as the CR. In addition, the CR is considered located away from the coast, to separate it from coastal upwelling, although the association with coastal waters must still be established.

The objectives of this research can be expressed as the following key questions:

- **What is the nature of the seasonality of the shelf ocean on the Agulhas Bank?**

  The AB water column in summer is described to be a two-layer system separated by a strong, shallow thermocline whilst in winter it is uniform and associated with deep mixing. The advection of warm waters from the AC and its associated eddies and plumes at the surface enhance the thermocline from above. From below, strengthening occurs by the advection of cool water driven by Ekman veering or dynamic upwelling

onto the bottom of the AB. In summer, these factors combined with weak winds and solar surface heating allow for a stable water column. In winter, stronger winds and less heating destabalise the water column and mixing occurs, breaking down the two-layer system.

A ROMS model simulation using climatological forcing is used to investigate the seasonal structure on the AB and in particular, the ability of the model to represent the CR. Since the description and observations of the CR are limited, a comparison to available measurements is somewhat subjective.

- **What is the effect of the Agulhas Current on the Agulhas Bank?**
  The dominant feature of the southern African oceanic region is the AC. Its proximity to the AB and the presence of its eddies and plumes imply, its dynamics should have a marked influence on the structure and circulation over the AB. In a comparison between the AB with the AC and without the AC (through an adjusted model run), this thesis aims to qualify the AC influence and its role in the formation of the CR.

- **What processes affect the formation of the cool ridge?**
  Two main hypotheses have been put forward for the formation of the CR. One CR hypothesis attributes the feature to a coastal upwelling plume driven by the wind. The other hypothesis attributes it to oceanic forcing. Using the climatological model run and an adjusted model run without the AC, the processes that contribute to the structure of the AB are investigated.

- **What is the seasonal behaviour and fate of the cool ridge?**
  The CR may persist for a few months or appear to be absent. The previous question alludes to its origin. This question refers to the seasonal structure of the CR. Once the CR has formed what happens to the cool water? Does it move westward and cool the rest of the AB or does it advect offshore with the AC? Cyclonic flow due to the CR has been described and it is a possible mechanism for retention of organisms on the AB. Does the fate of the CR play a role in the structure of the AB?

Chapter 2

Methods

This thesis uses the Regional Ocean Modelling System (ROMS) to investigate the features of the Agulhas Bank and the process through which the cool ridge forms. ROMS is a split-explicit, free-surface ocean model which solves the incompressible, hydrostatic, primitive equations on a rotating frame based on the Boussinesq approximation and hydrostatic vertical momentum balance, a full description is available by Shchepetkin and McWilliams (2003) and Shchepetkin and McWilliams (2005). The model is discretized in the horizontal by curvilinear coordinates and terrain-following coordinates in the vertical. Subgrid-scale vertical mixing is parameterized by the K-profile planetary (KPP) scheme (Large et al., 1994).

This thesis uses the ROMS model's nesting capability to achieve higher resolution over the Agulhas Bank. A coarser resolution model (the parent model) at 1/4° resolution, SAfE (Southern Africa Experiment) is used to provide boundary conditions for a higher resolution model (the child model) at 1/12°. This chapter describes the model configuration for the parent and child models and the datasets used in the analysis of the model.

2.1 Parent configuration: SAfE

SAfE is a ROMS model configuration which resolves the large-scale oceanic features off southern Africa (Penven et al., 2006b). This includes the Agulhas Current, the Southern and Northern Benguela Upwelling Systems, the Mozambique Channel and the Subtropical Convergence. In this region, eddy length scales are of O(100–200km) or more: Lutjeharms (1981) reports rings spun off from the Agulhas Current are of average 324km with most features found in the 100-200km scale. SAfE incorporates the domain enclosed by 4.8°S to 54.7°S and 2.5°W to 46.75 5°E (Figure 2.1). Specifically for this configuration, to dampen the effects of the strong western boundary current, a parameterization of horizontal viscosity

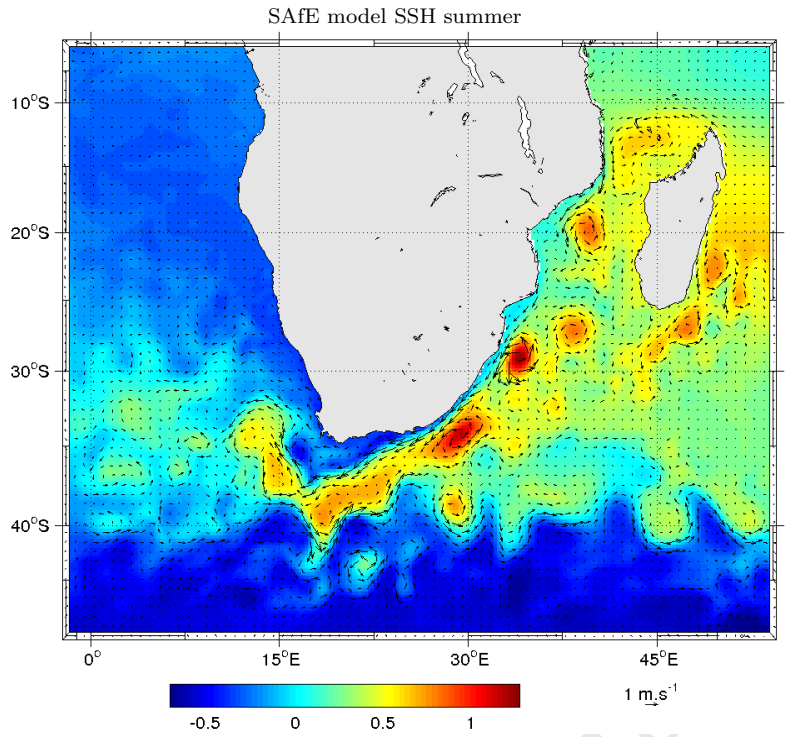

Figure 2.1: Two-day average sea surface elevation and superimposed current vectors for 17 January Year 5 showing the SAfE model domain.

has been added based on the Smagorinsky formulation (Smagorinsky, 1963) as described in Penven et al. (2006c):

$$A_h = 0.025 \times \frac{\delta x \delta y}{2} \times |deformation\,tensor|$$

where A_h is the horizontal turbulent viscosity coefficient and $\delta x, \delta y$ are the lateral grid size.

In this model configuration, the KPP scheme for vertical mixing at the surface and bottom are defined. The KPP scheme of Large et al. (1994) was designed for mixing processes in the ocean interior, the considerations to incorporate a bottom boundary to the KPP scheme in ROMS, as well as for the surface, is discussed in Durski et al. (2004). This is relevant for shallower regions such as the continental shelf. For this study of the Agulhas Bank, model processes in the bottom boundary layer were found to be important, for example in Ekman veering. Bottom boundary layer processes in ROMS can be specified as a drag-coefficient expression (either linear or quadratic) or wave-current sub-models which incorporate bottom bed roughness (Haidvogel et al., 2008). In SAfE, the former method is used: bottom stress for the model configuration is applied as a quadratic function of bottom velocity, the nondimensional drag coefficient is assigned ranging from minimum 0.0025 to 0.02. The simpler method is used as this study uses monthly climatological forcing and is not concerned with

small-scale processes as in sediment transport in which the sub-model is used.

The SAfE configuration was created using ROMSTOOLS which is a toolbox of Matlab programmes and global datasets which assist and make available the data needed in putting together the model configuration and its necessary forcing files (Penven et al., 2008). The use of ROMSTOOLS is fully described in the guide by Penven and Tan (2007).

The SAfE model grid was created at 1/4° resolution (approximately 25km) and consists of 32 vertical levels. The 32 vertical levels are s-coordinate with emphasis toward the surface, the stretching parameters are $\theta_s = 6$, $\theta_b = 0$ (Haidvogel and Beckmann, 1999).

The bathymetry (h) for the SAfE configuration is derived from the GEBCO 1-minute grid dataset (The GEBCO Digital Atlas published by the British Oceanographic Data Centre on behalf of IOC and IHO, 2003). To prevent the generation of noise due to under-sampling the new higher resolution topography from GEBCO is coarsened to reach the resolution of the SAfE grid in an iterative smoothing procedure (Penven and Tan, 2007). This new topography is then interpolated onto the SAfE grid. Further smoothing with a hanning filter is done to reduce any noise remaining in the topography. This is done to keep the slope parameter ($r = \frac{\nabla h}{h}$) below a certain threshold ($r = 0.2$). The minimum depth is set at 50m, thus any topography shallower than 50m is reset to 50m. The coastline is represented by land-sea masking.

SAfE is forced at the surface by monthly climatologies derived from the Comprehensive Ocean/Atmosphere Data Set (COADS) (Da Silva et al., 1994). In regions where the values are missing, such as at the coast, objective analysis is used to replace the values. The forcing is interpolated onto the ROMS grid using cubic interpolation method. Ocean-atmosphere heat exchange is driven by a net heat flux (Q_{net}) with contributions from infrared short and long wave radiation, sensible and latent heat (Penven, 2000). Since the surface heat flux is not updated from the model ocean to atmosphere flux, drift can occur in the model fields. Therefore SST feedback in the atmosphere-ocean interface (SST_{model}) is represented in the model by the linearisation of the thermal forcing around climatological SST (SST_{clim}), using $\frac{\delta Q}{\delta SST_{clim}}$ (Penven, 2000; Barnier et al., 1995). Total heat flux applied to the surface is thus:

$$Q_{Total} = Q_{net} + \frac{\delta Q}{\delta SST_{clim}}(SST_{model} - SST_{clim})$$

The $\frac{\delta Q}{\delta SST_{clim}}$ term may induce a weak nudging which could dampen small scale processes. The cool ridge is a subsurface feature, combined with the low resolution of COADS, the

cool ridge will not be resolved by the $\frac{\delta Q}{\delta SST_{clim}}$ term. Thus, the term can not induce a spurious forcing of the cool ridge. Freshwater flux, based on salt fluxes from evaporation and precipitation, is corrected similarly.

The model is initialised with data from World Ocean Atlas 2001 (WOA2001) (Conkright et al., 2002). The model is initialised using temperature and salinity for January and is started from rest. At the four open boundaries of SAfE, mean-monthly climatological values are derived from WOA2001. To provide information for velocities at the lateral open boundaries, geostrophic and Ekman velocity components are derived from COADS winds and WOA2001. The level of no motion for the geostrophic calculation of the velocities for the open boundaries of SAfE is set at 1000m.

Sponge and nudging layers at the open boundaries are assigned to coarsen the model solution to correspond with the large scale incoming signal (Penven and Tan, 2007) Within the SAfE domain, away from the open boundaries, there is zero horizontal viscosity. However, within the sponge layer there is assigned lateral viscosity: within a specified width of 200km at each of the lateral boundaries, viscosity increases from 0 to 1000 m^2s^{-1} in a half cosine curve from the inner-edge of the sponge layer to the boundary, respectively (Penven et al., 2006b). A sponge layer at the lateral boundary of the parent model allows for enhanced diffusivity at the lateral boundaries ensuring there is no discontinuities introduced at the boundary. Nudging occurs in the same layers. The model solution is nudged toward the WOA climatological data when information passes into the model domain through the open boundaries (Penven et al., 2006b).

2.2 Reference Experiment: The Climatology of the Agulhas Bank

Features on the Agulhas Bank include coastal upwelling on the EAB, which is sporadic and localised, uplift of the thermocline occurs in "a coastal band a few tens of kilometers wide" (Schumann et al., 1982, pg. 238) while the CR appears to be a larger feature which can extend over 100km offshore (Swart and Largier, 1987, see Figure 1.9a). In order to investigate the continental shelf region, a model resolution that resolves the features of the AB is required. This has been achieved using a one-way embedded ROMS model placed within the coarser grid configuration, SAfE. The setup of SAfE at 1/4° was described above. The child grid, refines the model solution by a factor of three, thus resolving the Agulhas Bank at 1/12° resolution. One-way embedding or nesting involves using a coarser resolution

model to provide the lateral boundary conditions for a finer resolution model as a form of local refinement. However, in one-way nesting the parent solution is not updated with results from the child as is the case of two-way nesting. Embedding is a method that allows for the refinement of the model resolution at reduced computational cost (Blayo and Debreu, 1999). The nesting technique in ROMS (Penven et al., 2006b) uses the package AGRIF (Adaptive Grid Refinement in FORTRAN) for mesh refinement (Blayo and Debreu, 1999). AGRIF is a FORTRAN 90 programme that applies the adaptive mesh refinement technique by Berger and Oliger (1984) for use in ocean models. AGRIF runs as a library, independent of the type of ocean model. In a simple test case, AGRIF was shown to better improve the local model solution as compared to other nesting methods (Blayo and Debreu, 1999). ROMS nesting using AGRIF has been successfully tested for the Californian upwelling system (Penven et al., 2006b). In this study, there were three open boundaries to the greater California upwelling system, few discontinuities were found at the parent-child boundary. A smooth transition between the parent and child were observed and the interpolation technique by AGRIF was confirmed to be able to conserve properties from the parent to child (Penven et al., 2006b).

Time stepping in the ROMS child model is done within the duration of the parent time step. It is handled using a recursive integration procedure (Penven et al., 2006b). To maintain the CFL criteria, the time step in the child model has to be decreased, such as in the refinement of the grid spacing between parent and child. For this experiment, the refinement of the grid spacing from parent to child is by a factor of three, i.e. the coefficient of refinement, ($r_{coef} = 3$). For each parent time step, the child time step will be advanced by the parent time step divided by r_{coef} (3), thus for each parent time step in this model the child will be advanced through 3 time steps to reach the parent time step. The parent-child coupling occurs at the baroclinic level in this experiment, i.e. for each baroclinic parent time step, the boundary conditions are interpolated in space and time to get the boundary conditions for the child grid (Penven et al., 2006b). For each parent time step, baroclinic prognostic variables (temperature, salinity, u, v) are bilinearly interpolated along each sigma level and linearly interpolated for each child time step. To preserve properties, the topographies of both parent and child sigma levels must be matched at the parent-child boundary.

The child has 4 open boundaries which are forced by the parent solution. To conserve mass and energy through the open boundaries, open boundary conditions for the child model are as described by Penven et al. (2006b). Dirichlet (i.e. fixed) boundary conditions are

used for the child baroclinic variables. Barotropic radiation conditions at the parent-child boundaries are by Flather radiation conditions (Flather, 1976).

There is a sponge layer between the parent and child model allowing for a smooth transition at the boundary. As in the parent model, the child model domain has zero horizontal viscosity. Within the sponge layer viscosity increases from 0 to $100\text{m}^2\text{s}^{-1}$ in a half cosine curve over a width of 50km.

2.2.1 Model Setup: Nesting Procedure

Preparation of the child grid and interpolation of the child model forcing, boundary and initial conditions were performed using the Matlab nesting tool which is a graphical interface incorporated into the ROMSTOOLS Package (Penven and Tan, 2007; Penven et al., 2008). Forcing, boundary and initial files are interpolated from the parent files. On the other hand, to obtain finer resolution of the bathymetry, the child grid interpolates from the original GEBCO dataset instead of from the coarser parent topography.

The embedded child model was chosen to cover an extensive region off southern Africa, incorporating the AB and the Southern Benguela Upwelling system. The child domain was defined to range from 27.7 to 39°S and 11.5 to 27.4°E (Figure 2.2) and comprises of 190 x 160 grid points. To ensure the consistent behaviour of the model solution close to the child boundaries, the corners of the child model were chosen away from strong circulation parallel to the lateral boundaries, steep topography and directional changes in the coastline. The child solution refines the parent solution by a factor of three thus yielding a resolution of 1/12° (approximately 8km). As in SAfE, the child has 32 vertical layers.

The child model obtains its topography from the GEBCO dataset. The process of interpolation and smoothing is similar to that of obtaining the parent grid topography, r-factor is 0.2. The minimum depth at the coast is set at 10m. Since the parent model is smoothed more than the child, the topographies of the two models differ and thus a smooth connection between the two are needed to allow for a smooth transition of features at the parent-child boundary. The following formula is applied to connect the child to the parent topography:

$$h^{child} = \alpha h^{parent} + (1 - \alpha) h^{fine}$$

where h^{child} is the bottom topography of the child grid; h^{parent} is the bottom topography of the parent grid; h^{fine} the high-resolution bathymetry; and α is a parameter which ranges

from zero to one within a given number of grid points ("nband") at the lateral parent-child boundary (Figure 2.3). At this parent-child boundary it is necessary to maintain the volume as well as to assist in the smooth transition of features from parent to child. In this experiment, the width of the connection band is set at to 25 grid points. For the (2 first) points closest to the child boundary, the child grid is forced to have the same vertical section and volume as the parent grid (Penven et al., 2006b). Thus, a consistent vertical section for this boundary region means volume is conserved between the parent and child (Penven et al., 2006b).

The surface forcing of the child grid is derived from the parent forcing (Penven and Tan, 2007). The parent forcing file created when the parent, SAfE, was configured (using data from the COADS dataset), is interpolated onto the created child grid. The CR has been observed in monthly satellite climatologies and persisting over several months (Demarcq et al., 2003). Thus, high frequency wind forcing should not be essential to reproduce this process. A temporally coarser product, such as monthly wind forcing, was used for this configuration. The following figure (Figure 2.4) displays selected wind stress vectors in the child forcing files. It shows mean winds in October (Figure 2.4d) and January (Figure 2.4a)

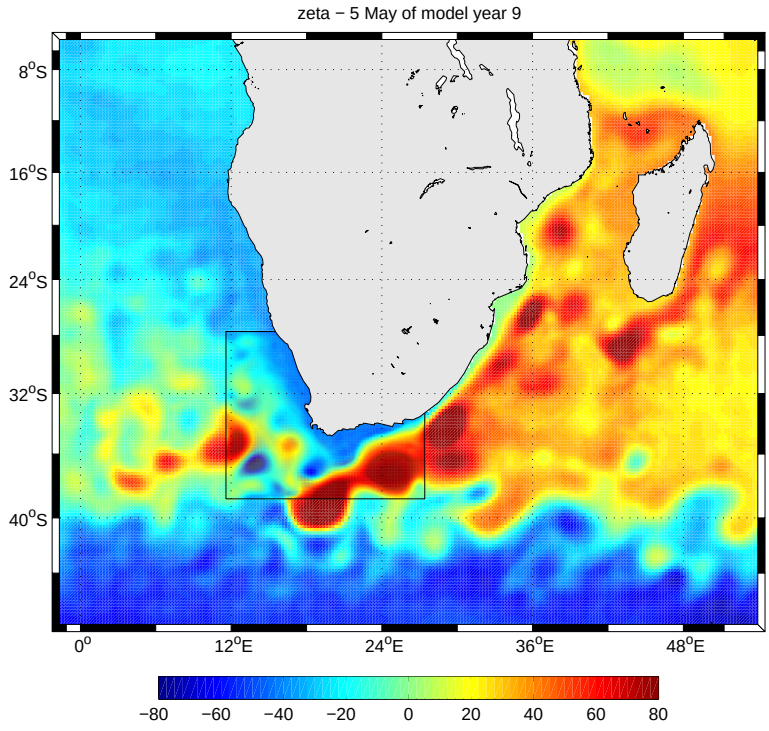

Figure 2.2: Two-day average sea surface height for 5 May Year 9 for SAfE with the embedded child domain for the Reference Experiment.

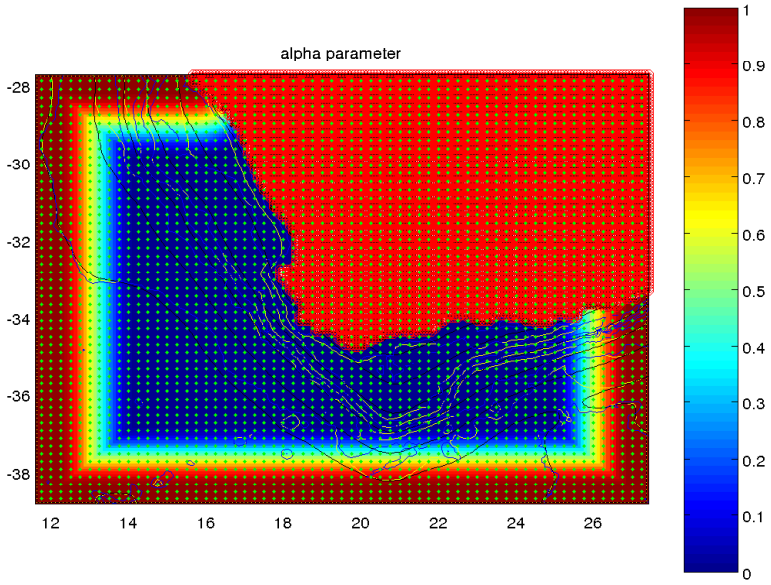

Figure 2.3: The outer coloured bands represents the width of "nband". The blue line is the new topography, the black line is the parent topography and the yellow line is the interpolated child topography. Within the band, the parent and child topography are connected and the isobaths overlap.

are southerly over much of the AB particularly close to the coast, varying to southwesterly further south of the shown domain. Mean winds in April (Figure 2.4b) show the strengthening and rotating of winds over the AB to become strong westerly winds as seen in July (Figure 2.4b). December-January and June-July mean wind direction shown by Shannon and Nelson (1996) in Figure 1.4 show similar direction. Consideration was given to the spatial coarseness of the wind data. The source of the wind data, COADS (Da Silva et al., 1994), can be poorly resolved at the coast and biased to the open ocean. Alternative products show this problem is not unique to the COADS wind product. Blanke et al. (2005) showed that QuikScat winds also showed problems at the coast: the wind stress curl close to the coast is not completely resolved and nearshore processes are not measured. In the child model, COADS winds were able to produce reasonable seasonal upwelling on the WAB and off the Cape Peninsula. For the EAB, wind direction fluctuates with a period of 2 to 6 days (Schumann, 1999) thus monthly-averaging of winds on the coastal EAB are expected not to produce a dominant direction, such as produced in Figure 2.4(a), nor strong upwelling at the surface. Cold coastal waters on the EAB is not observed in satellite monthly climatology (Demarcq et al., 2003). It is possible that with constant equatorward monthly-mean winds in comparison with fluctuating winds on the WAB and Cape Peninsula, seasonal coastal upwelling in this region may be overestimated in the model. Subject to the monthly forcing, the child model

was able to reproduce the CR and reasonable coastal upwelling west of Cape Agulhas. For this thesis, the questions, based on a seasonal analysis, could be addressed by the spatial and temporal resolution used in this model and the winds were not further refined. For analysis on a shorter scale, better horizontal resolution of winds close to the coast, to include effects such as topographic steering around headlands on the EAB, as well as temporally finer resolution is required.

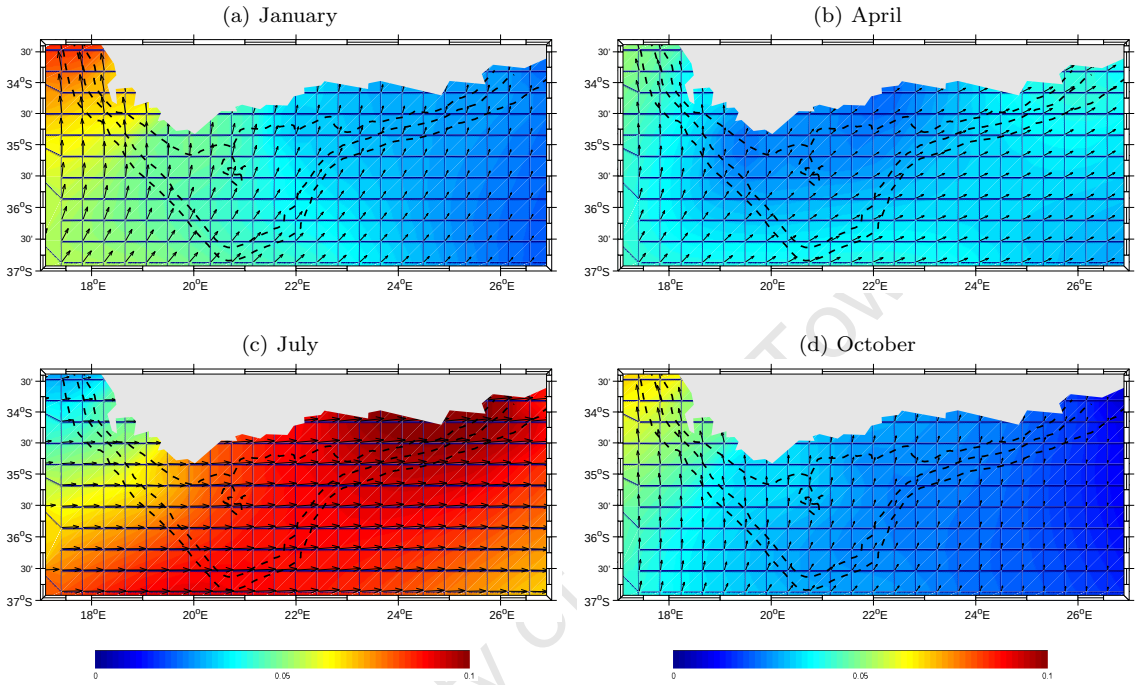

Figure 2.4: Child model wind forcing: wind stress magnitude ($N.m^{-2}$) and wind stress vectors over the Agulhas Bank.

Initial conditions of the child model are interpolated from the parent initial conditions. As the parent and child topographies differ, child initial conditions must be vertically re-interpolated.

The model was run for a total of ten years, spin up of the model to reach statistical equilibrium took approximately two years. Surface-averaged temperature and salinity were stable and no drift in the model solution was apparent. Years 3 to 10 were used for the analysis.

2.3 No Agulhas Experiment: The Adjusted Agulhas Bank

To test the sensitivity of the AB to the influence of the AC, the AC was removed close to the AB. This was done by placing an obstruction in the topography, in the form of a dam, upstream of the AB, thus causing the AC to move away from the shelf-edge and thus not affect the AB (Figure 2.5). This is dynamically possible as the retroflection of the AC is characteristic of the current, early and late retroflections of the AC are observed in nature (Rouault and Lutjeharms, 2003). Thus, the model simply forces a very early retroflection of the AC. This method maintains the stability of the parent model, SAfE as conditions at the boundary remain the same, only the dynamics within the model change.

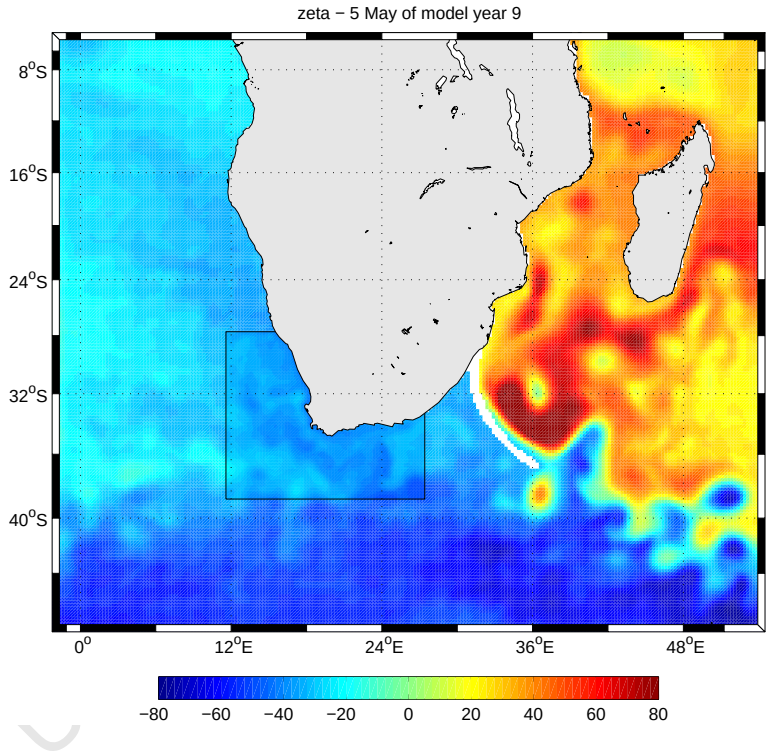

Figure 2.5: Two-day average sea surface height for 5 May Year 9 for SAfE with the embedded child domain for the No Agulhas Current Experiment. The white band extending off the east coast of South Africa is the dam which causes the early retroflection of the AC away from the AB.

However, adjusting such a large scale feature may possibly have dynamical consequences to the region. The AC transports substantial amounts of heat and salt around the southern tip of Africa into the Atlantic Ocean (Bryden and Beal, 2001). By placing the dam upstream and removing the AC, the region may lose the influx of the water masses brought to this region by the AC, such as Subtropical Surface Water and central and deeper waters. It is expected that the surrounding waters in the region of the AB still maintain the signature of

the adjacent ocean water masses such as Indian and Atlantic Ocean Central Waters. In this experiment, the effect of the AC removal on the processes on the AB is more important than the change in water mass distribution. Although, when analysing the structure on the AB, the change in water masses from the removal of the AC must be considered.

The dam as an extension of the coastline may experience "coastal" upwelling and wind-driven currents parallel to the dam. However, when compared to the fluxes of the AC, which normally dominate this region, the effect of these processes on this region is minimal. The position of the child model away from the dam could also possibly minimise the effect of any spurious features arising from the dam on the AB.

Surface-averaged kinetic energy as well as salinity and temperature show the parent model to reach equilibrium within 2 years. However, the AC does not fully form a stable stream and mesoscale eddies from further upstream may remain in the vicinity of the dam for longer than expected. This effect on the kinetic energy could possibly be moderated by the lack of eddies that are usually created by the interaction with the AC. However, increased temperature and salinity may be present in the model while these eddies are in the region.

2.3.1 Model Setup

For this experiment, SAfE is set up as indicated in the previous experiment, with the exception of the inclusion of the dam. After the SAfE grid file has been created, the dam is inserted into the topography. The dam is created using three points to indicate the start, mid and end points of the feature. A curve is fitted to these three points to make up the length of the dam. In this experiment, the dam connects to the coastline in the region of Durban at 30°S and 30°E and extends to around 37°S, 36°E covering a length of over 1000 km. These points are then interpolated onto the ROMS grid by masking the grid points of the dam. Masking or the creation of a mask, consists of assigning points on the grid either a value of 1 or 0, 1 for grid points overlying the sea and 0 for land points. The grid points corresponding to the position of the dam are assigned land values of 0 for the all the grid points: u, v, psi and rho points in the SAfE grid file. Interpolation of initial and forcing conditions are performed on the new grid as described for the Reference Experiment. Initial conditions are calculated using data which includes the Agulhas Current in its mean position, i.e. the effect of the dam is not included in the calculation. However, after suitable spin up the model solution adjusts to the presence of the dam. Furthermore, the placement of the

dam away from the boundary negates any complications that may arise in the calculation of initial and boundary conditions.

The embedding procedure for the AB is done as described for the previous experiment. The size of the child model remains the same as well as the surface fluxes. However, the lateral boundary conditions of the child will differ from the Climatology Experiment due to the dam in the parent model.

2.4 Datasets

AVISO MSLA

AVISO MSLA (Maps of Sea Level Anomalies) data is used to calculate eddy kinetic energy (EKE) to compare with EKE from the SAfE. The data used are objectively analysed 1/3° gridded maps derived from satellites such as TOPEX/Poseidon, ERS-1/2 and Jason (Ducet et al., 2000). Geostrophic current components can then be derived to calculate EKE.

WOA2005 Annual Temperature Climatology

WOA2005 temperature data (Conkright et al., 2002) is used for comparison to the large-scale baroclinic structure of the parent model. The annual climatology consists of objectively analysed data on a horizontal 1° grid with 33 vertical levels covering depths up to 5500m with more coverage in the upper 250m.

2.5 Visualisation and Analysis

Visualisation of the model results were performed with ROMSTOOLS, the visualisation tool by Penven and Tan (2007). The data presented is a subset of this domain for the AB up to approximately the 500m isobath (33.3 to 37.5 °S and 17 to 27°E).

Horizontal Structure

To represent the horizontal structure of the AB, the following depth levels were chosen: 10m, 50m and the model sigma level 1 (z1). 10m was the preferred level to the surface as it represents the surface mixed layer whilst excluding additional complications from the surface. 50m, which is generally below the thermocline, provides structure at mid-depth over the AB. The model's lowest terrain-following level, z1 is considered to represent the bottom boundary layer (bbl), the model bbl (as given by the model output parameter "hbbl" - the averaged depth of bbl), ranges in thickness from approximately 2.5 to 30m varying seasonally and may

be deeper where the AC impinges onto the shelf due to bottom friction. In winter when the thermocline may be deeper than 50m, the bottom waters are captured by the z1.

Horizontal sections were plotted for the following variables at the above depths: temperature, salinity and current vectors superimposed on current speed. Current vectors for every three points were plotted for the region, the current vectors for the AC were removed as they dwarfed the slow flow on the AB, being a magnitude of 7–8 times greater. Current speeds in excess of 0.8m.s^{-1} were removed, the points represent grid point flow which the currents were removed. The current vectors are plotted over the current speed which is calculated from the zonal and meridional current components.

Vertical Structure

Figure 2.6 shows the vertical sections chosen to represent the vertical structure for the WAB, CAB and EAB. The vertical section on the WAB was chosen as it shows the AC filament offshore as well as coastal upwelling. The section chosen for the CAB at 21°E was chosen to sample the AC on the shelf edge, the Mid-AB region and the coastal region as well as the cold bottom water observed moving westward in that region (Figure 4.4a–b). The section on the EAB was chosen to capture the AC on the shelf-edge and the cool water tongue in the vertical. Temperature and salinity are similar over the AB, therefore temperature was chosen to represent the vertical structure for the vertical sections.

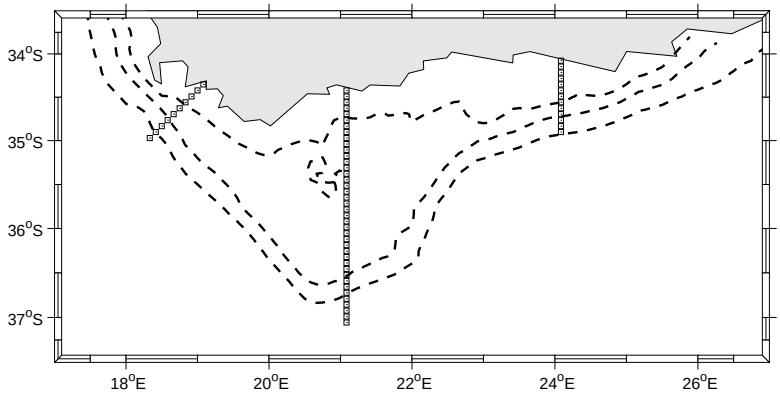

Figure 2.6: Position of vertical sections for WAB (19°E), CAB (21°E) and EAB (24°E).

Thermocline depth

The thermocline was calculated as the depth of the maximum vertical temperature gradient at each grid point. Due to the noisiness of the result, the thermocline depth map was smoothed horizontally using a Gaussian filter.

Temperature Difference

For comparison between the the Reference Experiment (ref) and the No Agulhas Experiment (noagulhas), the seasonal mean temperature difference at 10m, 50m and for z1 was calculated. The seasonal mean temperature for a specific depth for the No Agulhas Experiment is subtracted from the seasonal mean temperature at the same depth for the Reference Experiment:

$$T_{diff} = T_{ref} - T_{noagulhas}$$

The colour scale was chosen to such that the red colours indicate that the Reference Experiment is warmer than the No Agulhas Experiment, while the blue scale indicates that the Reference Experiment is cooler.

Advective contributions to temperature variations

This analysis investigates the influence of the Agulhas Current and the forcing of waters that contribute to the cool ridge by studying the horizontal and vertical temperature advection terms for mean and eddy (deviation from the mean). The advection terms are obtained from the division of the terms of the heat flux momentum equation into their respective components.

Consider the temperature terms from heat budget equation:

$$T_t + uT_x + vT_y + wT_z = D + F$$

where T is the temperature, u, v, w are the velocity components and T_x, T_y, T_z are partial derivatives. The LHS of the equation represents the time derivative and advection of temperature. The RHS of the equation represents the driving forces (D) as well as the other forcing terms which contribute to the heat budget (F), such as mixing.

The terms are used at depths where the total heat budget is balanced by the horizontal and vertical advection for example, where influences such as wind mixing are stirring are negligible. Therefore using only the LHS of the equation, the average total advection is:

$$\overline{adv} = \overline{uT_x + vT_y + wT_z} = \overline{uT_x} + \overline{vT_y} + \overline{wT_z}$$

If the instantaneous quantity is decomposed into mean and deviation, for example, $u = \overline{u} + u'$ (where $\overline{u'} = 0$), $T = \overline{T} + T'$ (where $\overline{T'} = 0$) etc., the individual advection term for x becomes:

$$\overline{uT_x} = \overline{(\overline{u} + u')(\overline{T} + T')_x}$$

$$\overline{uT_x} = \overline{\overline{u}\overline{T_x} + \overline{u}T'_x + u'\overline{T_x} + u'T'_x}$$

The mean of the time varying fluctuations are zero, $\overline{u'} = 0$ and $\overline{T'} = 0$, thus:

$$\overline{uT_x} = \overline{u}\overline{T_x} + \overline{u}\underbrace{\overline{T'_x}}_{0} + \underbrace{\overline{u'}}_{0}\overline{T_x} + \overline{u'T'_x}$$

$$\overline{uT_x} = \overline{u}\overline{T_x} + \overline{u'T'_x}$$

In summary, total advection in the x direction is the sum of mean and eddy contributions:

$$\textit{Total advection} = \textit{mean} + \textit{eddies}$$

Similarly, for the y and z components:

$$\overline{vT_y} = \overline{v}\overline{T_y} + \overline{v'T'_y} \text{ and } \overline{wT_z} = \overline{w}\overline{T_z} + \overline{w'T'_z}$$

These terms represent the x and y horizontal and vertical heat advection terms.

The total advection is the sum of these terms:

$$\overline{uT_x + vT_y + wT_z} = \overline{u}\overline{T_x} + \overline{u'T'_x} + \overline{v}\overline{T_y} + \overline{v'T'_y} + \overline{w}\overline{T_z} + \overline{w'T'_z}$$

Total mean advection term (LHS) and the mean advection term can be obtained from the model results. The deviation (u', T') is computed by subtracting the mean $(\overline{u}, \overline{T})$ from the model output.

Horizontal maps at 50m and 100m of these components for the Reference Experiment are displayed in Chapter 6. Due to the influx of waters by the AC, cooling and heating by advection below 50m is more marked on the EAB than on the WAB and west coast. Therefore results are displayed for the EAB only. At depths of 50m and below, the difference between summer and winter advection terms is small. Therefore the annual-mean terms will be used to investigate the contributing processes. The following terms are plotted: the mean horizontal temperature advection $(\overline{u}\overline{T_x} + \overline{v}\overline{T_y})$, the mean vertical temperature advection $(\overline{w}\overline{T_z}$), and the mean horizontal eddy temperature advection $(\overline{u'T'_x} + \overline{v'T'_y})$. The mean vertical eddy temperature advection term $(\overline{w'T'_z})$ is small in comparison with the other terms and has not been included in this study.

Chapter 3

South African Experiment (SAfE): the large-scale environment

The Agulhas Bank (AB) is positioned between two dynamic regimes: with the Agulhas Current (AC) and its large scale influences upstream and the Benguela Upwelling System downstream. SAfE is a ROMS model configuration designed to incorporate the main features of the southern African oceanic region and thus provides the large-scale dynamics surrounding the AB. Although its resolution is too coarse to resolve the finer detail of the shelf, SAfE is used to supply the boundary conditions for a finer-resolution child model embedded within the SAfE domain.

The dynamics of a western boundary current, such as the AC, being highly non-linear and interacting with topography poses challenges specifically in terms of kinetic energy. EKE in the Agulhas Retroflection Region exceed those found elsewhere in the world's oceans such as the Gulf Stream (Richardson, 2007). In order for the features on the AB to be resolved, an accurate representation of the large-scale oceanic features surrounding the AB is required.

This thesis aims to describe the dynamics on the AB using a higher-resolution ROMS model embedded in SAfE. In order for the dynamics on the AB to be reproduced, its forcing must be representative of the observed oceanic forcing. As with other ROMS studies, the EKE, transport and seasonal signal are important for comparison with observations.

This section presents the output of the model, particularly the horizontal large-scale features in order to describe the larger oceanic region and the SAfE model configuration. The following images, provide a view of typical output of SAfE.

3.1 SAfE: General Description

Figure 3.1, displays a 2-day average of sea surface height (SSH) with overlaid current vectors and temperature at 10m, representative of summer conditions. It shows the Indian Ocean with its warmer waters and positive SSH and the cold denser Atlantic Ocean with negative SSH. To the south, the cold waters of the Southern Ocean interact with the warmer waters. The Mozambique Channel and east of Madagascar are turbulent regions, rich in eddies both cyclonic and anticyclonic as indicated in SSH.

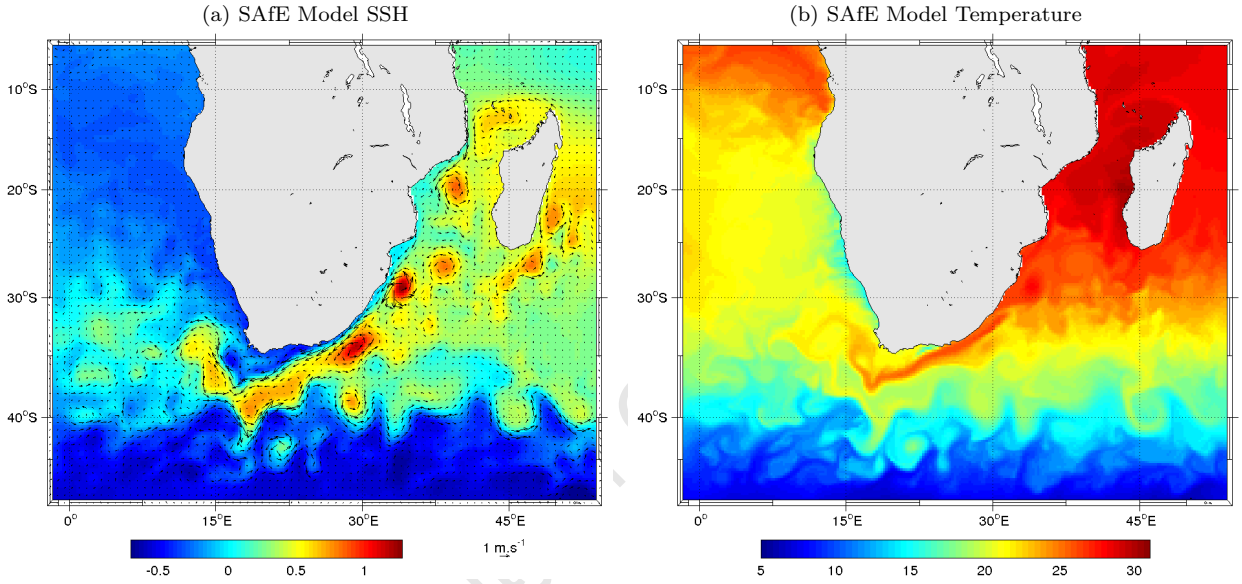

Figure 3.1: "Snapshots" of (a) model sea surface height (cm), (b) model temperature (°C).

The two disparate regimes of the AC and Benguela are apparent on either side of southern Africa. The AC with a core of approximately 26°C flows adjacent to the southeast continental shelf (Figure 3.1b). SSH shows the AC and retroflection region, with Agulhas rings being spun off into the Atlantic (Figure 3.1a). Associated with these rings, warm AC water moves into the southern Benguela as an AC filament. To the east of the AB an anticyclonic feature is present, either from recirculation or early retroflection. West of the AB, a cyclonic lee eddy is observable. The AB at 10m is, in general, warm with a cold tongue (13–16°C) located inshore of the AC.

Upwelling of cold waters (12–14°C) are found along the whole west coast, there is some interaction between the cold upwelling filaments and warm water offshore, consistent with the Benguela Upwelling System in summer.

Evolution of Kinetic Energy

The average kinetic energy of the model increases from zero at the start of the model (Figure 3.2). Within 2 years, the average kinetic energy reached equilibrium. This suggests that the model is stable, results are thus calculated for years 3 to 10, post spin-up.

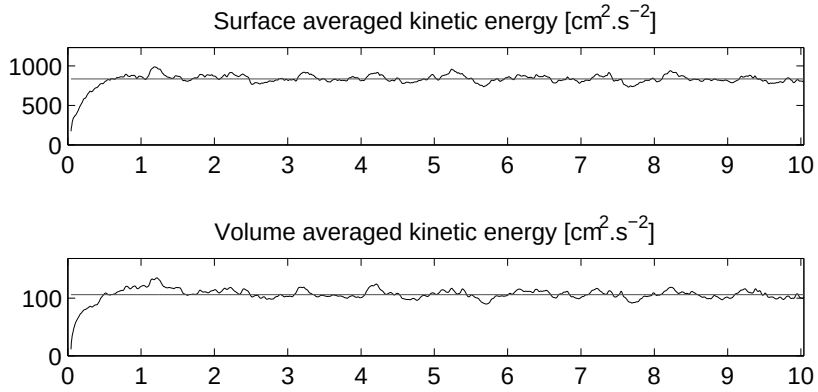

Figure 3.2: Averaged kinetic energy for the (a) surface and (b) volume for model duration.

After equilibrium was reached, intra-annual variations are observed in the averaged kinetic energy (clearer in the surface-averaged plot). There is a small peak in average kinetic energy at the beginning of the year and a minimum in the last half of the year. This suggests seasonality. As the AC is a large source of kinetic energy this could provide a source of the seasonality in the region.

Annual Eddy Kinetic Energy

The model eddy kinetic energy (EKE), shown in Figure 3.3, displays the highest EKE in the region of the Agulhas Retroflection Region (ARR). Although the ARR dominates the SAfE domain, other regions of variability are found: the Mozambique Channel, east of Madagascar and the path along which the eddies move east of the continent. The AC close to the coast does not display much variability as the AC is mostly stable where the shelf is narrow.

The model EKE, as a whole, reproduces the regions of high variability as displayed by the AVISO altimeter data. The model places the highest EKE in the ARR and although comparable in magnitude to the AVISO-derived EKE, the model EKE distribution surrounding the ARR is more extensive and extends further into the Atlantic.

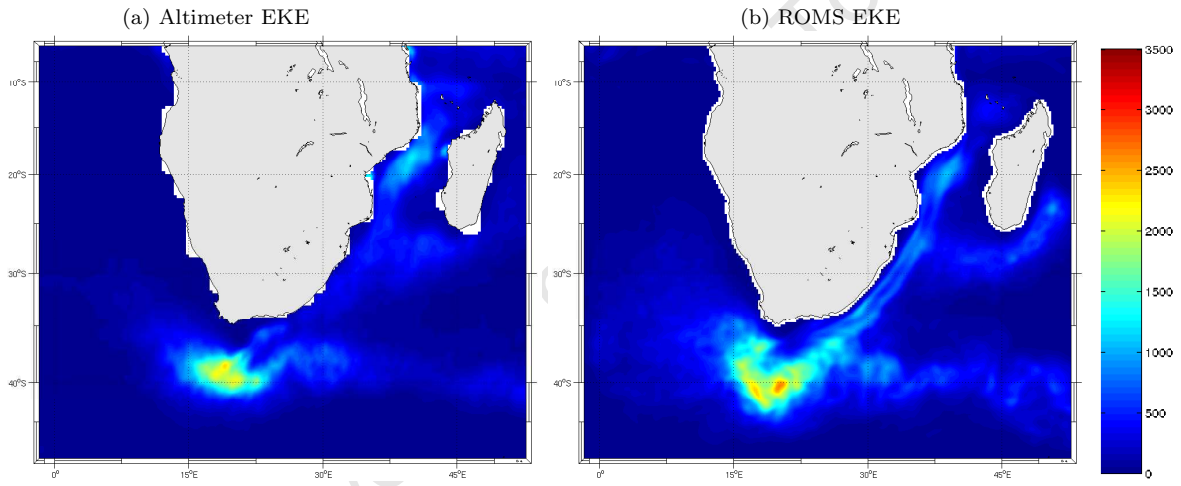

Figure 3.3: Annual mean surface eddy kinetic energy (cm^2s^{-2}) for (a) AVISO altimeter data (b) ROMS SAfE configuration.

Annual Transport

The AC produced by SAfE displays an annual-mean transport of approximately 50–60Sv relative to 1500m (Figure 3.4), when it is fully constituted off the EAB. It derives contributions of approximately 15Sv from the Mozambique Channel and 30Sv in the region south of Madagascar. In addition, substantial recirculation is found in the region, for example, centered at 30°E, which contributes around 20Sv to the AC. Approximately 70Sv are found in the ARR and 50Sv reaches the Agulhas Return Current at 23°E.

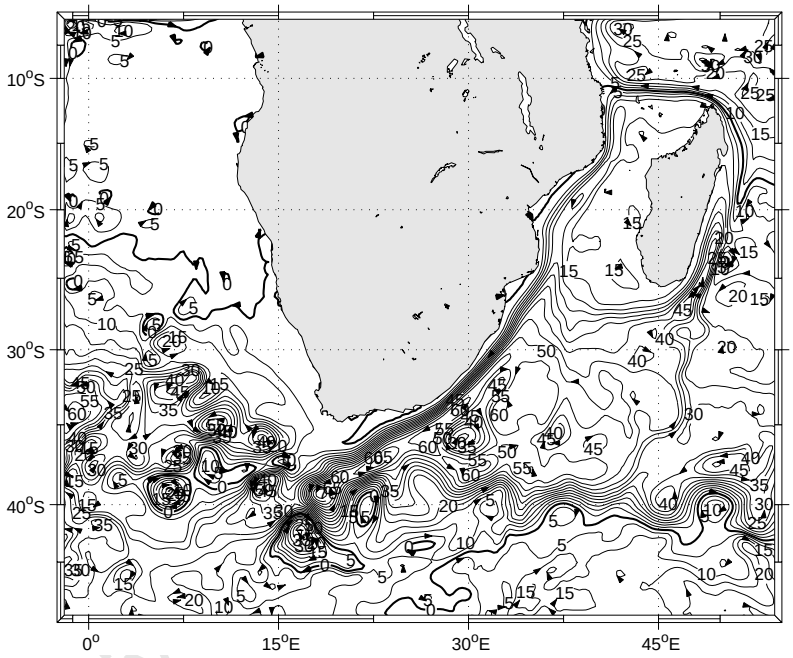

Figure 3.4: Annual mean model transport streamfunction relative to 1500m (Sv). Contour interval is 5Sv.

Annual Vertical Section

Figure 3.5 shows vertical zonal sections off 31.5°S of annual-mean temperature for the model, SAfE (Figure 3.5a) and WOA2005 (Figure 3.5b) data. The sections extend from the coast up to 47°E, which is approximately the eastern boundary of the SAfE domain. This latitude was chosen as it represents where the AC is stable and fully formed. In addition, around this latitude, literature is available, detailing sections performed crossing the AC (Biastoch et al., 1999). Figure 3.5 shows that the upper 1500m is warm and stratified. In both the model and WOA2005 sections, the upper ocean temperature structure is comparable, although WOA2005 does not resolve the shelf and slope nor the bottom topography in detail.

(a) SAfE Temperature (b) WOA2005 Temperature

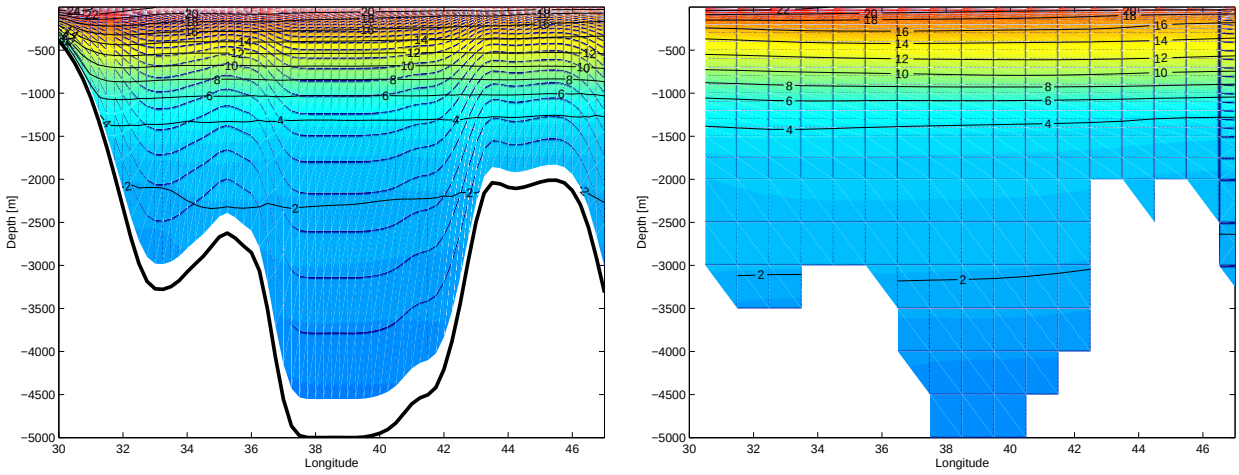

Figure 3.5: Annual mean temperature (°C) vertical zonal section at 31.5°S for (a) the model SAfE and (b) the World Ocean Atlas 2005 (WOA2005) dataset.

WOA2005 data show the isotherms to be flat and do not reflect the presence of the AC on the slope. This is possibly due to the coarseness of the data resolution, requiring interpolation where data is missing. The surface temperatures in both transects are 20–22°C. The 12°C isotherm is located between 500 and 600m and 4°C at about 1400m for both.

The transects differ at the bottom of the water column, initially apparent is the difference in the depth of the bottom bathymetry. The SAfE bathymetry shows a continental slope deepening to 3500m at 33°E. There are two ridges apparent in both sections, roughly centered at 35 and 45°E. The ridges in the bathymetry are coarsely resolved in the WOA2005 section. The ridge centered at 35°E is shallower by approximately 500m in the model compared to WOA2005. This could possibly contribute to the 2°C water being present at shallower depths (700m shallower) in the model than the WOA2005 data. The vertical resolution of the model must also be considered, due to its effect on the structure of the bottom of the water column. At water depths of greater than 2000m, the vertical resolution of the model grid is greater than 200m and increase in size with water column depth to approximately 750m in water depths of 5000m.

3.2 The Southern Agulhas Current Region

Figure 3.6 shows a summer-winter comparison of the southern Agulhas region for the SAfE domain. Presented are SSH, which indicates the general geostrophic flow patterns, SST and surface salinity in the region. At the surface, typical seasonal differences are observed with

the surface being warmer and saltier in summer than winter.

In summer, the SSH contours (Figure 3.6a) show the general flow in the region. The 200 and 500m isobaths are indicated in the figures and show that the topography of the SAfE grid is relatively coarse. It shows the the AC moving along the EAB and past the tip of the AB. The AC core in summer has a mean temperature of 25–26°C (Figure 3.6b) and salinity of 35.3–35.6psu (Figure 3.6c). At approximately 18°E, the AC retroflects and moves eastwards as the Agulhas Return Current. At approximately 25°E the flow moves northwards around the Agulhas Plateau. In summer, relatively higher SSH, as compared to the surrounding region, occurs in a band extending northwestwards from the retroflection region into the Atlantic Ocean. This band is in summer is associated with a large contribution of warm saline waters into the South Atlantic from the Indian Ocean of 20–21°C and 35.3–35.6psu. This region is associated with the passage of eddies and rings spun off from the AC. In winter, SSH contours on the EAB slope are similar to the levels in summer. However, further off the shelf, winter-mean SSH associated with the AC and Agulhas Return Current, is higher than summer. Three cores of SSH are distinguishable in winter that were not observed in summer, these are centered at approximately 18, 22.5 and 27°E. This could possibly suggest changes in the flow regime between summer and winter, with winter showing more recirculation. However, these features might be due to the averaging of mesoscale features and recirculations which are regular occurrences in the flow of the AC.

On the shelf, summer SSH levels on the AB are similar to winter levels (Figure 3.6a). On the AB, inshore of the AC in summer there is a tongue structure of low SSH possibly indicating denser water and cyclonic motion. On the AB in summer, the temperature is warm at 20°C (Figure 3.6b) and 35.3–35.5psu (Figure 3.6c). In winter, the AB is cooler at 16–18°C in winter and less saline at 35.2–35.4psu.

At this resolution in the SSH maps (Figure 3.6a), features such as upwelling on the EAB and WAB are not well resolved and off the Cape Peninsula the intense upwelling is not clearly distinguishable nor is the Good Hope Jet in spring and summer (Figure 3.6a–c). The southern Benguela region in summer, shows a band of cool, less saline water along the coast of 14–19°C and 35.2–35.35psu (Figure 3.6b–c). This region is associated with the wind-driven coastal upwelling of cool waters. Even with the coarse topography, the SSH, SST and SSS structure suggests that this region is less topographically controlled than the AB and east coast of South Africa.

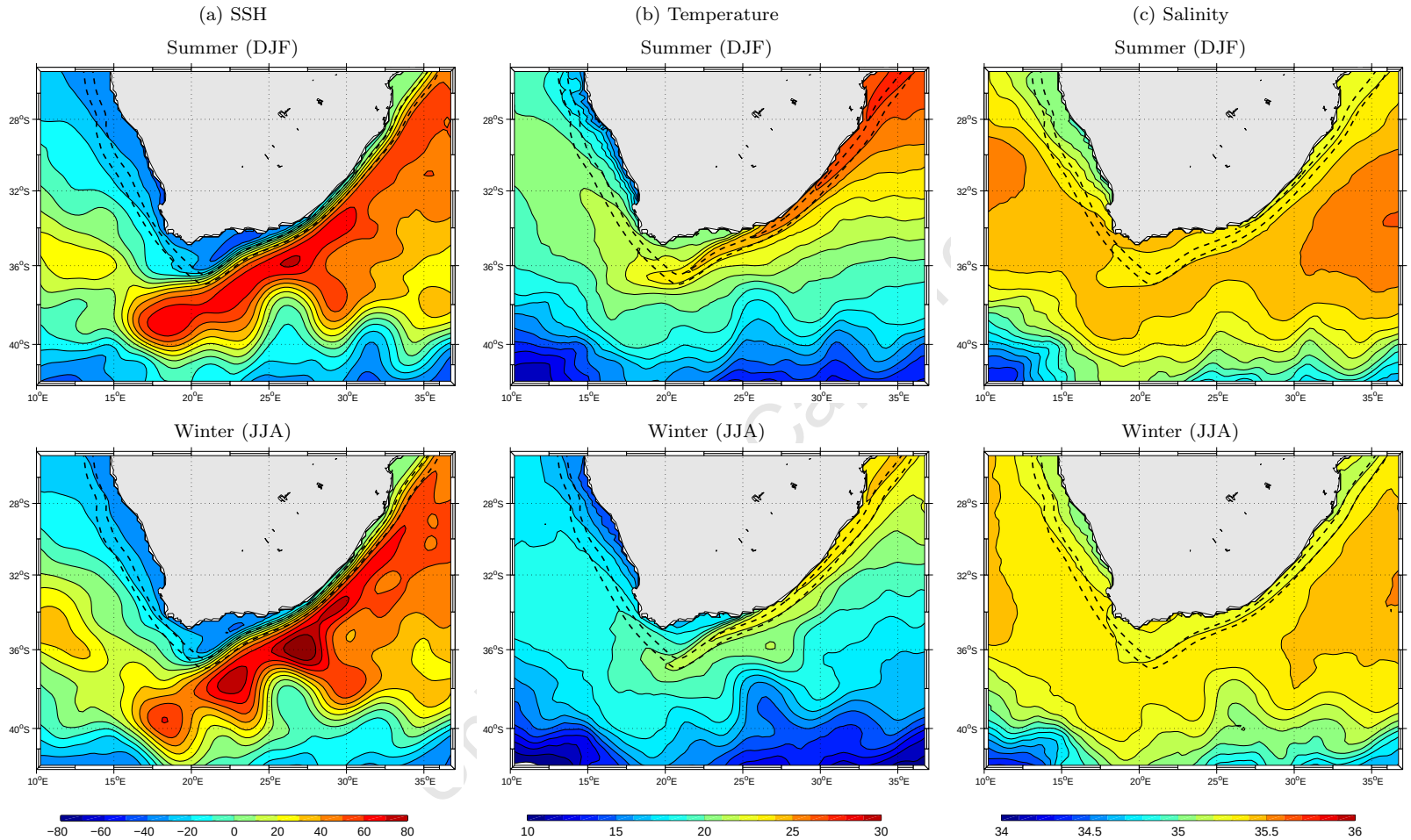

Figure 3.6: Seasonally-averaged summer and winter model (a) sea surface height (cm), (b) sea surface temperature (°C), (c) surface salinity (psu) for the Agulhas Current Region.

3.3 Discussion

The model AC is presented as a warm current subject to mesoscale processes such as eddies and meanders. Filaments and rings produced by the AC in the ARR are also reproduced as well as input into the South Atlantic. Limited seasonal variation is observed in the surface temperature and salinity. From the SSH, it is not clear whether there is seasonality in the flow of the AC due to the large variability and mesoscale structures associated with the AC. Surface mean temperature in summer for the AC lies within the expected range for surface waters although salinity may be slightly lower, expected surface salinity for the AC region exceed 35.5psu (Valentine et al., 1993). Mixing and decreased solar warming contributes to the lower values in winter.

In the vertical the model mean temperature structure is comparable to that of WOA2005 climatology. The upper layer shows annual mean warm temperatures. The depth of the 4°C isotherm, regarded as the permanent thermocline (Beal and Bryden, 1999), in the model compared well to WOA2005 climatology. Beal and Bryden (1999), measured the 4°C isotherm at 1100m off the continental shelf deepening to 1500m offshore, similar depths are obtained by the model.

Annual mean transport of the AC by the model off the Natal Valley is approximately 60Sv. Bryden and Beal (2001) calculated a net transport by the AC of 66.5Sv off 32°S. In situ measurements of the AC depend on the location and time period the measurements are taken as well as the method the calculations are performed. Matano et al. (2002) discuss that diagonal or non-zonal sections may produce larger transport by including the inertial recirculation cell and increased flow occurs with the passage of eddies. A POCM study on Agulhas variability showed a 43Sv transport of the AC at 32°S (Matano et al., 2002).

EKE maps show that the model EKE is in the same order as that calculated using AVISO satellite data, it suggest that the model is not overly turbulent although the distribution of EKE differs. EKE may be higher in the model as the model was calculated based on a resolution finer resolution that that of the AVISO data (1/4° vs 1/3°). On the other hand, large EKE values are found in the the region. Calculations from drifter data show EKE in the ARR exceed 3000cm^2.s^{-2} with a maximum value of EKE at 3650 cm^2.s^{-2} at 39°S 19°E (Richardson, 2007).

The distribution of the annual mean EKE shows a western bias possibly increasing the input of heat and salt into the south Atlantic. This bias could be due to the model Retroflec-

tion favouring a more westward position or due to ring spawning in the model. Position of the Retroflection has been observed to vary, even showing seasonal variations (Matano et al., 1998). It is primarily located between 15 and 20°E (Lutjeharms, 1996) but has been observed further to the west (Walker, 1986) and in an extreme event at 5°E (Lutjeharms, 1996) or early to the east at 25°E (Rouault and Lutjeharms, 2003). Also the AC along the EAB shows more variability than indicated by the AVISO.

The dynamics of a western boundary current, such as the AC as well as the ARR poses challenges. It has the largest kinetic energy signature in the world. A comparison with other models show that these problems are common, biases are found in the westward termination of the Agulhas Retroflection but also the recirculation of water within the southern Indian Ocean (Penven et al., 2006a). ROMS has been shown to perform reasonably well in dealing with these issues than the other models.

The AC appears to be the dominant signal in the region. SAfE, subject to its particular forcing at the boundary and surface, produces a seasonal signal as seen in the SSH map. The actual seasonality or seasonal variation of the AC is contested. Pearce and Grundlingh (1982) found no significant seasonality in the core speed of the AC based on historical accounts, fluctuations that were detected in the strength of the AC were attributed to mesoscale variability.

On the contrary, seasonality of the AC is found in other ocean models. Biastoch et al. (1999) used MOM2 to show a strong seasonality in the source regions of the AC, particularly the Mozambique Channel, thus affecting the AC. At 32°S, the transport was shown to be weakest in January and March whilst strongest in October and November. Matano et al. (2002), found in their POCM simulation transport to be maximum between winter and spring and minimum between summer and autumn.

Matano et al. (1998) studied satellite sea surface height to investigate the seasonality in the ARR. Over a relatively short period (October 1992 to April 1996), a seasonal signal was found which was maximum in summer and minimum in winter. The maximum in summer is associated with high variability, this was postulated that summer conditions favour "an early retroflection or bifurcation of the current at approximately 25°E" (pg. 4363). This theory is described as consistent with observations of decreased inflow into the Benguela in summer by Garzoli and Gordon (1996).

In SAfE, the large recirculation in SSH at 25°S suggests early retroflection could be

present in winter. The model SSH gradient could also suggest stronger flow in winter supporting larger transport, similar to that obtained by the POCM model (Matano et al., 2002). However, due to the variable nature of the AC and high mesoscale variability this interpretation should be treated with caution.

3.4 Summary

This chapter shows that SAfE produces a stable solution after a spin up of 2 years in which averaged kinetic energy for the model run reached equilibrium. SAfE is also able to reproduce a reasonable approximation of the processes governing the southern African oceanic region, specifically the AC. The model AC is found at approximately the right location in the vertical and horizontal mean. The westward bias is not expected to influence the seasonal mean behaviour of the Cool Ridge which is a feature on the EAB and upstream from this region. Seasonality in the AC of the SAfE model is not apparent. At 1/4° resolution, SAfE is unable to represent features of the AB and therefore placing a higher resolution child within SAfE is necessary.

Chapter 4

The climatological structure and circulation of the Agulhas Bank

As described in Chapter 1, the Agulhas Bank (AB) displays a marked seasonality. In summer, the thermocline is shallow and the shelf waters are highly stratified. The water column is warmed by solar insolation in combination with the effects of the adjacent Agulhas Current (AC) in the upper layers and cooled from cold bottom waters below. In addition, easterly winds are more frequent in summer thus introducing cold water by coastal upwelling along the south coast, whilst the dominant southeasterly wind introduces coastal upwelling on the WAB. In winter, the AB waters are cooler with strong westerly winds mixing and destabilising the water column thus deepening the thermocline. The bottom waters in summer have been shown by several studies to be colder than the winter waters, although the source of these waters were not qualified. The Cool Ridge (CR), the cold tongue of water extending over the EAB is a feature of the AB. Its forcing is not well understood, it has either been attributed to coastal upwelling or oceanic influences.

In situ studies described in literature mostly consist of long-term investigations with coarse spatial resolution or are short-term with limited spatial coverage. Shipboard surveys are expensive and thus selective in region and duration: they are generally performed for fisheries applications over specific time periods, particularly spring and summer and thus other times of the year may be excluded. Moorings are used for longer studies but their locations must be chosen as spatially representative of a region and may not capture all the dynamics. Satellite images are used to clarify the overall structure but this method is limited to the uppermost layer of the ocean and affected by factors such as cloud cover and the areal coverage of the satellite; often measured values are used to derive other information

such as circulation is inferred from temperature. Thus to get an overall representation of the AB, these studies are generally combined and averaged despite their differences, such as measuring technique. In comparison, a model simulation provides results that are both of relatively high spatial resolution (in this case approximately 8km, with 32 terrain-following vertical levels) and high temporal resolution (data was saved every 2 days for 10 years) and can thus describe processes and structures in greater detail.

This section uses the results of the high-resolution embedded model to investigate the seasonal structure of the AB and compares it to that described in literature. The seasonal mean CR is also described.

4.1 Model Results: Structure of the Agulhas Bank

4.1.1 Sea Surface Height

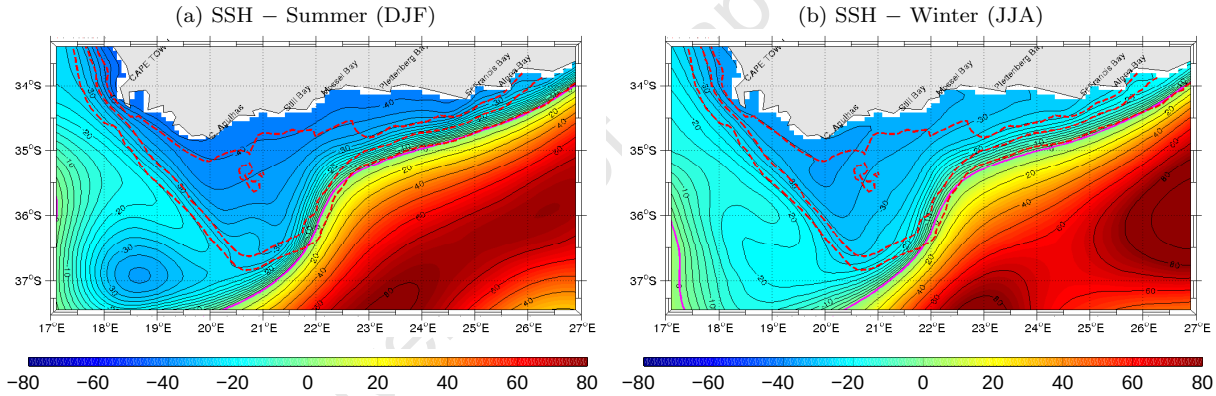

Figure 4.1: Seasonal mean model sea surface height (cm). Negative contour intervals are 2.5cm apart, positive contour intervals 10cm, 0cm contour marked by magenta line.

Figure 4.1 shows the seasonal mean sea surface height (SSH) over the AB, averaged over 8 years, and surrounding ocean.

The Outer-AB and Adjacent Oceanic Region

Dominating this region, is the SSH gradient associated with the warm AC off the EAB. The narrowly-spaced contour lines indicate the speedy flow of the AC which extends onshore up to approximately the 100m isobath on the EAB in summer. In general, flow in the region is subject to topographic steering. In particular, SSH contours of the AC follow the topography more closely where the flow is stronger such as on the EAB. In the region of the

Agulhas Bight, the contours show the AC flowing onto the AB and turning southwards. The AC appears to leave the AB at its southern tip between 21 and 22°E and flows southwesterly off the 500m isobath. Although the maximum SSH for summer and winter is comparable at 80cm, the orientation and structure differs, thus the winter flow along the shelf edge appears slightly weaker.

Off the WAB (37°S, 18–19°E), a trough of SSH is found in summer. This trough is possibly associated with cyclonic circulation, probably cyclones found in the lee of the AB. The outer AB west of 20.5°E inshore of the 500m isobath does not change significantly between summer and winter. This could be attributed to domination by oceanic influences in contrast to seasonal patterns of wind and solar insolation on the Inner and Mid-AB.

The Inner-AB

The AB itself is a large trough of SSH. At the coast, SSH is deeper by 7.5cm in summer as compared to winter, deepening from east to west. The Inner-AB east of Cape Agulhas differs in structure from winter to summer, forcing by westerly winds appear to have shifted the isolines in a more meridional direction in winter as opposed to the zonal flow in summer.

The Inner-AB west of 20.5°E maintains a similar structure from summer to winter. Northwesterly-aligned SSH contours from the wider WAB converge off Cape Peninsula where the shelf is narrow. The offshore SSH gradient off Cape Peninsula indicates that the flow is stronger there (greater in summer than winter). This region coincides with the location of the Good Hope Jet and suggests that the currents on the WAB may contribute to the flow of the Good Hope Jet. In summer, the coastal trough of SSH in this region is seen as a drop of 15cm from the 500m isobath toward the coast compared to 7.5cm in winter. This drop indicates stronger coastal upwelling in summer than winter.

Summary

The main features indicated by the SSH contours are the seasonal change in the AC off the EAB and coastal upwelling on the WAB. In winter, the SSH contours associated with the AC appear further offshore as compared to summer and thus the flow on the EAB appears weaker. On the Outer-AB, west of 20.5°E there is no significant difference in SSH between the seasons. On the Inner-WAB, SSH indicates that coastal upwelling and the associated coastal jet is stronger in summer.

4.1.2 Seasonal Mean Structure and Circulation

Figures 4.2, 4.3, and 4.4 show the AB at horizontal levels of 10m, 50m, and z1 (the first vertical, topography-following grid level), respectively. The depths chosen represent the section above the thermocline, below the thermocline and along the shelf bottom. To review the AB in the model, the AB is divided into three subregions as suggested by the various forcings: the wind-driven Inner-AB, the oceanically-forced Outer-AB and the transitional region of the Mid-AB. Subsequently, the AB is analysed at these depths and discussed with reference to the three subregions.

Outer-Agulhas Bank and Oceanic Region

The Agulhas Current

The model results show the Outer-AB to be dominated by the AC. The AC has the largest speeds in the region which obscures the slower circulation on the adjacent AB, with currents of generally less than 0.2m.s^{-1}. In comparison, off St Francis Bay, the AC has a maximum speed of 1.1–1.2m.s^{-1} in spring and a minimum in winter of 0.9–1.1m.s^{-1} (see Appendix). The AC, also supplies the warmest waters in the region. The core of the AC is 23–26°C at 10m in summer (Figure 4.2b) and 2°C cooler in winter (Figure 4.2d). Salinity (Figure 4.2e–h) is fairly uniform with AC salinity around 35.25–35.45psu at 10m. The most apparent feature in salinity is the lower salinity tongue in summer (Figure 4.2f) which extends from Algoa Bay southwestwards to approximately 21.5°E. Temperatures in the core of the AC decrease with depth. At 50m, maximum temperatures are found in autumn at 22–24°C (Figure 4.3c). At the bottom, z1 (Figure 4.4), temperatures under the AC core, are 5–7°C and salinity below 34.9psu.

Temperature structure at 10m, from spring to autumn (Figure 4.2a–c), suggests the presence of an AC filament (20–22°C). At the tip of the AB, the AC moves off the shelf edge. The AC filament, on the other hand, is observed as an extension of the AC running along the Outer WAB at 10m (Figure 4.2a–c). At 50m, summer mean temperature (Figure 4.3b) of 19–20°C, shows no apparent continuity between the warm AC waters and the AC filament; these water shows the filament to move around a cyclonic feature. This discontinuity is shown in the circulation at 10m (Figure 4.2i–l) and particularly at 50m (Figure 4.3i–l) at approximately 20.5°E and 36.5–37°S. In this region, the mean currents are weak and variable

in direction. This could be due to the warm filament not being directly forced by the AC and/or the averaging of highly variable transient flow patterns in this region (such as cyclonic lee eddies as well as AC filaments). Warm AC filaments are not observed at z1. Thus these filaments are shallower than 50m in spring and slightly deeper in summer and autumn.

The Outer-AB (21.5–27°E): 10m and 50m

The strong currents and temperature and salinity structure of the AC extend onto and affect the AB. This can be seen by the horizontal temperature gradient east of 23°E (Figure 4.2 and Figure 4.3). In spring and summer, when the AC is stronger (see Appendix), this front extends up to approximately the 100m isobath. In winter (Figure 4.2d,l), the influence of the AC on the AB does not reach as far inshore as the other seasons, particularly in the region of the Agulhas Bight.

Waters on the Outer-AB, east of 21.5°E, correspond to AC waters, which were described in the previous section to vary seasonally.The Outer-AB includes Algoa Bay, where the shelf is very narrow. In general, the Outer-AB waters, east of 21.5°E, exceed 18–19°C and 35.25–35.3psu at 10m (Figure 4.2). At 50m (Figure 4.3a–d), the front between AC water and cold AB water (less than 15°C) is more marked.

The currents shown by the model output (Figure 4.2i–l, Figure 4.3i–l) indicates that the outer EAB is influenced, both in magnitude and direction, by the AC. On the outer EAB, where the AC follows the slope in the mean, shelf currents at 10m and 50m are predominantly westwards throughout the year and generally exceed 0.2m.s^{-1}. The strongest flow on the shelf is found between Algoa Bay and St Francis Bay (Figure 4.2), where the shelf is narrow. In the region of the Agulhas Bight (35–35.5°S, 22–23°E), the AC impinges onto the shelf before turning polewards. Current shear produces shelf currents higher than 0.1m.s^{-1} throughout the water column and the mean current direction turns anticyclonically to become southwesterly south of the Agulhas Bight.

The Outer-AB (21.5–27°E): z1 / bottom

On the Outer-AB, east of 21.5°E, bottom waters on the slope are colder than above (Figure 4.4a–d). East of Mossel Bay, the cold bottom waters shows seasonal variation in magnitude and lateral extent. In spring, 10–11°C (34.9–34.95psu) bottom water is found in Algoa Bay and along the outer shelf up to the 100m isobath in some regions. In summer and autumn, this region is warmer, showing 11–12°C water in this region. Maximum mean

bottom temperatures for this region are found in winter at 12–13°C. This movement of cold water onto the shelf edge is probably a result of the seasonal changes in the location of the AC on the slope (Figure 4.1) as opposed to wind mixing. South of the Agulhas Bight, there are cores of warmer (12–13°C) and saltier water (35.0–35.1psu) than the surrounding region.

Where as shelf and slope currents at 10m and 50m show mostly westward flow, east of Plettenberg Bay, z1 currents (Figure 4.4i–l) show cross-isobath flow. Currents are rotated to the right as compared to the interior flow above, suggesting the mechanism for this flow is Ekman veering[1]. This probably assists in bringing the cool 10–12°C waters found on the slope closer to the coast. These waters cross the 100m and 200m isobaths and are then subjected to the prevailing westward currents.

The vicinity of the Agulhas Bight is another region of cross-isobath currents at the bottom (Figure 4.4i–l). These currents (less than $0.1 m.s^{-1}$) cause the water to move up the topography in a northwesterly direction. In spring (Figure 4.4a,e,i), 10–11°C (34.9–34.95psu) water flows onto the AB at the Agulhas Bight and extend westward along the 100m isobath up to about 20.5°E. In summer (Figure 4.4b,j,f), this process continues, but the water is slightly warmer and saltier at 11–12°C (34.95–35.0psu). This bottom water in summer, appears to contribute to and constitute the majority of the water on the AB bottom. This process decreases in autumn and appears to be limited in winter, as the 11–12°C water does not fully reach across the AB onto the WAB.

South of the Agulhas Bight, the shelf currents on the Outer-AB is faster (exceeding $0.2 m.s^{-1}$).

[1]Ekman veering can be explained simply by the alongshore flow in the interior interacting with bottom friction causes cross-shelf ageostrophic transport in the turbulent boundary layer (Perlin et al., 2007, Cushman-Roisin and Malai, 1997, Brink and Shearman, 2006). This momentum balance is between horizontal presure gradient, Coriolis and frictional forces. Ekman theory predicts the flow in the bottom is 45° to the right (left) of the interior flow in the Southern Hemisphere (Northern Hemisphere). However, the veering angle shown in observations is normally less than 20° (Perlin et al., 2007). The transport in the bottom Ekman layer is proportional to the flow in the interior (Cushman-Roisin and Malai, 1997). Convergence or divergence in the bbl transport must be compensated by vertically upward or downward velocity (Ekman pumping) by the continuity of fluid (Cushman-Roisin and Malai, 1997 and Brink and Shearman, 2006).

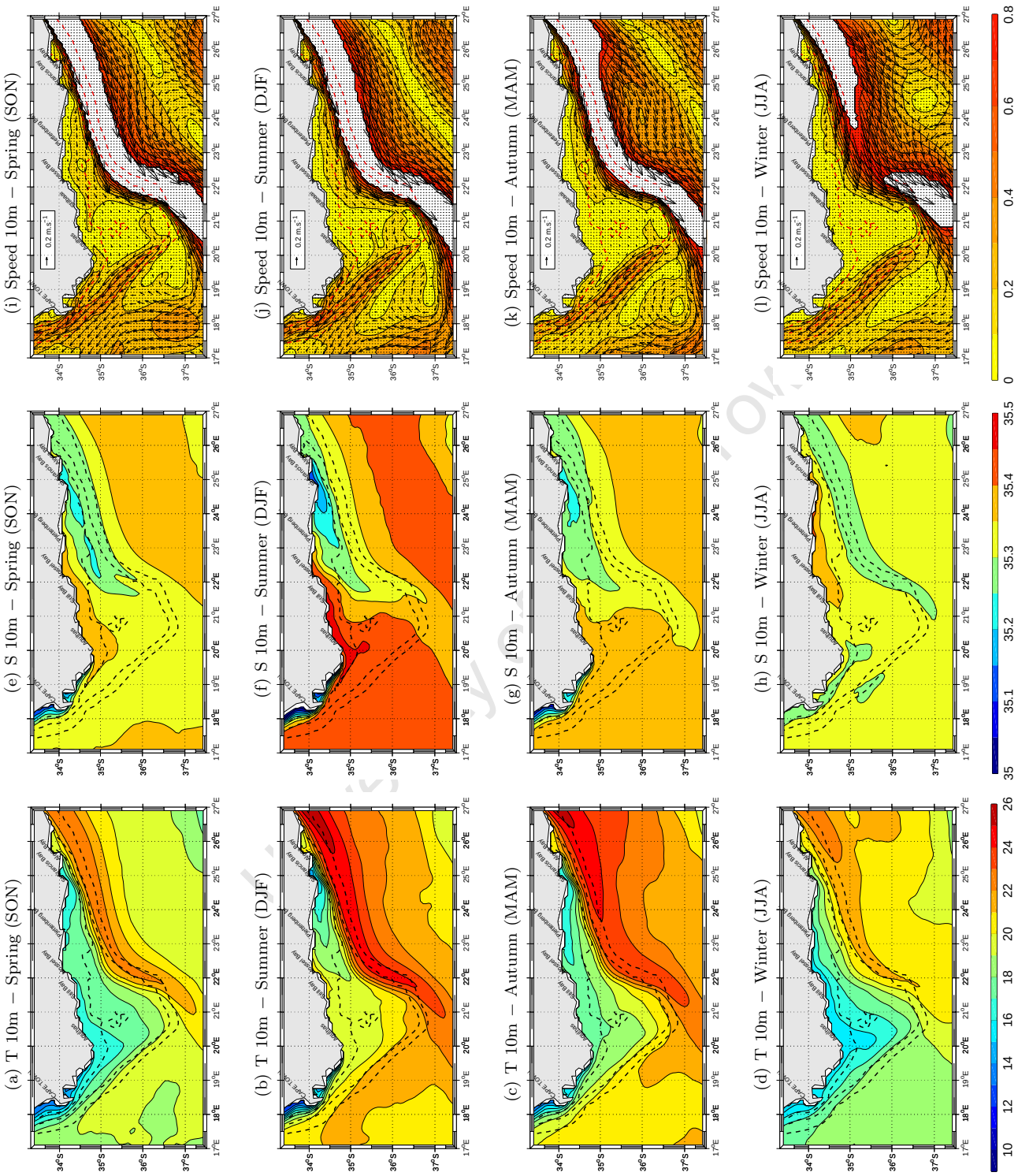

Figure 4.2: Seasonal mean (a–d) temperature (°C), (e–h) salinity (psu) and (i–l) speed ($m.s^{-1}$) and current vectors for the model AB at 10m.

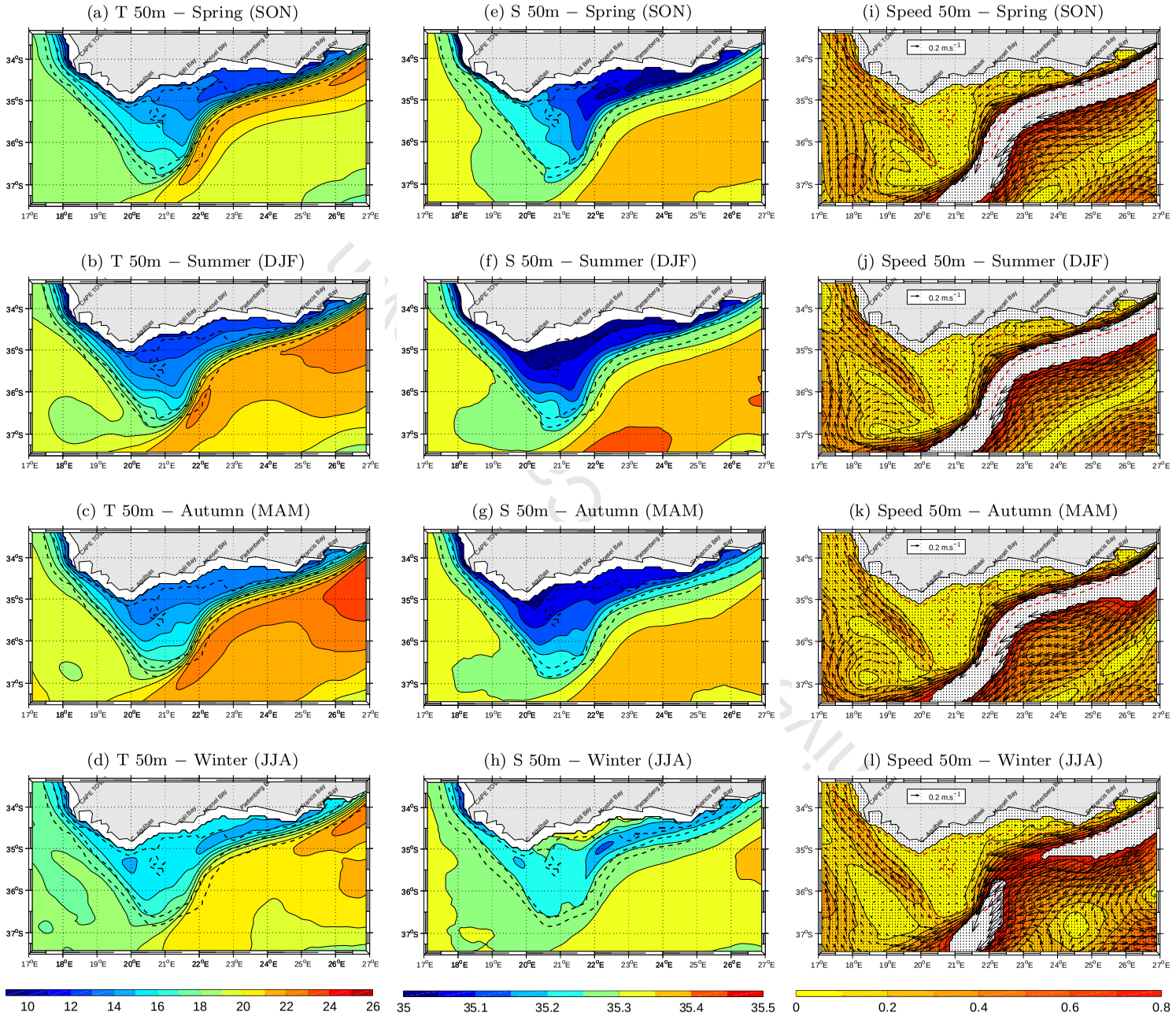

Figure 4.3: Seasonal mean (a–d) temperature (°C), (e–h) salinity (psu) and (i–l) speed (m.s^{-1}) and current vectors for the model AB at 50m.

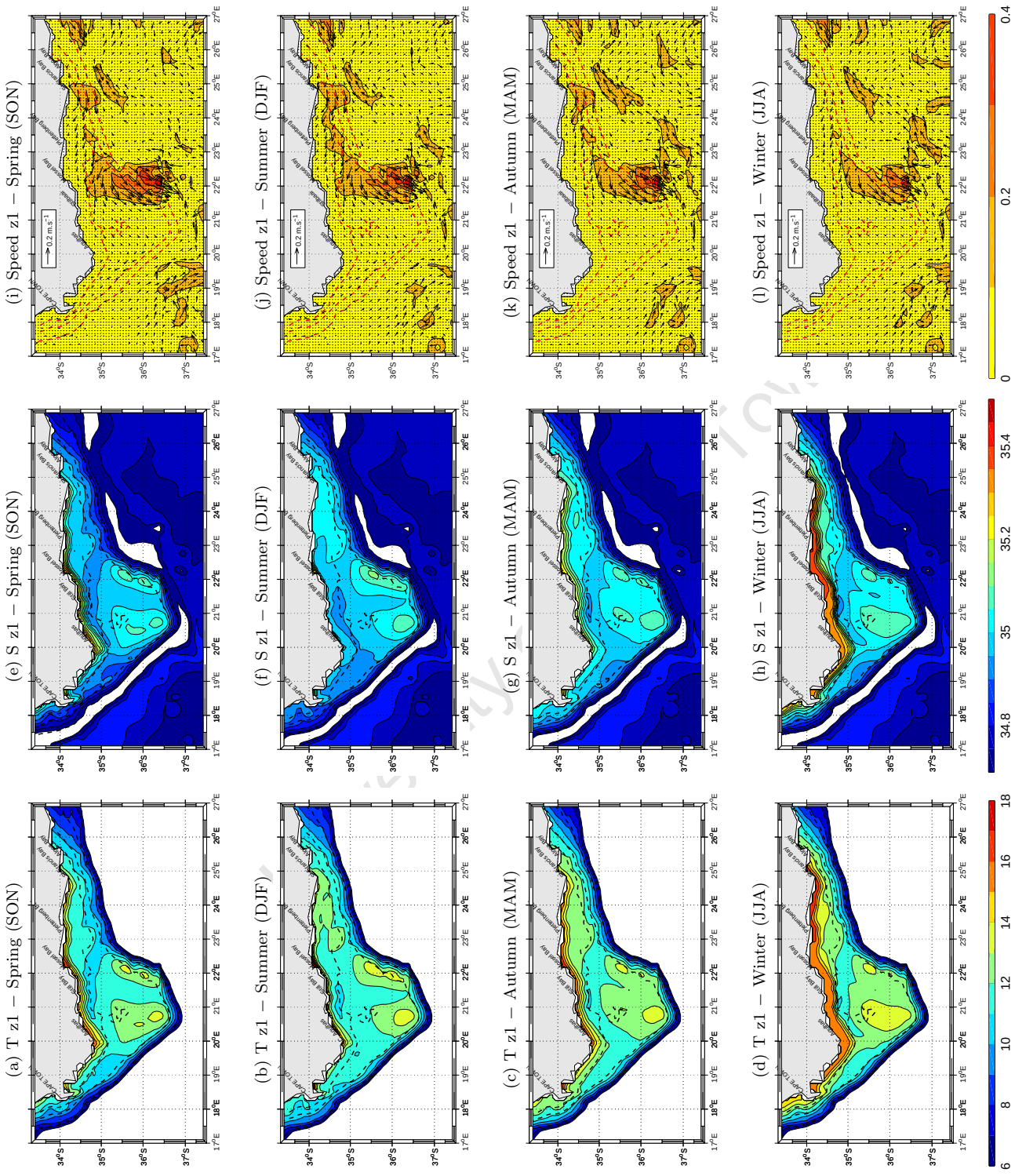

Figure 4.4: Seasonal mean (a–d) temperature (°C), (e–h) salinity (psu) and (i–l) speed ($m.s^{-1}$) and current vectors for the model AB z1 representing f the bottom boundary layer. The displayed range of temperature, salinity and speed have changed from that used at previous depths.

Southern tip of AB (20–21.5°E)

At the southern tip of the AB (approximately 20.5°E), the AC appears to leave the AB slope. However, the temperature and salinity on the outer shelf appear are still determined by the AC. At 10m, the Outer-AB in this region is 18–19°C in winter and spring, warming to 20–21°C in summer and autumn (Figure 4.2a–d). At 50m (Figure 4.3), at the tip of the AB the mean temperature and salinity structure remain consistent throughout the year at 16–17°C and 35.2–35.3psu. At the bottom (Figure 4.4a–h), a core of warmer saltier water (12–13°C, 35.0–35.1psu) is found.

In this region, faster currents (exceeding $0.1 m.s^{-1}$) associated with the AC are found offshore the 200m isobath at 10m and 50m (Figure 4.2i–l, Figure 4.3i–l). Although the AC moves offshore in this region, in autumn and winter, some flow on the shelf edge moves around the tip of the AB and, instead of moving offshore. This flow follows the topography and moves onto the outer WAB, joining the northwestward flow on the Outer-AB. Inshore of the 200m isobath, the mean currents in this region are extremely weak, less than $0.1 m.s^{-1}$ (Figure 4.2i–l, Figure 4.3i–l).

In summary, for the apex of the AB, seasonal changes are mostly experienced in the upper layer, while 50m and the bottom remains relatively constant through the year.

The Outer-AB (18–20.5°E): 10m and 50m

The Outer-AB, west of 20.5°E (the outer WAB), appears predominantly oceanically driven. Temperature and salinity structure show offshore influence, while currents show little change with fluctuations in the seasonal-mean wind stress and direction.

The outer WAB appears to be influenced by the warmer temperatures associated with the AC filaments (Figure 4.2a–d, Figure 4.3a–d). Waters on the outer WAB from spring through autumn exceed 19°C (35.3–35.45psu). Deeper in the water column at 50m (Figure 4.3b–c), 19–20°C waters are found in summer and autumn, possibly from AC filaments, but these waters are located off the shelf offshore the 500m isobath. Temperature and salinity in this region remain consistent throughout the year at 50m (Figure 4.3a–h), ranging from 15–19°C and 35.2–35.3psu.

The influence of AC filaments on this region is not apparent at 10m in the winter temperature map, but at 50m 18–19°C waters might suggest involvement of an AC filament. In winter, mean temperatures are 17–19°C.

The region is dominated by strong northwesterly flow at 10m and 50m throughout the

year (Figure 4.2i–l, Figure 4.3i–l). Currents exceed 0.2 m.s^{-1} at 10m (Figure 4.2i–l), with the speed decreasing with depth. The fastest speeds are found in summer and autumn (0.4–0.5m.s^{-1}) and centered around 19.5°E and the 200m isobath. In winter, the fastest current speeds are 0.3–0.4m.s^{-1}. With westerly winds being dominant in autumn and winter, the consistent direction throughout the year on the outer WAB suggests that this region is mostly oceanically driven and the strengthening observed in summer results from the addition of summer-mean southwesterly wind stress.

The Outer-AB (18–20.5°E): z1 / bottom

Bottom structure and circulation on the outer WAB is characterised by cold, fresh waters and weak northwesterly flow. Temperatures at z1 (Figure 4.4a–d), are 11–14°C throughout the year. Bottom waters in the region are coldest in spring at 10–11°C (34.95–35.0psu), these waters are found up to the 100m isobath (Figure 4.4a,e). In summer, these cold waters are found deeper, the shoreward extent is limited to the 200m isobath (Figure 4.4a). Mean summer bottom temperatures are 11–12°C in this region.

Bottom flow on the outer WAB (Figure 4.4i–l), is predominantly weak (less than 0.1m.s^{-1}). In spring and summer, the currents are mostly northwestward but cross-isobath flow is found crossing the 200m isobath at 19.5°E. This cross-isobath flow could assist in the movement of the cold (10–12°C) waters onto the shelf in spring an summer. The general northwestward flow then spreads this water further onto the AB up to the 100m isobath. In autumn and winter, the general flow appears weaker. Reverse (southeasterly) currents may be found in winter around 20°E.

Inner-Agulhas Bank / Coastline

The Inner-AB (22.5–25.5°E)

Cool coastal waters are found east of 22.5°, at 10m, from spring to autumn (Figure 4.2a–c). In summer, these waters are the coldest and are not confined to the coastline. Instead, these waters extend westwards across the EAB along the 100m isobath, in the form of a colder, fresher tongue or plume, reaching 22°E (Figure 4.2b). The core of the tongue is coldest at Cape Recife (western point of Algoa Bay) at 14–15°C (35.1psu) and warms to 18–19°C (35.25psu) at 22°E. The tongue appears bound onshore by the coast and offshore by the AC. The size of the tongue suggests that this is not related to coastal upwelling which

is expected to be limited in this region.

A similar tongue can be observed deeper in the water column at 50m. In spring and winter at 50m(Figure 4.3), the tongue formation is observed in temperature and salinity. This tongue in spring has a core of 12–13°C and a corresponding salinity of 35.0psu and in winter it is 14–15°C(35.1–35.2psu). The similarity in structure suggests a similar forcing.

The horizontal temperature gradient (Figure 4.4a–d), along the bottom distinguishes the Inner-AB from the rest of the AB. Bottom temperatures on the Inner-AB are warmer than the rest of the AB. The coldest bottom waters are found in summer at 12–13°C (Figure 4.4b) and warmest in winter at 15–17°C (Figure 4.4d).

Inner-AB mean currents are predominantly westward from spring to autumn (Figure 4.2i–k, Figure 4.3i–k). These currents are aligned to the coastline and are less than 0.1m.s^{-1}. The tongue, while not having a distinguishable current pattern, appears to be influenced by the prevailing westward currents. Off Plettenberg Bay, when the currents move offshore, the tongue detaches from the coast. Bottom currents from spring to autumn (Figure 4.4i–k), have an onshore component probably related to further offshore cross-isobath currents. This suggests that cool waters at the bottom are advected into shallower regions from the shelf edge. Since the AC appears to vary seasonally, the waters found on the shelf edge vary seasonally. Thus waters advected into the tongue from this shelf edge region will display seasonal changes. In winter (Figure 4.4l), currents are weak and eastwards between 22–23°E and offshore bottom flow is found east of Plettenberg Bay (see Appendix). This suggests, winter westerly winds induce downwelling. This assists in creating a well-mixed water column as seen by similar temperature and salinity structure at 10m and z1 of 15–17°C (35.3–35.35psu).

The Inner-AB (20–22.5°E)

Inner-AB waters between Cape Agulhas and Mossel Bay show seasonal warming and cooling. Waters at 10m, are warmest and more saline in summer at 19–21°C, 35.45–35.5psu (Figure 4.2b,f) and coldest and freshest in winter at 15–16°C, 35.3–35.35psu (Figure 4.2d,h).

Current speeds east of 20.5°E for this region are slow (less than 0.1m.s^{-1}) throughout the year. In spring and summer, the mean currents in this region are westwards (Figure 4.2i–j). In autumn, with the onset of strong westerlies, currents between Cape Agulhas and Plettenberg Bay average out to almost zero (see Appendix). In winter, westerly wind stress continues, resulting in opposite (eastward) flow close to the coast from Cape Agulhas to

Mossel Bay (Figure 4.2l).

The Inner-AB: 18–20°E

Between Cape Point and Cape Agulhas on the Inner-AB, coastal upwelling is predominant from spring to autumn as observed by the isotherms at the coast (Figure 4.2a–c). Upwelling is strongest in summer with water as cool as 14°C (35.05psu) found close to the coast. At the bottom, summer temperatures (Figure 4.2b) are the coldest for the year at 12°C (34.9psu). In winter, the water column is uniform at 15–16°C and 35.25psu (Figure 4.4d,h).

Concurrent with the upwelling fronts, there is an alongshore northeasterly jet of 0.2–0.3m.s^{-1} with a core of 0.3–0.4m.s^{-1} in summer (Figure 4.2j), at the bottom the flow is slow (less than 0.05m.s^{-1}) and northerly (Figure 4.4j). Currents at 10m in this region are northwestward throughout the year (Figure 4.2i–l). The flow in this surface jet moves equatorward and around Cape Point to join the flow off the Cape Peninsula (the Good Hope Jet). In autumn (Figure 4.2k), with the increase of westerly wind stress, upwelling as well as the current speed decreases reaching a minimum speed of less than 0.1m.s^{-1} in winter (Figure 4.2l). In winter, the bottom flow (Figure 4.4k) is very weak at less than 0.025m.s^{-1}.

The Cape Peninsula: Good Hope Jet

Off the Cape Peninsula, the isobaths converge from wide WAB as the shelf narrows. The Cape Peninsula Upwelling cell occurs here, with intense upwelling, from spring to autumn (Figure 4.2a–c,e–g), bringing the coolest, freshest water up to 10m for the study region (12–13°C, 35.1psu). In winter (Figure 4.2d), mean temperature and salinity of 14–17°C and 35.25–35.35psu, respectively, is found off the Cape Peninsula.

Consistent with the sharp temperature gradient there is a strong northwestward to northward coastal jet (Figure 4.2i–l). The location of the jet (maximum mean speed occurs over the 200m isobath), identifies this feature as the Good Hope Jet, a shelf-edge jet (Bang and Andrews, 1974). The Good Hope Jet is maximum in summer at 0.5–0.6m.s^{-1} at 10m (Figure 4.2j). Speeds decrease with depth: weaker flow (less than 0.1m.s^{-1}) with similar direction is found at the bottom (Figure 4.4j). Bottom flow with an onshelf component is found at 34°S. In autumn, upwelling decreases as well as the associated coastal current, reverse southward flow is observed at the bottom between 200 and 500m isobaths (see Appendix for zoom). In winter (Figure 4.2d), the Good Hope Jet is still present but with decreased magnitude of approximately 0.3–0.4m.s^{-1} (Figure 4.4l) .

Mid-Agulhas Bank

The Mid-AB is the region around the Alphard Banks (approximately 20–21°E, 35°S). It is the region in the center of the AB which is a transitional region between the regions dominated by oceanic or wind forcing. From the description of the above regions, it is clear that the region east of Mossel Bay and that west of Cape Agulhas can be explained by either wind-driven or oceanic processes. Cape Agulhas and Mossel Bay are therefore roughly the west and east boundaries of the Mid-AB, respectively. Its northern limit is the edge of the Inner-AB which is driven by the wind. Its southern border is approximately 36°S, inshore of oceanic influence found on the shelf-edge (which characterises the Outer-AB).

The Mid-AB shows marked seasonal fluctuations, reflecting seasonal changes in solar insolation. In summer (Figure 4.2a–h), near-surface (10m) waters are the warmest (19–21°C, 35.35–35.5psu) while winter displays the coolest temperatures (15–18°C, 35.3–35.4psu). A transitional temperature structure is found in spring and autumn. At 50m (Figure 4.3a–h), temperature and salinity increase with latitude. In summer, 50m waters are 12–14°C (35–35.1psu). The Mid-AB is horizontally uniform in winter at 15–16°C (35.3–35.3psu). Except for the warmer cores described in the Outer-AB which span into the Mid-AB region, the Mid-AB shows similar temperature structure throughout the year at the bottom, z1 (Figure 4.4a–d). Bottom temperatures are generally 11–13°C and 34.9–35.1psu with the exception of spring (Figure 4.4a–h). In spring, 10–11°C (35.85psu) water is found in the region from further east (Figure 4.4a,e). In summer and autumn, remnants of the 10–11°C water remain on the AB at 21°E along the 100m isobath (Figure 4.4b,c). It is not clear why it is not advected west with the rest of the flow.

Currents on the Mid-AB, at 10m and 50m, are weak and directions appears determined by the currents of the surrounding regions. Mean currents (Figure 4.2i–l, Figure 4.3i–l), are generally weak at 10m (less than $0.1 m.s^{-1}$) and decrease in magnitude with depth. At 50m, currents are directionally similar to that at 10m although slightly weaker. Mean currents, are westwards to southwestwards due to currents found east of the region. This suggests that the current in this region are indirectly driven by the AC which influences the currents to the east of this region.

Summary

The main features of each of the above regions is summarised below.

Outer-AB

The Outer-AB shows oceanic influence, this is due to the AC and an associated AC filament which is found off the WAB. In summer when the AC and filament are warmest, waters in the upper water column on the Outer-AB are warmest. In contrast, bottom waters are the coldest and freshest in summer. Bottom waters on the shelf-edge vary in temperature seasonally, with spring being the coldest. Bottom currents show cross-isobath flow, attributed to Ekman veering, east of 23°E. This provides the mechanism to advect these cooler shelf-edge waters closer to the coast. Similar cross-isobath flow at the Agulhas Bight, force cold, fresh waters westwards along the bottom of the AB.

West of 20.5°E, outer WAB mean currents are northwestwards throughout the year and slightly stronger in summer (0.4–0.5m.s^{-1}) than winter (0.3–0.4m.s^{-1}). In this region, bottom cross-isobath flow is found on the Outer-AB, bringing bottom waters, which are coldest in spring and warmest in winter, further onto the shelf.

Inner-AB

East of 20.5°E, upwelling is limited although temperatures at the coast are cooler than the shelf waters. Mean currents east of 20.5°E are weak, generally below 0.1m.s^{-1} and westward except in winter where limited eastward flow is observed.

Despite, limited upwelling, a tongue of cool, fresh water occurs on the EAB. The tongue is largest and coldest in summer, a smaller tongue is found at 50m in winter.

Strong coastal upwelling is found west of 20.5°E from spring through autumn along with their associated northwestward coastal jets. Upwelling and the associated jets fluctuate seasonally maximum speeds and sharpest offshore temperature gradients occur in summer with speeds of 0.3–0.4m.s^{-1}. In winter, this jet and coastal upwelling are not found.

Off the Cape Peninsula, strong coastal upwelling is found from spring to autumn. The Good Hope Jet, the strongest shelf jet in the region, is present throughout the year with a mean-summer maximum of 0.5–0.6m.s^{-1}; in winter speeds drop to 0.3–0.4m.s^{-1}. These upwelling jets are maximum at the surface.

Mid-AB

Mid-AB currents are generally slow throughout the water column (less than 0.1m.s^{-1}) and westwards. Temperatures vary seasonally showing solar insolation changes, it is warmest in summer and coolest in winter.

Cold bottom waters from the Agulhas Bight moves westwards through this region along the bottom towards the WAB.

4.1.3 Thermocline Structure

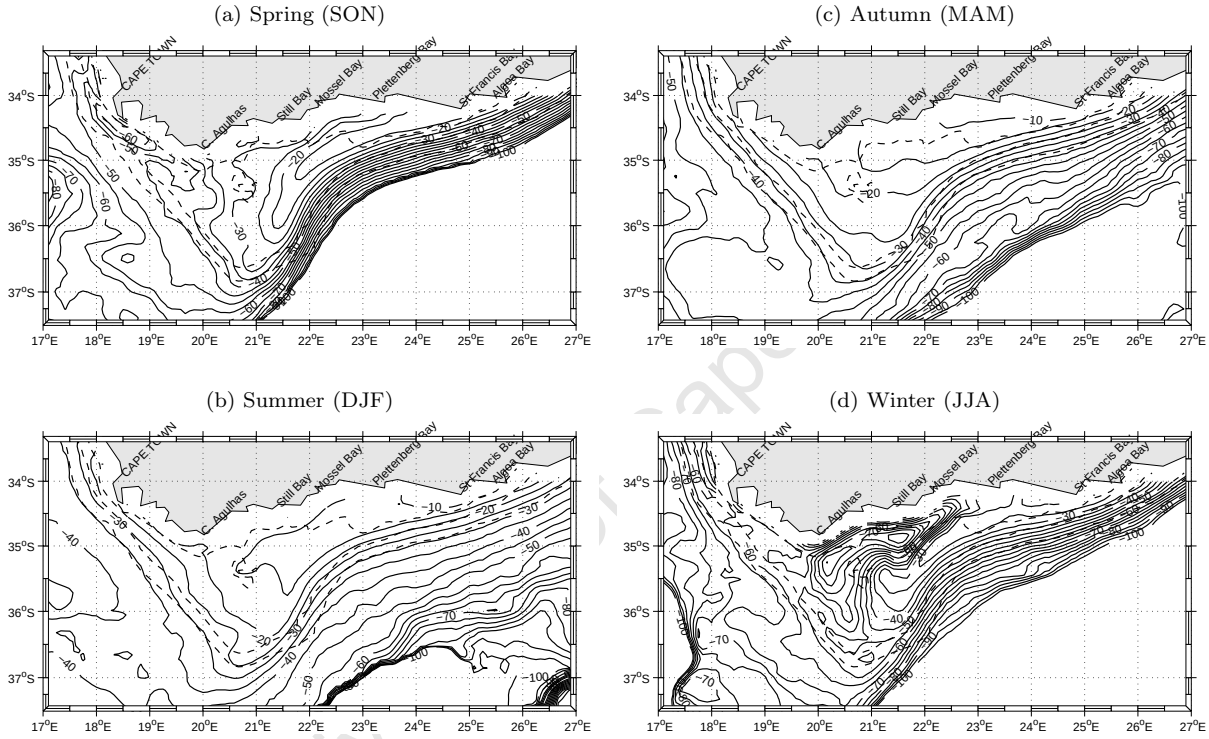

Figure 4.5: Seasonal mean model thermocline depth (m). Contour intervals are 5m, plotted to a depth of 100m.

Figure 4.5 presents the thermocline depth structure over the AB. The thermocline represents the stratification and separates surface warm waters with the cold bottom waters. The previous section has shown surface waters are warm whilst deeper in the water column (at 50m) and at the bottom waters are relatively much colder. In addition, these waters at different depths were shown to change seasonally. This suggests that the thermocline will vary seasonally. The seasonal changes in stratification over the AB may aid in the interpretation of the seasonal structure over the AB. The thermocline depth has been computed using the greatest vertical temperature gradient. The depth of the maximum temperature gradient was calculated at every grid point and the results were "noisy", thus horizontal

smoothing was applied. Due to this smoothing, the Inner-AB is not resolved. The Inner-AB has narrowly-spaced shoaling thermoclines, shallowest at the coast, particularly on the WAB (not shown). This could be attributed to wind-driven upwelling.

Thermocline Orientation

The thermocline structure of the AB (Figure 4.5) tends to align with the bathymetry. The orientation change between the thermocline structure of the EAB and WAB occurs at approximately 20.5°E. On the Outer-AB, thermocline depth reflects the major features of the flow in the region as seen in the mean SSH (Figure 4.1), in particular, the AC on the EAB and the northwestward flow on the outer WAB.

Thermocline Depth

In general, the thermocline on the EAB is shallow and deepens to the west. The shallowest thermocline depths are found east of 22°E at a depth of 10m in summer and autumn (Figure 4.5b–c). Spatial distribution of the thermocline depth on the EAB is in a southwesterly orientation aligned with the oceanic thermocline depth structure, related to the AC. Thermocline depth in this region shows the major features of the AC. The shallow nature of the thermocline can be attributed to the above surface warming combined with weak wind stress. Additionally, cold water input from greater depths on the shelf (as described in the above section) would contribute to elevating the thermocline from below. On the WAB during summer and autumn (Figure 4.5b–c), the thermocline shoals over the shelf, possibly indicating upwelling in response to southeasterly winds in those seasons. As seen in Figure 4.2, this could also be attributed to the warm waters of the AC filament that affect the AB. Both these influences could contribute to the northwesterly orientation of the thermocline structure.

In winter (Figure 4.5d), strong westerlies and cooling at the surface incite mixing and are responsible for deeper thermocline depths. Depths of 50m and 60m are observed on the EAB and WAB, respectively. The deepest mixing is found on either side of the Alphard Banks, up to 75m. The thermocline appears to have strengthened through summer such that even with the onset of the westerly winds in autumn it is only in winter that the structure set up in summer is seen to destabilise. In spring, the thermocline starts rebounding to summer levels.

EAB Thermocline Ridge

The pattern formed by the thermocline shoaling / ridging on the EAB forms a tongue structure on the shelf. This ridging appears inshore of the shallowing of the thermocline associated with the AC. Using the 15m isoline as an indicator for the tongue from spring to autumn and the 25m isoline in winter, this tongue extends southwestwards up to the Alphard Banks, although the orientation and distance from the coast differs with season. This is expected as SSH suggests that the position of the AC changes inter-seasonally. This tongue feature is possibly associated with the CR.

Summary

The thermocline shows seasonal changes and is shallowest in summer and deepest in winter. The thermocline follows the topography with the orientation changing east and west of 20.5°E. The thermocline structure is aligned to the dominant flow on the Outer-AB, that is: the AC on the EAB and the northwesterly flow on the WAB. Thermocline depth increases from east to west. The shallowest depths associated with the cold tongue in the region of Cape St Francis. Inshore of the AC, doming of the thermocline is found in a tongue structure on the EAB. The tongue structure inshore of the AC, changes depth and size over the seasons. The deepest thermocline pattern on the AB occurs in winter on the Mid-AB.

4.1.4 Vertical Structure

Figure 4.6 shows the vertical sections chosen to represent the vertical structure for the WAB, CAB and EAB. The location for these sections were shown in Figure 2.6. The vertical section on the WAB was chosen as it shows the AC filament offshore as well as coastal upwelling. The section chosen for the CAB at 21°E was chosen to sample the AC on the shelf edge, the Mid-AB region and the coastal region as well as the cold bottom water observed moving westward in that region (Figure 4.4a–b). The section on the EAB was chosen to capture the AC on the shelf-edge and the cool water tongue in the vertical. Temperature and salinity structure reflect similar variation over the AB, therefore temperature was chosen to represent the vertical structure for the vertical sections.

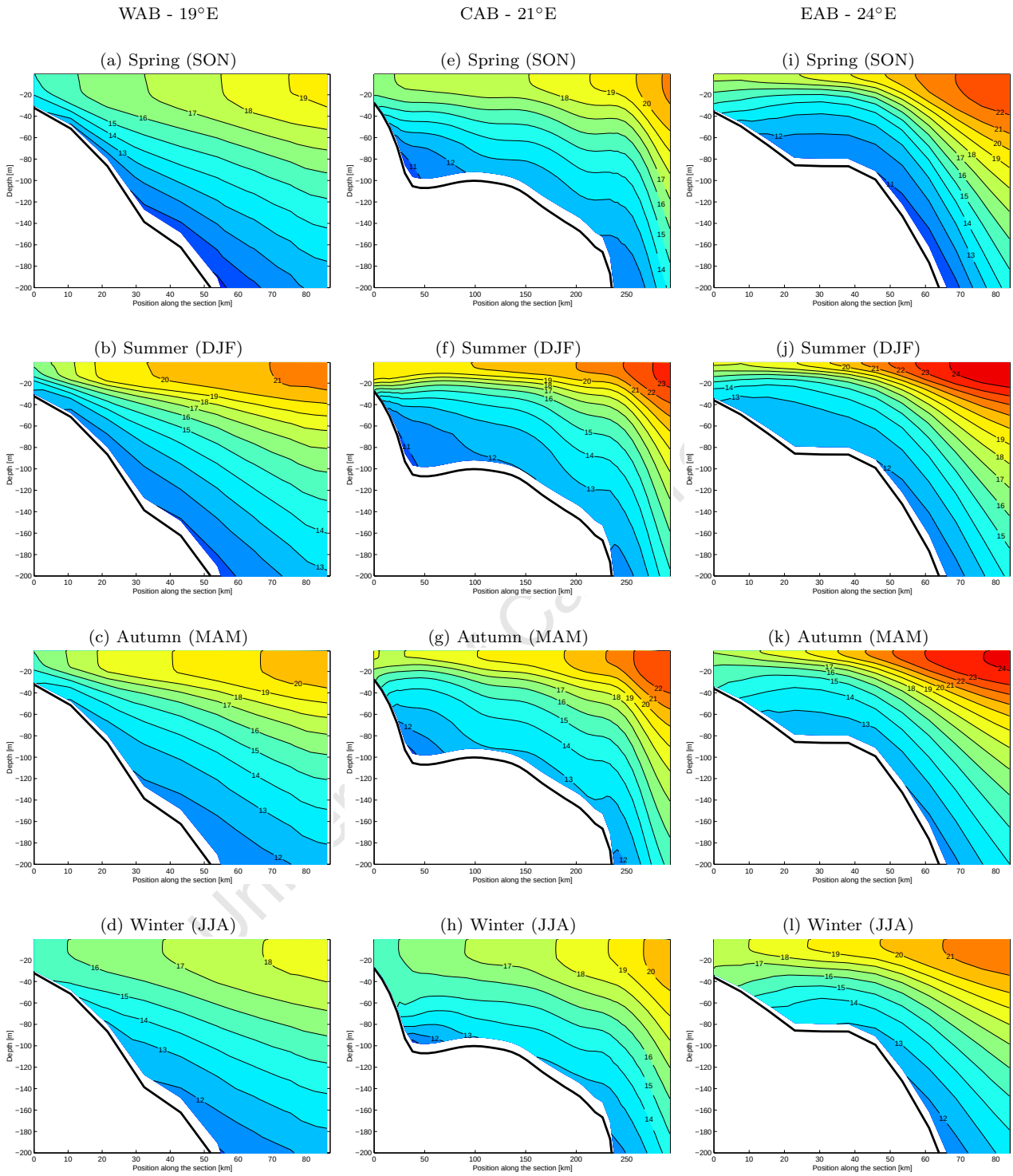

Figure 4.6: Seasonal mean model vertical temperature structure (°E) up to 200m depth for the (a–d) WAB (19°E), (e–h) CAB (21°E), and (i–l) EAB (24°E). Contour intervals are 1°C.

WAB

In the vertical, the WAB (Figure 4.6 a–d) is dominated by upward tilting isotherms throughout the year.

Outer-AB

The influence of the AC is apparent off the shelf edge in summer and autumn with waters greater than 18°C (Figure 4.2b–c). In the horizontal, it appears as an AC filament (Figure 4.2b–c). In the vertical, this feature is shallow: less than 60m deep. In winter and spring, the AC filament is cooler with maximum temperatures of 18°C and 19°C, respectively.

Mid-AB and Inner-AB

In spring (Figure 4.6a), the onset of equatorward winds upwells 14–15°C water at the coast. Waters of 11–13°C water reach above 50m and 10–11°C water reaches 120m.

In summer (Figure 4.6b), upwelling intensifies, isotherms tilt upward more sharply but the progression of 10–11°C onto the shelf is limited. It reaches only 160m. Waters of 12–13°C line the shelf bottom at the coast. At the coast, there is a stronger cross-shore temperature gradient due to the intensification of upwelling. Waters of 16–18°C are present at the surface originating from 80m depth 90km offshore. Even though upwelling has intensified, waters upwelled to the surface in summer are slightly warmer. This is possibly due to the AC filament offshore or general warming of the region.

In autumn (Figure 4.6c), warm 20–21°C water is still present offshore. Coastal upwelling has weakened, although 16–17°C waters are still found on the Inner-AB. Bottom waters are warmer at 11–13°C, 12–13°C waters are found below 50m.

Winter on the WAB (Figure 4.6d) is characterised by flatter isotherms and a well-mixed water column of 15–16°C at the coast.

CAB

The CAB shelf at 21°E (Figure 4.6e–h) is wider than the other chosen sections. At nearly 250km offshore, the section displays three patterns of isotherms, reflecting the different subregions of the AB: the Outer-AB with isotherms tilted upwards under the influence of the AC and warm AC waters in excess 20°C; the Mid-AB and Inner-AB with relatively flat isotherms associated with a stable stratified water column.

Outer-AB

In spring (Figure 4.6e), the isotherms rise under the current and dome over the shelf edge, this brings 11–12°C water onto the shelf edge and 12–13°C water which is found lining the bottom of the section. In summer (Figure 4.6f), warm AC waters are shallow and the influence on the thermal structure is not as marked as spring. Although there is still an uplift of isotherms under the AC, 11–12°C water does not reach as far up the slope as in spring. From autumn through winter (Figure 4.6g–h), although the AC is closer inshore and the structure is deeper, the size / depth of the 12–13°C layer which forms the AB bottom waters decreases. In winter this water does not move entirely up the slope. This suggests that although doming occurs under the AC, any shelf-edge upwelling in this region is not sufficient to feed the bottom waters.

Mid-AB

At mid-shelf, from about 40km to 200km offshore, the isotherms are relatively flat (Figure 4.6e–h). A stronger thermocline is apparent in summer (Figure 4.6f) with the warmest waters of 19–20°C at the surface and a thick layer of 12–13°C bottom water below. The region is cooler in winter (Figure 4.6h) with 16–18°C at the surface and 13–14°C at the bottom.

At 50km, around the 100m isobath, the coldest waters are found on the AB at 10–12°C (Figure 4.6e–h). The layer is thinnest in winter at 10m and thickest in summer at about 40m thick. These waters are detached from that similarly cold water on the slope. Thus the source of these waters are further east since currents in the region are westerly, probably the cold water that enters the AB bottom layer at the Agulhas Bight (Figure 4.4a–d). Since the currents are mostly westwards in this region, the major contributor to waters on the CAB are from the shelf further east.

Inner-AB

The inner CAB shows simple structure, upwelling at 21°E is not found in the seasonal means. In spring (Figure 4.6e), isotherms tilt only slightly upward but do not reach the surface. In summer (Figure 4.6f), the Inner-AB is uniform and warm at 19–20°C with a strong thermocline, below this cold bottom waters tilt upwards. In autumn (Figure 4.6g), the water column starts mixing and the downward tilt of isotherms at the coast suggests downwelling and wind-driven eastward flow such that by winter (Figure 4.6h), the Inner-AB is uniform at 15–16°C down to 80m.

EAB

On the EAB at 24°E (Figure 4.6i–l), the shelf is narrow. Thus, the uptilt of the isotherms associated with the AC over the shelf edge onto the AB shows considerable influence on the vertical structure across the entire section.

Outer-AB

On the Outer-AB, uplift of isotherms of the AC is apparent. In spring (Figure 4.6i), the sharpest offshore temperature gradient is observed with the coldest water introduced to the AB: 10–11°C water reaches up the slope and 11–12°C forms the AB bottom waters up to the 60m isobath. Spring 11–12°C bottom waters are replaced with 12°C waters in summer (Figure 4.6j) by doming onto the AB. Through autumn and winter (Figure 4.6k–l), the offshore temperature gradient decreases and less cold water is uplifted onto the AB with 13–14°C making up the winter bottom water at 24°E. This could be attributed to the seasonal change in position of the AC as seen in SSH (Figure 4.1). Less upwelling by Ekman veering would occur when the AC is further offshore or slower.

Mid-AB

The mid-shelf region is hard to define in this section. Although there is overlap of influences in this region, the section between 20 and 30km offshore display mostly flat isotherms in the upper water column. For the bottom layer there is doming of the cool water isotherms. This doming effect is enhanced in autumn and winter when the Inner-AB experiences downwelling of isotherms.

Inner-AB

Although coastal upwelling is a summer phenomenon on the EAB, corresponding to easterly wind stress (Schumann et al., 1995), upwelling is not apparent in the seasonal mean temperature sections except in autumn (Figure 4.6k). The Inner-AB appears highly stratified with flat isotherms in spring and summer (Figure 4.6i–j). Cool waters as cold at 15°C are available relatively close to the surface in the upper 20m. In autumn (Figure 4.6k), the 17°C isotherm uplifts to the surface at the coast, this could be from the influence of AC surface waters or due to the cumulative effect of easterly winds from summer. In winter (Figure 4.6l), the Inner-AB is mixed with 17°C surface water overlying 16°C bottom water.

Summary

The main features indicated by the vertical sections are summarised subsequently.

Outer-AB

On the Outer-AB, warm waters of the AC affect the surface of the adjacent AB, particularly in summer. Below the thermocline, isotherms associated with the AC incline over the slope. For the CAB, this water sits on the bottom at the shelf edge but does not move onto the shelf. On the EAB isotherms dome over the shelf edge and line the bottom of the EAB. These waters reach far onto the narrow shelf on the EAB. In spring and summer, the cold water lines the bottom of the AB contributing to the wide extent of the cold waters seen in the horizontal. In autumn and winter, within 20km of the coast, isotherms are subjected to local effect such downwelling and mixing, this enhances the dome shape in the vertical. The doming of cold waters in the vertical contribute to the thermocline ridge on the EAB.

On the outer WAB, the AC filament is shallow and does not show a significant effect like the incline of isotherms under the AC. It does, however, contribute to surface warming. Below the AC filament, isotherms do tilt upwards over the WAB bottom but the role of coastal upwelling can not be discounted.

Mid-AB

Mid-AB isotherms are relatively flat, summer shows the strongest thermocline for this region. Cold bottom waters in this region appear to be from futher east. The cold westward moving bottom water of 10–12°C from the Agulhas Bight is found around the 100m isobath in this region.

Inner-AB

The Inner-AB shows coastal upwelling on the WAB from spring through autumn. Coastal upwelling is not apparent for the CAB. In spring, isotherms tilt upwards but remain subsurface. Isotherms close to the coast on the inner EAB, are flat in summer and do not show upwelling but upwelling is found in autumn. The Inner-AB in winter, shows the effects of mixing with the deepest surface mixing found on the CAB.

4.2 The Cool Ridge

The CR of the model AB manifests itself, in the horizontal, as a tongue of colder and fresher water extending from the coast west-southwestwards across the comparatively warmer and more saline waters of the AB in summer and autumn at 10m (Figure 4.2b–c, f–g) and deeper in winter and spring at 50m (Figure 4.3a,d,e,h). This roughly coincides with the ridging of the thermocline structure inshore of the AC (Figure 4.5). The seasonal mean CR is predominantly subsurface as seen by vertical doming in Figure 4.6(i–l). The maximum mean horizontal appearance of the CR occurs in summer at 20m, therefore this depth was chosen to study the CR.

Horizontal Structure

Figure 4.7 shows the temperature and salinity structure of the CR at 20m as well as the current speed and vectors for the EAB. The tongue structure of the CR is more clearly expressed in the salinity than the temperature. The CR does not have its own distinctive current structure but appears to move with the prevailing currents.

No tongue feature in temperature or salinity is apparent at 20m in winter (Figure 4.7d). A doming of isotherms and a tongue-like feature is, however found deeper in the water column at 50m consisting of 14°C water (Figure 4.3c).

The CR at 20m, appears to develop in spring (Figure 4.7a,e). The CR core at this depth consists of 14–16°C (35.15–35.25psu) water. Its direction appears related to the shelf currents, which are generally southwestward and less than 0.2m.s^{-1}. The CR appears to start along the coast west of Algoa Bay but salinity indicates it is part of a larger structure that includes Algoa Bay. The CR temperature structure extends across the EAB up to 22°E. Its offshore limit is the AC; east of Plettenberg Bay it extends onshore up to the coast. In the region of Plettenberg Bay, the current has an offshore component: the CR appears to detach from the coast in this region after which it moves southwestward. The CR salinity signature shows the tongue extending in a southerly direction, west of 22°E, corresponding to the currents in the region.

In summer (Figure 4.7b,f), the CR reaches its maximum expression, being the widest and extending past 21°E. The CR is the coldest and freshest in summer, with a core of 12–13°C (35.05–35.15psu) ranging to 16°C (35.2psu). In comparison with the temperature and salinity range of the CR in summer (Figure 4.7b,f), the CR in autumn is not as intense

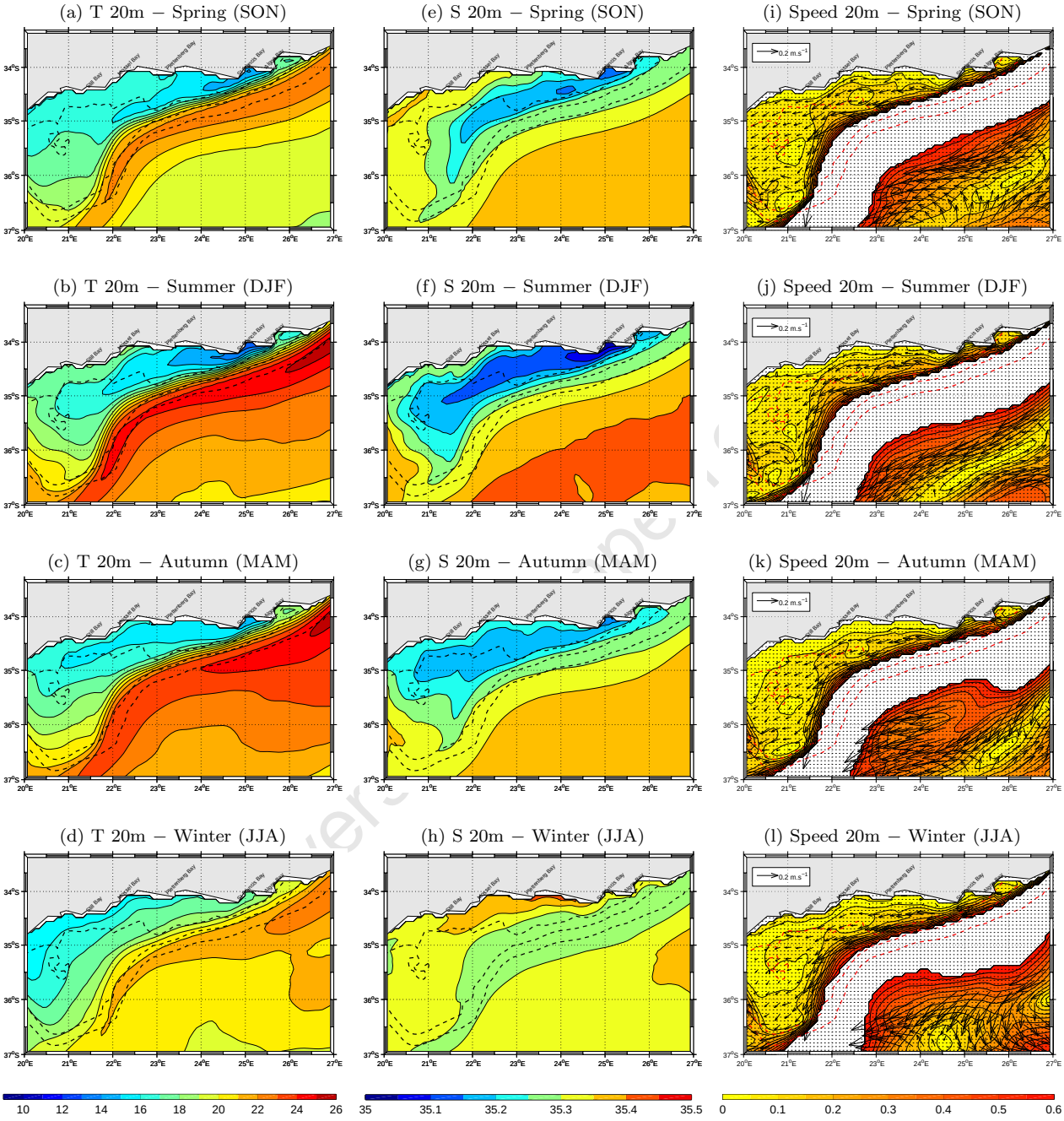

Figure 4.7: Seasonal mean (a–d) temperature (°C), (e–h) salinity (psu) and (i–l) speed ($m.s^{-1}$) and current vectors for the model AB at 20m showing the maximum extent of the CR in summer. Speed contour interval is $0.05 m.s^{-1}$ up to $0.6 m.s^{-1}$, current vectors plotted for speeds less than $0.4 m.s^{-1}$.

(Figure 4.7c,g). The tongue-like structure in temperature of the CR is 15–16°C but the salinity structure suggests that the 16–17°C water may also be part of the larger CR structure. Salinity for the CR ranges from 35.15–35.2psu. The offshore front of the CR at 16°C remains positioned inshore of the AC. Seasonal changes such as the destabilisation and mixing of the upper water column due to decreased insolation and increased winds in autumn or from less advection of the colder waters that feed the CR may contribute to the weakening of the CR in the horizontal. In winter, the CR is not apparent at this depth (Figure 4.7d,h).

Vertical Structure

Figure 4.8 shows a vertical section through the CR. In the horizontal, in summer (Figure 4.7b), the CR appears fully developed at 24°E and may start detaching from the coast, thus this vertical section was chosen. In the vertical, the doming of the isotherms, isohalines and isopycnals over the shelf-edge and onto the shelf can be observed throughout the year (Figure 4.6). The 17°C isotherm appears to indicate the bottom of the upper mixed layer and top of the thermocline. It rises over the slope and lies flat over the AB, separating the warm surface waters above and the doming of cool waters below.

Doming occurs under the AC and onto the shelf. The narrowness of the shelf probably allows the cool waters to reach far into the shelf. The doming appears to be controlled by the AC and displays seasonal changes discussed previously.

From the horizontal sections (Figure 4.7) and these vertical sections (Figure 4.8) it appears the CR has a distinguishable temperature and salinity signature. The waters involved in doming over the shelf edge range from 11–16°C and between 34.9 and 35.2psu. Thus, a particular density structure is implied. This appears to be indicated by the 26–26.5kg.m^{-3} isopycnals associated with the density structure of the AC. The isopycnal shows that the density structure imposed by the AC on the AB shelf reaches all the way to the coast. Presumably, changes in temperature and salinity inshore are due to local effects such as wind-mixing or currents. The structure remains fairly similar throughout the year, the 26kg.m^{-3} isopcynal rises from approximately 100m at 80km offshore to 20m at the coast in summer and autumn. In spring, the isopycnal is shallower at 110m, 80km offshore but also reaches 20m at the coast. In winter, the 26kg.m^{-3} isopycnal is located offshore at 90m but only reaches 40m close to the coast. Ekman veering, as seen at level z1 (Figure 4.4i–l) , is related to the mean current speed.

Figure 4.8(i–l) shows a seasonal pattern in the speed of the AC off 24°E. The strongest

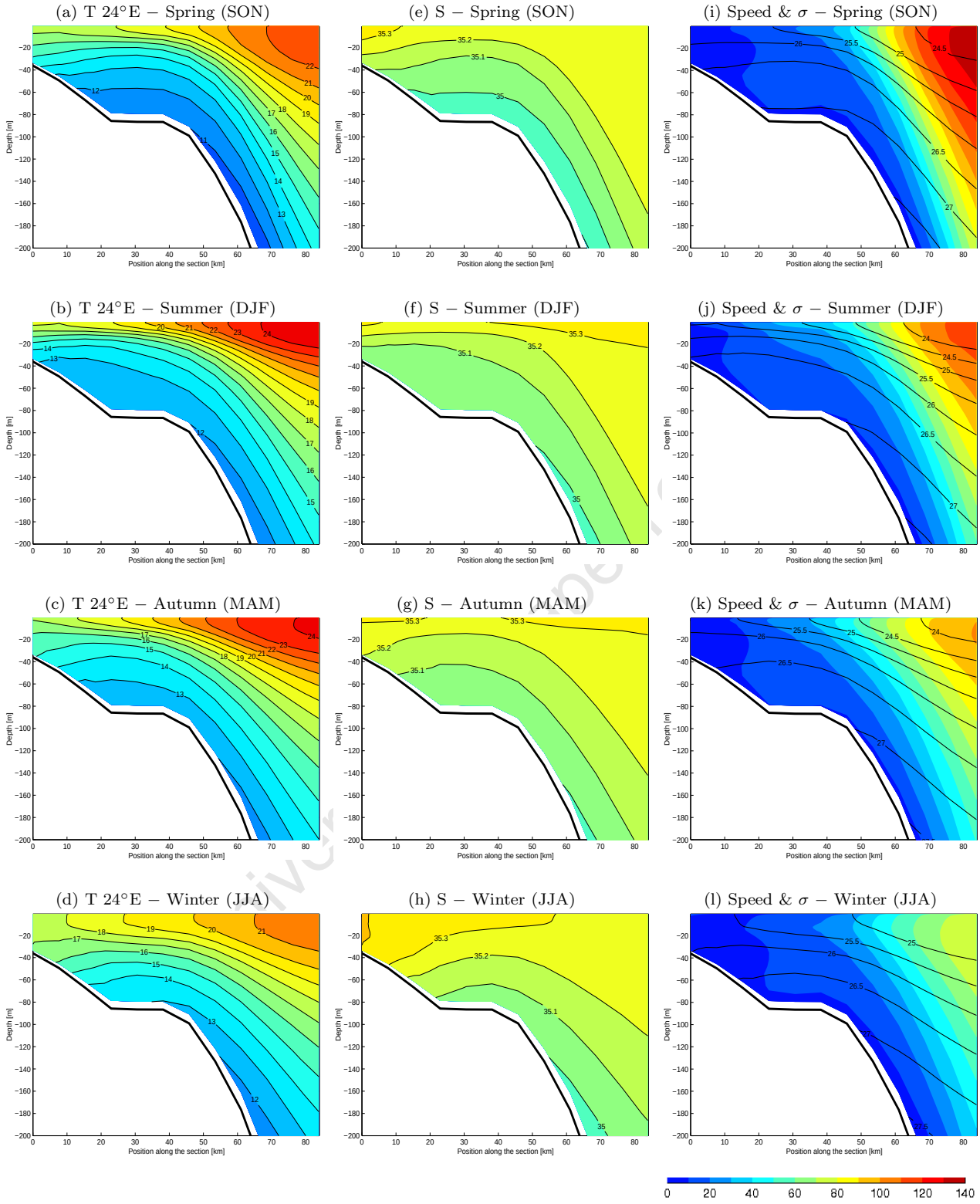

Figure 4.8: Vertical sections at 24°E for seasonal mean (a–d) temperature (°C), (e–h) salinity (psu) and (i–l) speed (cm.s^{-1}) with density (σ) contours (kg.m^{-3}) overlaid for the model AB. Speed contour interval is 10cm.s^{-1}, density contours are 0.5kg.m^{-3}.

flow is observed in spring where the AC at 80km offshore the coast at 24°E exceeds 1.3–1.4m.s^{-1} and the slowest in winter at 0.8–0.9cm.s^{-1}. Thus, stronger flow would correspond to increased advection onto the shelf through the bbl such as in spring and conversely less transport in winter.

The AC appears to impose its density structure on the AB which displays seasonal variations. This accounts for the upwelling of isotherms onto the shelf but does not fully account for the slight downwelling of isotherms closer inshore seen in the vertical temperature and salinity. This could be attributed to local effects on the AB. In autumn and winter, when strong westerly winds occur over the AB, the coast is conducive to downwelling, also very weak even eastward flow were found in the model. The mixing at the coast could thus contribute to the deepening observed in these seasons. In spring and summer, the CR is at its widest. This could be due to the increased advection onto the shelf combined with the lack of limitation at the coast from wind effects such as downwelling. As the shelf is narrow, the upwelling winds could possibly encourage the uplift isotherms in the Inner-AB region, increasing the onshore extent of the uplifted thermocline across the AB.

Summary

Horizontal expression of the CR

In the horizontal, the CR is expressed as a cold, fresh tongue of water extending across the AB with the prevailing currents which are generally southwestwards (although it does not have its own associated current structure). It is attached to the coast west of Cape Recife, where the shelf is narrow and the currents are alongshore, aiding in the movement of cold water westward. The CR detaches from the coast in the region of Plettenberg Bay where currents have an offshore component. Its offshore limit appears to be the inshore front of the AC. At 20m, it shows seasonal changes, being widest and coldest in summer, its orientation also changes depending on the seasonal mean currents in the region. In winter, it is not found at 20m but is located deeper in the water column.

Vertical expression of the CR

In the vertical, the CR manifests as doming of isotherms and isohalines over the shelf edge under the AC. Seasonal mean water properties range from 11–16°C and between 34.9 and 35.2psu, thus the CR is composed of Indian Ocean Central Water. It is subsurface in the

seasonal mean and shallower in summer than winter. Close to the coast, local effects on the Inner-AB affect its shape in the vertical. Seasonal position changes of the AC, as seen in the SSH maps, are reflected in the density structure and adjacent current speeds on the slope. When the AC is closest and fastest, the coldest waters dome onto the AB. With this influx the thermocline shallows and the CR is relatively shallow. In winter, slower speeds and less input of cold water on the bottom limit the size of the CR.

4.3 Discussion

This section compares the previously presented results to that found in literature and puts these results in context of the various forcings of the AB.

4.3.1 Sea Surface Height

SSH maps were used to infer the general flow pattern and the density of water in the AB region.

Using the mean seasonal SSH of the model, documented oceanic features of the AB are distinguishable, including: summer upwelling west of Cape Agulhas, the AC and cyclones in the lee of the AB. Cyclonic eddies are spun off the AB by the interaction of the AC with the southern tip of the AB at irregular intervals (Penven et al., 2001a). From the mean model SSH, the model AB was shown to be seasonal. Thus this model simulation of the AB is forced by an AC that is seasonally variable in position on the shelf edge as well as in intensity. Seasonality on the shelf interior is also inferred from SSH, probably forced by both the atmosphere and the AC. SSH shows the coastal trough on the WAB and off the Cape Peninsula, associated with intense upwelling and the Good Hope Jet, which is also subject to seasonal variation. SSH also shows that the coastal region east of Cape Agulhas extends up to Cape St Francis. The coastline further east of Cape St Francis appears part of the offshore circulation pattern.

4.3.2 Sources of water on the AB

This section suggests the sources of water for the AB for above and below the thermocline. Due to processes on the shelf, such as mixing, the character of the water masses on the shelf change from their origin.

Sea surface temperatures on the AB were found to be fairly horizontally uniform whilst at 10m the structure included the cooler waters on the EAB. The seasonal variability for the

upper water column of the AB is apparent from the maps. The model layer z1, representing the bbl, shows little change except for the additional influx of cold water in spring and summer both on the EAB and WAB.

Surface waters

Temperatures at 10m, representing the layer above the thermocline, of the model AB are warmest in summer at 19–20°C in summer with corresponding salinities greater than 35.35psu and are coldest in winter 15–18°C (35.3–35.45psu). A large contributor to the warm AB waters appears to be the AC and the AC filament. In general, these temperatures agree with the expected ranges found in literature. Satellite SST climatology (1992–1999) found SST of 20–23°C in summer, cooling to 15–19°C in winter (Demarcq et al., 2003). Data from various sources over the years 1930 to 1978 were averaged to yield surface temperatures of 20–21°C on the AB while cooler for the coastal upwelling on the EAB (17°C) in summer and 15–18°C in winter (Schumann and Beekman, 1984). Seasonal mean temperature and salinity values for the model AB above the thermocline indicate that these waters are Subtropical Surface Water, 16.0–26.0°C and salinities greater than 35.5psu. Although the salinity may be slightly lower, lower salinities have previously been noted on the AB and were attributed to mixing with deeper waters of lower salinity (Swart and Largier, 1987).

Bottom waters on the outer EAB

In general, bottom temperatures on the AB, as shown by level z1, range from 15–17°C (greater than 34.9psu) on the Inner-AB and 10–14°C (34.9–35.1psu) over the rest of the AB and are colder in summer than winter. On the AB, between the 30m and 500m isobaths, Roberts (2005) reported bottom temperatures (from 86 surveys involving CTD measurements), ranging from 3.2 to 16.4°C and an average bottom temperature of 14°C (range 10–19°C) east of 26°E, attributed to the proximity of the AC. Although mean bottom temperatures in the model fall within that shown by Roberts (2005), the model shows the warmest bottom temperatures east of 26°E to be 12–13°C, slightly colder than the *in situ* value. The TS character of the bottom water on the model Outer-AB suggest these waters are Central Waters of either Indian (8.0–15.0°C, 34.6–35.5psu) or Atlantic Origin (6.0–16.0°C,34.5–35.5psu) (Valentine et al., 1993). Chapman and Largier (1989) show AB bottom waters to be Central Waters although the oceans from where the waters originate are distinguishable by nutrient profiles.

4.3.3 Seasonal Structure and Circulation of the AB

The Outer-AB

The outer EAB

Temperature, salinity and currents in the model show the AC to dominate the Outer-AB. Model SSH showed a seasonality to the orientation of the AC off the EAB, offshore temperature gradients suggest that the current appears stronger in summer than winter, this has been observed by Schumann and Beekman (1984) who noted the temperature gradient marking the inshore edge of the AC was observed in summer and not in winter. SADCO data from 1930 to 1978, show the maximum mean temperature of the AC core was 26°C in core decreasing by 3–4°C in winter (Schumann and Beekman, 1984), similar temperature for the model AC were found. Currents on the Outer-AB are stronger than the rest of the AB and follow the direction set up by the AC, southwestwards east of 20.5°E and northwestwards west of 20.5°E. Where the shelf is relatively narrow, east of St Francis Bay and Algoa Bay the entire shelf appeared to be forced by the AC. As it flows along the EAB, the AC directly forces its structure onto the adjacent AB. Thus, the outer EAB is warm in the upper layers with relatively strong currents on the shelf, below the thermocline the waters are cold from Ekman veering up the slope. The model shows currents exceeding 0.2m.s^{-1} these speeds correspond to typical current speeds of 25–100cm.s^{-1} indicated by Boyd et al. (1992). The model AC moves past the tip of the AB and moves off the shelf. Current speeds and direction for the upper layer are similar to the typical values and direction by Boyd et al. (1992) in Figure 1.7 although seasonal-mean model currents do not show the flow reversal indicated in the image. Boyd et al. (1992), analysed shipboard ADCP currents near the surface for November 1989 and 1990 and found that the region east of 24°E is dominated by the AC, this is apparent in the model.

Algoa Bay

The model indicates that the Algoa Bay region, despite being a shallow coastal region, is part of the Outer-AB. The influence of the AC on the temperature structure has been shown to influence this region by meanders and upwelling from the AC core and within eddies and plumes (Goschen and Schumann, 1988). Model mean temperatures in the region of Algoa Bay show the region to be warmer at 19–21°C in summer. Mean temperature observations

from various data sources (over the period 1960–1992), show that Port Elizabeth located in Algoa Bay shows a maximum mean summer temperature (21.03°C) greater than that further west (Schumann et al., 1995). At z1, temperatures in the Algoa Bay region are coldest in summer at 11–12°C. Although, in the model the relatively cooler waters associated with the CR are found west of Algoa Bay, the temperatures along the bottom of the entire outer EAB appear of similar range and thus possibly similarly sourced. Similar cold waters have been found for PE compared to that further west (Schumann et al., 1995).

Bottom waters

East of Plettenberg Bay, cool waters move up the slope through Ekman veering and line the bottom of the Outer-AB in the model. In the vertical, this water is shown to range from 10–14°C. For the bottom layer, z1, 10°C is found on the outer slope in spring, this is the season in which this water reaches the furthest on to the shelf up to the 100m isobath along the bottom. This is associated with the CR and will be discussed later.

The Agulhas Bight

Cold water is also shown at z1, the bottom, to move westwards in the region of the Agulhas Bight. This cold (12°C) water appears to be introduced to the AB from spring as it is not present in winter. The spring thermal structure shows a tongue of 12°C extending westwards. Presumably, this water spreads westward where it is found up to Cape Agulhas in summer and where it joins the 12°C water on the WAB. At 10m and 50m, the flow is southwestwards with the AC but bottom flow shows Ekman veering across the Bight, which upwells the cold water then moves westward with the westward flow aligned to the 100m isobath. No literature describes this pathway of cold water. The AC is known to directly affect the AB at the Agulhas Bight, eddies are concentrated in this region (Lutjeharms et al., 1989) particularly cyclonic eddies which assist in the vertical movement of cold water (Lutjeharms et al., 2003). However, these do not describe the lateral movement of this water.

The outer WAB

The flow on the outer WAB is northwestward throughout the year, except for the region between 20 and 20.5°E, which shows weak mean currents from spring to autumn. The northwestward flow on the outer WAB converges at the Good Hope Jet, which is fastest in summer and slowest in winter. The outer WAB is warmed by the AC in the form of an AC

filament, which is clearly identifiable from spring to autumn. The AC filament is identified by warm water, exceeding 18°C, and in the model is shallower than 60m. This model shows that, in the vertical mean, shallow AC filaments are prevalent as opposed to to Agulhas rings, which generally have a deeper thermal structure (Lutjeharms and Cooper, 1996). Furthermore, the weak currents between 20 and 20.5°E, which were previously attributed to averaging, can also be due to the behaviour of AC filaments. Lutjeharms and Cooper (1996) describe that many AC filaments detach from the AC only after the AC has moved past the southern tip of the AB. Thus, the filament generally does not flow directly along the shelf edge from the outer EAB to WAB but moves off the shelf before affecting the outer WAB, leaving a region of weak currents with no direct forcing. Lutjeharms and Cooper (1996) also indicates, based on a small sample, average speeds associated with a filament of 0.8m.s^{-1}, double the speed shown by the model means. This is probably due to the seasonal averaging of highly variable flow on the outer WAB. A mean speed of 0.3cm.s^{-1} for two months from December 1986 was measured by Largier et al. (1992). Based on eight drifters launched on the WAB, Lutjeharms et al. (2007), show that the outer WAB is highly variable due to the passage of both cyclones and anticyclones which affect both the direction and speed of the flow in the region. Seasonality of the warm water on the outer WAB was described by Largier et al. (1992), the appearance of the warm AC water was observed to coincide with the upwelling system in summer. Largier et al. (1992) suggested that the northwestward flow on the outer WAB may play a role on the upwelling of cold water over the shelf edge through bottom stress. On the outer WAB, upward tilting isotherms are present deeper than 40m in all seasons as is the northwestward flow. However, flow at the bottom in the model shows cross-isobath flow occurs only in spring and summer. Speed of the northwestward flow are of a similar magnitude in winter and spring thus if the flow did support shelf edge upwelling, it should be observed in the other seasons as well. It is possible that the isotherm structure imposed by the warm AC filament, although shallow, may play a role in the upwelling of cold waters along the WAB shelf bottom, even in winter. This is supported by the lack of correlation between velocity and temperature at the shelf edge (Largier et al., 1992), that the thermal structure is not altering the speeds of the region.

Mean bottom currents do not indicate longshore reversals in the flow described by Chapman and Largier (1989). The model does show reversed bottom flow between the 200m and 500m isobath in autumn but this flow does not move up the shelf. This flow is the mecha-

nism attributed to supplying the WAB with bottom waters of Atlantic origin. In the model, water introduced by Ekman veering over the shelf edge, moves northwestward rather than southwards.

The Inner-AB

The seasonal contrast between summer and winter on the Inner-AB is apparent from the structure of this region. In winter, the Inner-AB is vertically well-mixed with the vertical sections on the WAB and CAB showing a vertically uniform water column at the coast. It is, however, the other seasons that show rich structure on the Inner-AB and this is emphasised in the following discussion. The Inner-AB west of Cape Agulhas in the model responds to seasonal winds and is dominated by coastal upwelling from spring through autumn. Although wind-driven upwelling has been documented for the Inner-AB east of Cape Agulhas, averaging produced no discernible seasonal-mean coastal upwelling at 10m. Vertically, the CAB shows limited subsurface upwelling in spring but this is suppressed by the surface layer of warm water in summer.

The inner WAB and the Cape Peninsula

Model temperatures on the WAB in winter correspond to the expected range of approximately 15–16°C (Boyd et al., 1985). Upward sloping isotherms and no upwelling of isotherms to the surface as seen in the model in winter are expected as winds are not conducive to upwelling in this season (Boyd et al., 1985). Upwelling west of Cape Agulhas is distinguishable from spring through autumn. In the horizontal, waters in the upper layers show cold waters decreasing towards the coast; while in the vertical, isotherms were shown to slope upwards towards the coast. In summer, upwelled waters at the coast on the WAB are the coldest and freshest (14–16°C, 35.05–35.25psu). An alongshore jet associated with the coastal upwelling extends along the inner WAB and is maximum in summer, averaging 0.3–0.4m.s^{-1}. This jet forms part of the Good Hope Jet off the Cape Peninsula. Off the Cape Peninsula, coastal upwelling is stronger than the WAB with waters as cold as 10°C and 34.85psu. Model mean temperature and salinity values fall within the range measured by Boyd et al. (1985). Upwelling on the WAB has been observed to bring waters with temperatures as cold as 10–12°C to the surface, particularly off the Cape Peninsula (Boyd et al., 1985).

The Good Hope Jet

The Good Hope Jet, off the Cape Peninsula, was found with maximum mean speed

in summer of 0.5–0.6m.s^{-1} and minimum in winter 0.3–0.4m.s^{-1}. In general, mean model currents within the Inner-AB fall within the range indicated in Figure 1.7 (Boyd et al., 1992). Boyd et al. (1992) show speeds associated with the Good Hope Jet of between 50–75cm.s^{-1}. Summer mean speeds for the model Good Hope Jet fall within this range. However, the Good Hope Jet is still present in winter with mean speed below the range indicated by Boyd et al. (1992) even though the Good Hope jet is primarily associated with seasonal upwelling (Bang and Andrews, 1974; Nelson et al., 1998). However, variability in the Good Hope Jet has been noted by Nelson et al. (1998), who found the presence of the jet outside of the upwelling season: a speed of 35cm.s^{-1} between 20 and 60m in May 1992 is given as an example. This suggests that the model flow for the Good Hope Jet may be a reasonable representation. Northwestward flow on the outer WAB appears to contribute to the Good Hope Jet in the model. In winter, when upwelling has ceased, this flow on the outer WAB is still present and appears to contribute to the winter presence of the Good Hope Jet. This is particularly noticeable in winter at 50m (Figure 4.3l). Part of this flow has been attributed to AC water moving around the AB tip at 50m as well as from shallow AC filaments (from spring to autumn). Thus, the Good Hope Jet appears to be not solely due to wind-driven upwelling but also due to the effect of the AC on the WAB. This is also suggested by Boyd and Nelson (1998) who noted that in a study from August 1996 to July 1996, strong NNW flow occurrences off the Cape Peninsula coincided with the presence of AC water in the region.

The Inner-AB, east of Cape Agulhas

Coastal upwelling east of Cape Agulhas in the model is not apparent in the seasonal mean structure at 10m. Although temperature and salinity at 10m may suggest that the cool tongue observed in Figure 4.2 is part of the Inner-AB due to its attachment to the coast, structure deeper in the water column and currents in this region suggest that this structure is part of the CR and will thus be included in the discussion of the CR. Cool coastal waters in the model appear associated with the CR rather than coastal upwelling. Vertical sections show mean upward sloping isotherms at the coast in upwelling seasons. However, no significant mean upwelling signal is found in the model temperature at 10m. This could also be attributed to the nature of upwelling in this region. Upwelling between Mossel Bay and Cape Agulhas was shown by Eagle and Orren (1985) to be a small-scale process occurring within 10km from the coast while for east of this region is "a few tens of kilometres offshore" (Schumann et al., 1982, pg. 242). The spatial scale of upwelling combined with relatively coarse wind

resolution could possibly imply that the model (at approximately 8km resolution) may not adequately resolve coastal upwelling nor the effect of the many headlands. Effects such as topographic steering due to features on the coastline are also not taken into account at this resolution. Temporally, upwelling in this region is a short-lived process, Schumann (1999) found that easterly winds are of short duration, upwelling events followed by relaxation occur over a relatively short period of time and does not allow distinct upwelling cells to develop. The surface signature of the upwelling is quickly covered by warm water when upwelling winds weaken (Boyd et al., 1985) by as little as 12 to 18 hours after cessation of easterly winds (Goschen and Schumann, 1995). Upwelling east of Cape Agulhas is a complicated process. Schumann et al. (1982) note that in the presence of easterly winds, upwelling may not always be observed at the surface. Averaged surface temperature maps do not clearly show cool waters associated with coastal upwelling east of Cape Agulhas, for example, in monthly SST satellite climatology (Demarcq et al., 2003) and in seasonally averaged *in situ* data from 1930–1978 (Schumann and Beekman, 1984) .

Weak mean currents (less that $0.1 m.s^{-1}$) are found on the model Inner-AB east of Cape Agulhas and were generally aligned to the coastline and topography. The model currents are slightly stronger in spring and summer and are westward. In autumn, the model currents are extremely weak whilst in winter in some regions the model currents are opposite (eastwards). Boyd et al. (1992) shows typical current speeds of 10–40$cm.s^{-1}$ for this region. While this is larger than the mean model speeds, winds in this region have been observed to change from easterly to westerly and force the coastal waters accordingly, thus, average currents would be weak. Also, the model is forced by monthly climatology winds in which those highly variable winds have been averaged, the effect on the currents will therefore be reduced.

The Mid-AB

The Mid-AB in the model is characterised by strong seasonality, reflecting seasonal insolation patterns at the surface. The upper layer is warm in summer with a thermocline at 20–30m. In winter, the Mid-AB is cool and well-mixed, the thermocline deepens to greater than 60m. In the vertical, this region displays level isotherms throughout the year. Stronger stratification is observed in the vertical across the CAB in summer than the other seasons. Closer to the Inner-AB, the bottom layer is fed by westward moving cold water of 10–12°C, which has upwelled at the Agulhas Bight. On the Mid-AB, model mean currents are very weak throughout the water column (less than $0.1 m.s^{-1}$) and generally have a westward component.

Eagle and Orren (1985) studied cruise data from 1974 to 1979 for the CAB off Cape Infanta (20°50'E) and showed this region to have a marked stratification in summer and autumn although they showed a better developed thermocline in autumn. Although the weak mean model currents in this region is commonly observed *in situ* (Boyd et al., 1992), the cyclonic circulation apparently associated with the CR (Boyd and Shillington, 1994) was not found in the mean model currents.

Eagle and Orren (1985) found cold bottom water of 11°C off Cape Infanta (20°50'E) in late summer and autumn, also noted was slightly warmer bottom waters further offshore. It was suggested that that this could be due to advection from the west in contrast to the east via reverse plumes from the AC. The model provides an alternative explanation, this cold water could be from the waters entering the AB at the Agulhas Bight. Agulhas Bight upwelled waters in the model move westwards along the bottom in a narrow band across the slightly warmer AB. The waters to the south of this band would be warmer than the band creating a similar structure to that observed by Eagle and Orren (1985).

4.3.4 Thermocline Depth

The model thermocline on the EAB strengthens in summer and autumn by seasonal warming and warm AC water in the upper layers as well as the injection of cool water along the bottom, shallows the thermocline particularly where the shelf is narrow. Thus, the thermocline is shallowest on the far EAB. The thermocline deepens to the west, upwelling on the WAB produces a shallow thermocline on the inner WAB. By winter, the effect of autumn and winter westerly winds have deepened the thermocline with the deepest thermoclines found on the Mid-AB. Ridging of the thermocline associated with the CR, inshore of the AC, is limited by mixing along the coast in winter. In spring, the thermocline starts to shallow again with the onset of summer conditions. Vertical temperature sections show warm water from the AC influencing the AB, this would enhance the two-layer structure from above. Ekman veering of cold waters would enhance the layer below the thermocline. The ridging of the thermocline is aided by the processes at the coast. In summer, the CR detaches from the coast due to offshore currents, mixing and downwelling at the coast would deepen the thermocline on the shoreward side of the CR. Upwelling on the south coast is not well resolved by the model in the seasonal mean. Although cold water is found inshore east of Plettenberg Bay in summer, this is a result of the shallow thermocline from the CR allowing cool waters to be available very close to the surface.

On the WAB, upwelling produces the shoaling of the thermocline onshore in summer and autumn with the shallowest thermoclines on the Inner-AB at the coast. In winter and spring, these regions are mixed and the thermocline deepens. Thermocline depth changes depending on the local conditions and may vary from year to year. While in the model mean thermocline depth helps in understanding the features of the AB, *in situ* measurements of this are usually done to help understand events or shorter time periods. Thus, the value obtained by the model based on 8 years of data may differ from literature, which depends on the period over which averaging occurred.

Comparison to literature

In general, the thermocline behaviour agrees with the literature with the thermocline depth deepening from east to the west (Largier and Swart, 1987). Also the deep thermoclines observed in the model on the Mid-AB in winter are expected, Eagle and Orren (1985) found deep mixing thermocline close to bottom in winter and spring.

The model thermocline appears related to the AC. The shoaling of the thermocline on the EAB has previously been observed and suggested to be associated with the bathymetry and the AC (Schumann and Beekman, 1984). Largier and Swart (1987), noted the strong thermocline on the EAB is maintained by warm waters from the AC in the upper layers as well as by cold upwelled waters below the thermocline. Largier and Swart (1987) also attributed the deepening of the thermocline to the west due to decreased flow of bottom waters. This might explain deepening to the north on the EAB. In the model, deepening to the west appears as part of the change in the oceanic forcing. Upwelling of cold waters occurs on the both the EAB and WAB. It is therefore possible that the strengthening of the surface layer by the warmer AC may be contribute to the shallower thermocline on EAB, particularly where the shelf is narrow and the AC can reach further inshore.

For the WAB, thermocline depth in 1975 (Boyd et al., 1985) from January to April was calculated at 30m and from June and July at 80m and October to December at 55m. The model thermocline depth on the WAB is comparable to these values although is slightly shallower in summer. The thermocline on the CAB is slightly shallower (at 20m) than measured by Eagle and Orren (1985) who found the thermocline in autumn at 30m. The winter thermocline is expected to be close to the bottom in this region and the model shows the deepest thermoclines in this region in winter.

4.3.5 The Cool Ridge

Unlike the west coast of South Africa, which is well-supplied with nutrients through coastal wind-driven upwelling (Shannon and Nelson, 1996), upwelling on the south coast is small and localised along the EAB (Schumann et al., 1982) and appears insufficient to support productivity. Despite this, the AB supports spawning of species, such as sardine, anchovy and squid, and also provides a nursery ground for many species (Hutchings et al., 2002). This productivity is attributed to the CR; elevated levels of phytoplankton (Probyn et al., 1994) as well as copepods (Verheye et al., 1994) are associated with the CR .

A concise definition to the cool ridge is not available. An important aspect of the CR that has been observed, is its effect on the biology through the increase of nutrients (Boyd and Shillington, 1994). In order for this to occur, there must be vertical uplift of colder, nutrient rich water from greater depths. Thus, for this thesis, the CR is considered as the doming of isotherms or uplift of mid-shelf isotherms on the AB which results from the vertical movement of cool bottom waters into warmer shallower waters. The association with coastal waters and coastal upwelling must still be established.

CR Description

In the model, the mean vertical doming of isotherms is located on the EAB. In the horizontal, the vertical doming corresponds to a cool, fresh water tongue extending across the EAB. This brings cool water from the shelf edge to shallower depths. This pattern in the temperature and salinity, identifies this feature as the CR. The CR temperature and salinity show the CR is made up of Indian Ocean Central Water. The model CR is a tongue of cool water extending from west of Cape Recife in a generally southwesterly direction. This doming appears to vertically lift the thermocline. In the mean the CR is subsurface i.e the thermocline does not reach the surface. The CR is thus apparent in the horizontal thermocline depth structure over the AB, however in autumn the coastal upwelling signal obscures the CR structure. Typically, its seasonal mean offshore extent is the inshore AC front. Although the main horizontal structure of the CR starts at Cape Recife, cool waters are found, at depth, on the shelf east of Algoa Bay.

It is apparent from the horizontal and vertical temperature structure that the CR can be found in all seasons although the structure and orientation may vary. In summer, the CR is at its largest and coldest, extending across the AB up to 20.5°E, it is attached to the coast

up to Plettenberg Bay where it moves offshore. In summer, it is observed as shallow as 10m. In winter, the CR is narrow, deep and 2°C warmer. Its offshore limit is determined by the AC while its onshore boundary is determined by the structure of the Inner-AB particularly where the shelf is narrow, in the region of Cape St Francis. For example, in autumn coastal upwelling affects the CR signal and in winter, downwelling and mixing from westerly winds in the shallower inshore region confines this tongue away from the coast. In winter, the CR is only seen at 50m, although it starts close to the coast it does not appear attached to the coast. The CR also appears to be laterally confined to the EAB, it is not observed past Cape Agulhas in the model mean. This suggests its structure is dependent on the AC. Although the prevailing currents may play a role in spreading the cold water across the AB, the proximity to the AC, advectively maintaining the cool water is responsible for its vertical seasonal mean structure.

The CR does not appear to have its own associated current structure like the AC which transports warm, salty water. Its horizontal position and movement appears to be determined by the currents on the outer EAB which are in turn influenced by the AC. No dominant flow associated with the CR appeared in the seasonal-mean model SSH. This emphasises the subsurface nature of the CR and its association with the AC as the AC signal dominates the signal of the shelf-edge.

Drivers of the CR

The doming of the CR is associated with the Ekman veering / cross-isobath flow observed in the bottom Ekman layer. This influx of cool water onto the AB causes the thermocline to shallow and dome. Thus, cool waters are available relatively close to the surface. Ekman veering by the AC has previously been reported off Port Edward on the east coast (approximately 30°E, 31°S), using temperature and current data (Schumann, 1986). In this region, the shelf is less than 10km wide and in water depth of less than 50m, the bottom Ekman later extends throughout the water column only limited at the surface by effects such as the wind. This shows that Ekman veering under the AC does occur. Upwelling due to a western boundary current, the East Australian Current, was investigated by Oke and Middleton (2001). They found that where the shelf narrowed, acceleration of the current occurred which resulted in increased bottom stress which allowed upslope flow in the bottom boundary layer. Furthermore, this cold water moved laterally subsurface due to the currents in the region. In the East Australian Current case, the cold water upwells to the surface further downstream

due to current divergence.

Seasonality in the position of the AC implies that the magnitude of the currents over the EAB slope is weaker in winter when the AC is further offshore. Since Ekman veering is related to the speed of the flow in the interior of the water column, decreased speeds in winter imply less Ekman veering in winter as well. In addition, the position of the AC appears to determine the waters that upwell and dome onto the AB. The strength of cross-isobath flow is comparable in spring and summer yet colder waters are found at the bottom in spring. The position of the AC determines the imposed thermal structure and thus the doming onto the AB. Thus, the character of the CR appears to be related to both the position and speed of the AC.

The seasonality of the AC is still contested, but meandering of the AC is accepted, the winter / summer comparison may correspond to the movement of the AC away from / toward the AB. When the AC is further from the shelf, less Ekman veering occurs thus, less waters upwell and the CR is confined to the slope or deep in the water column. However, when the AC is closer to EAB, more cold water upwells onto the shelf where shelf currents assist in spreading these waters across the AB i.e. a larger CR. Also, the contribution of shelf edge features may slow down or speed up the flow against the slope as they pass, resulting in more or less veering.

Comparison to literature

The CR in the model does not contradict any descriptions of the CR. Previous descriptions of CR are based on few data, Boyd and Shillington (1994) tracked the CR in November for four years. The model shows that in the vertical, the 17°C isotherm and the thermocline appears in the upper 30m coinciding with observations by Boyd and Shillington (1994). Horizontally the CR is consistently described as a feature of the EAB. Its attachment to the coast may vary between studies but overall the mean CR feature is consistent in structure with previous descriptions of the CR (Hutchings, 1994). Satellite monthly climatology by Demarcq et al. (2003) indicated increased levels of chlorophyll-a on the AB in a tongue off the EAB, since elevated nutrients are associated with the vertical movement of cold waters and thus the CR, the model CR shows fair agreement to the horizontal location and orientation. Satellite observations by Walker (1986), show that the cold water tongues to start at the coast between Still Bay and Port Elizabeth with Cape St Francis showing the "most active tongue". This supports the model, which in summer produces the coldest waters off Cape St

Francis.

Largier et al. (1992) describe the coldest water on the AB to be contained on the AB within the CR. However, the model shows the cold water and the ridging of the thermocline over the cold water to constitute the primary CR. Water on the shelf, on either side of the CR in the model, are warmer than the CR itself. This is supported by Lutjeharms and Meyer (2008), who attribute the CR to the movement of cold bottom waters, however, their proposed mechanism and origin differ to that observed by the model. An assortment of widely-sourced data were incorporated to suggest to the authors that the upwelling at Port Alfred is the source of all the cold water on the EAB; the subsequent lateral movement of these cold waters along the 100m isobath constitutes the CR (Lutjeharms and Meyer, 2008). The model, on the other hand, shows the cold water and doming of the CR is determined by cross-isobath flow from Ekman veering along the EAB (from the Agulhas Bight to Cape Recife) as well as the position of the AC and assisted by the shelf currents for distribution. Lutjeharms and Meyer (2008) dismiss Ekman veering along the EAB shelf edge as a source of cold water onto the AB, having not found supporting evidence in somewhat disparate data. Hutchings et al. (2002), however, refers to upwelling along the shelf edge in this region in a review on the physical oceanography of spawning grounds around southern Africa.

The model shows that the CR is seasonal, maximum in summer. Roberts (2005) describes the CR as a summer upwelling phenomenon, mainly due to easterly winds. The model CR shows seasonal variation in assocation with variations in the AC. Since, the model is forced with monthly wind stress, the full contribution of winds on an event scale can not be explored. Easterly wind stress is expected to cause coastal upwelling, which would serve to bring the thermocline and the CR (where the shelf is narrow) to the surface at the coast. For example, in autumn, although the vertical structure distinguishes the CR, the thermocline structure and horizontal structure at 10m shows that it is dominated by the coastal upwelling signal. This would contribute to the CR, appearing as a wind-driven upwelling plume even though its primary mechanism appears to be by the AC. It also supports the absence of the CR in the presence of strong easterly wind stress (Roberts, 2005). If there is a weak or no CR doming the thermocline, then cold waters cannot breach the surface despite the strength of the winds. However, upwelling in autumn is weak and not strong enough to bring the deeper AB waters to the surface. Although being subsurface in the mean, the CR may be observed at the surface when Ekman veering is enhanced presumably from when the AC is

faster or where winds are able to further lift the thermocline to the surface. Thus, the CR could outcrop at mid-shelf as suggested by Jury (1994), the cyclonic shear resulting from the increase in wind velocity with distance from the coast could uplift the thermocline in the region of the 100m isobath. For the bottom waters to be available above the thermocline to enrich productivity, the thermocline must be uplifted close to the surface by AC action or lie shallow enough for erosion or uplift by wind action.

The AC advects cool water along the bottom along the shelf edge. Where the shelf is narrow, the cold water is available close to the coast but lies below the thermocline. Even though this cold water may be available at shallow depths, in the mean it lies below the surface. The AC does not drive this water up to the surface at the coast as seen for the East Australian Current (Roughan and Middleton, 2003). Therefore winds would play a necessary role in making nutrients available for production.

Thus, the ridging that is responsible for the CR is forced primarily by the AC but to get the signature observed in many of the studies the interplay of winds must also be considered.

4.4 Summary

To understand the structure of the AB, this chapter has used horizontal sections above and below the thermocline and at mid-depth as well as vertical sections for the EAB, CAB and WAB. The model has been shown to be stable and reproduces features expected and observed on the AB. In the seasonal mean, no obvious spurious features were found. The CR was resolved by the model.

The model AB is a complex and dynamic region and appears indeed divided into subregions depending on the major forcings. These subregions defined for the AB vary seasonally. This is predominantly due to the position of the AC which in the model varies seasonally as seen in the SSH. A tentative definition for the subregions identifiable from the model AB structure and circulation is presented in Figure 4.9 and Figure 4.10, respectively.

Thermal structure of the AB

Figure 4.9 shows a summary of the structure obtained by the model.

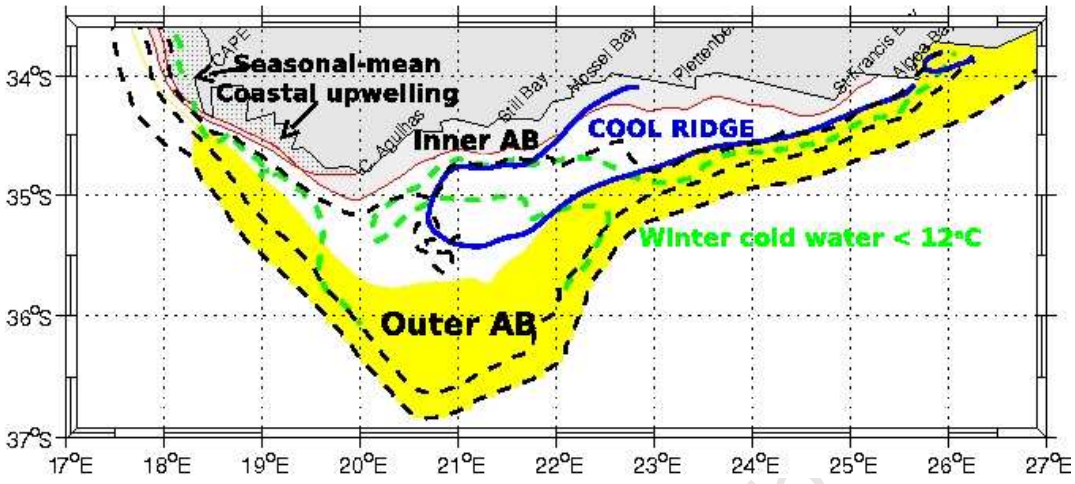

Figure 4.9: Main temperature features of the AB. Indicated are the 3 regions of the AB: Inner-AB (grey), Mid-AB (white), and Outer-AB (yellow); the region of strong upwelling in summer on the WAB; the largest extent of the Cool Ridge in summer is shown by the blue line; sub-12∘C water in winter is indicated by the green dashed line.

The Inner-AB is the region close to the coast, shallower than 50m, from Cape Point (tip of Cape Peninsula) to Cape St Francis. Also shown, are regions of strong summer upwelling west of Cape Agulhas.

The Outer-AB (in yellow) is the outer shelf influenced by the AC and its features such as the AC filament on the WAB, it spans from Cape Peninsula to Cape St Francis, also included is the entire shelf east of Cape St Francis which includes Algoa Bay. In the Outer-AB, cold water moves up the slope; the green dashed line indicates where cold water (less than 11°C) lies in winter on the EAB and WAB. The cold water lies on the slope of the EAB and enters the AB in the region of the Agulhas Bight where it moves westwards. On the WAB it lies offshore the 100m isobath. In summer, with increased veering along the slope this cold water moves further onshore and spreads further westwards over the AB, such that the Mid-AB in summer is 11°C at the bottom.

Mid-AB is the shelf region between these two regions. Mid-AB is the transitional region between the two directly forced regions, it shows flat isotherms in summer due to surface warming but with the influence of cold bottom water from further east, while in winter this

region has a deeper mixed water column and less influence of cold bottom waters from the east.

The maximum horizontal extent of the CR is shown in blue, it shows the CR may be found close to the coast west of Algoa Bay and extends southwestwards bordered offshore by the AC and its features. The inshore border of the CR is not distinguished as it may depend on the structure of the Inner-AB, for example, coastal upwelling will show the feature connected to the coast or winter mixing will show the CR further from the coast.

Current structure of the AB

The major features in the flow on the AB are summarised in Figure 4.10. The AC is the major driver of the Outer-AB with currents and thermal structure on both the outer EAB and outer WAB showing sympathy to the AC. On the outer EAB current direction appears determined by the AC. Along the EAB and parts of the WAB, Ekman veering creates upslope flow along the bottom which brings cool water onto the shelf. The schematic shows the path of cool water which enters at the Agulhas Bight and moves westwards across the AB. South of the Agulhas Bight, currents are aligned to the AC and are southwestwards. Flow Mid-AB is generally westwards and weak throughout the water column.

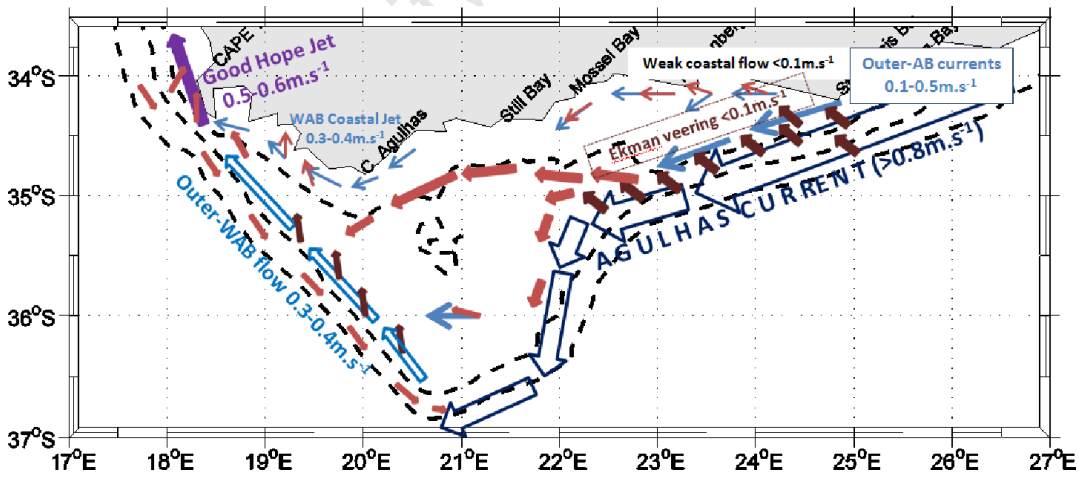

Figure 4.10: Schematic of the main current features on the AB in summer. Blue and purple arrows indicate flow at 10m with the summer-mean speeds. Red/pink arrows indicate flow along the bottom (z1).

Although the main arm of the AC moves southwards out of the shown domain (where it will retroflect), AC filaments show a seasonal mean influence on the outer WAB from spring

to autumn, creating a region of northwestward flow and warm oceanic waters. Together with the upwelling jet on the Inner-AB, west of Cape Agulhas, this northwestward flow contributes to the Good Hope Jet located off the Cape Peninsula. These jets are stronger on the surface than below and are not found at the bottom of the water column. Off the WAB, at the bottom between the 200m and 500m isobaths, the schematic shows the reverse flow seen in winter and spring.

On the Inner-AB, coastal flow in summer on the EAB is eastwards Figure 4.10, there is an offshore component to the flow of Plettenberg Bay, at the bottom flow is also eastwards. On the WAB, the Inner-AB near-surface flow is northwestwards, aligned to the coastline and joined the Good Hope Jet; currents at the bottom feed coastal upwelling and are onshore.

Chapter 5

The effect of the Agulhas Current on the Agulhas Bank 1: Description

The AC plays an important role on the AB. It contributes to the maintenance of the thermocline on the EAB by the advection of its warm waters and plumes at the surface whilst strengthening from below by mechanisms such as current-driven upwelling. Features of the AC such as meanders (like the Natal Pulse) and eddies and their associated plumes are often found on the shelf edge (Lutjeharms et al., 1989) and affect the circulation for the duration of their passing. While the AC generally follows the shelf edge, at the Agulhas Bight the AC has been shown to move onto the AB (Boyd et al., 1992) and may have dynamical consequences for the AB. Port Alfred located on the far EAB at approximately 26.5°E is a site of subsurface upwelling by the AC, winds then expose these cool waters to the surface (Lutjeharms et al., 2000).

The importance of the AC to this thesis, is that several authors have suggested the oceanic origin of the CR (Swart and Largier, 1987; Boyd and Shillington, 1994) and the AC and its features may possibly provide the mechanism that contributes to the formation of the CR. Hutchings et al. (2002) report sporadic upwelling at the shelf edge which enhances productivity. The Reference Experiment in Chapter 4 has shown that seasonal changes in the AC on the outer EAB produce seasonal changes in the behaviour of the upwelling of cool water onto the AB. This upwelling produced the seasonal doming of the cool water under the thermocline reproducing the CR. The CR was shown to be largest in summer and smallest in winter.

By removing the influence of the AC, the AB can be simplified. The main drivers are expected to be wind stress and solar insolation. In this chapter, the results of the Adjusted-

AB from the No Agulhas Experiment are used to describe the AB as a simpler shelf. Since Chapter 4 has shown that the largest contrast in the CR has been between summer and winter, the summer and winter means are explored in this chapter.

5.1 Model Results: Structure and circulation of the Adjusted-Agulhas Bank

5.1.1 Sea surface elevation

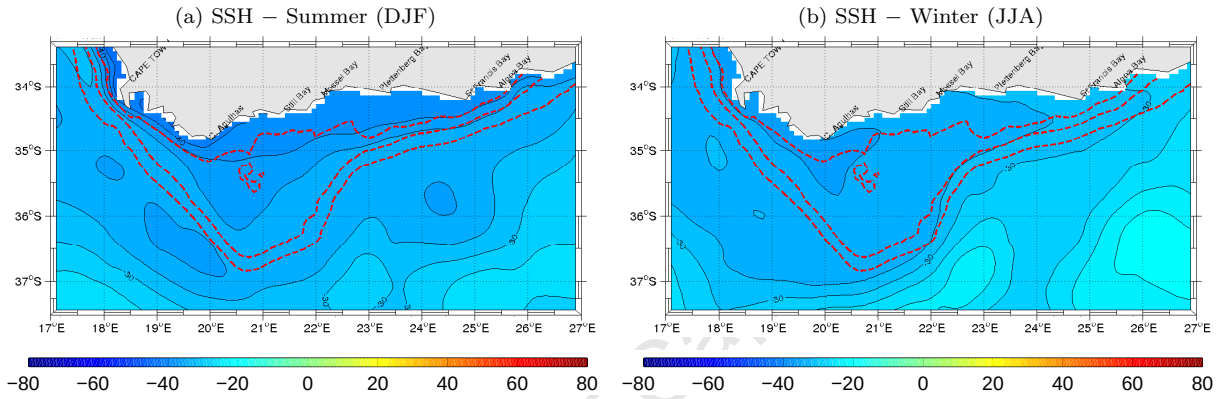

Figure 5.1: Seasonal mean model sea surface elevation (cm) for the No Agulhas Current Experiment. The same colour bar as 4.1 is used: negative contour intervals are 2.5cm apart, positive contour intervals 10cm, 0cm contour marked by magenta line. 100m, 200m and 500m isobaths plotted (red line).

Figure 5.1 shows the SSH over the AB and adjacent oceanic region without the influence of the AC. In the Reference Experiment, large positive SSH values (Figure 4.1) associated with the AC were obtained. In comparison to these strong features, the SSH in the No Agulhas Experiment is negative over the domain for both summer and winter.

Adjacent Oceanic Region

Without the AC supplying a steady flow in the seasonal mean, the mean flow off the shelf (beyond the 200m isobath) consists of mesoscale features. In the mean, these features are found away from the shelf and might not influence the AB. Off the EAB, the oceanic flow differs between summer and winter: the -32.5cm SSH contour level in summer (Figure 5.1a) is located offshore while in winter (Figure 5.1b) the contour is located around the 200m isobath. The position of this contour differs by over 1° of latitude from summer to winter, suggesting a difference in the oceanic regime off the EAB shelf in these seasons.

In winter (Figure 5.1b), at the southern tip of the AB there is an offshore gradient in SSH, therefore stronger currents are expected off the shelf in this region.

Off the WAB, the summer and winter mean SSH are similar. However, a core of low mean SSH is found off the WAB in summer (around 36–27°S, 19–20°E) which is not present in winter. This could suggest some recirculation in the mean, although the effect may be small. In the Reference Experiment, a cyclonic feature, which showed a drop in SSH of 10cm from the surrounding SSH, was found off the WAB in summer (Figure 4.1a). In comparison, the feature of the No Agulhas Experiment is small, 2.5cm lower than the surrounding region.

AB shelf

In winter (Figure 5.1b), the basic SSH structure over the AB remains similar to the Reference Experiment.

SSH contours over the EAB in summer (Figure 5.1a), suggests flow following the 100m and 200m isobaths. Where the shelf is narrow, such as east of Plettenberg Bay, the contours are closer suggesting that the flow is stronger there. This flow is not evident in winter (Figure 5.1a).

On the inner WAB and Cape Peninsula, low coastal SSH values in summer (Figure 5.1a), indicates coastal upwelling. The values obtained are comparable to the Reference Experiment, reinforcing the wind-forced nature of this region. The upwelling region on the WAB, in summer, appears to extend past Cape Agulhas up to approximately 21°E. The closely spaced SSH contours off the Cape Peninsula show that the speedy flow of the Good Hope Jet still remains and is a wind-driven feature. The -35cm SSH contour on the inner WAB is found at the same position in both experiments. This shows the coastal WAB is predominantly wind-forced.

Summary

Without the AC, the AB shows seasonal differences in the flow as suggested by the SSH. The low coastal SSH found on the Inner-WAB and off the Cape Peninsula confirm that this region is wind-forced.

Summer mean SSH on the AB, shows flow extending along the 100m isobath across the whole AB and is strongest where the topography is narrow, such as east of Plettenberg Bay and west of Cape Agulhas.

5.1.2 Horizontal Structure of the Adjusted-AB: Summer vs. Winter

Figure 5.2, Figure 5.3 and Figure 5.4 presents the seasonal mean summer and winter temperature, salinity and current speed with current vectors overlaid at a depth of 10m, 50m and z1, respectively. This shows the horizontal structure of the AB without the influence of the AC at depths representing the near-surface, above the thermocline (10m); mid-depth (50m) and representing the bottom boundary level (z1).

Without the AC, the subregions of the AB identified in the Reference Experiment are not readily distinguishable, especially as the driver of the Outer-AB (the AC) is absent. The Outer-AB and Mid-AB are analysed together as the previously defined limits, from the Reference Experiment, are not apparent.

Inner-AB / Coastline

Inner-AB: Cape-Agulhas – 27°E

Without the AC, seasonal changes are still found in this region. In summer (Figure 5.2a,c), 10m (near-surface) waters are warm and saline (20–21°C, 35.4–35.5psu) while in winter (Figure 5.2a,c) the waters are cooler and fresher (20–21°C, 35.4–35.5psu). Below this, z1 temperatures in this region are colder and fresher than the near-surface at 13–17°C, 35.1–35.2psu (Figure 5.4a and Figure 5.4c).

East of Cape Agulhas, coastal upwelling is not apparent in the temperature section at 10m, but a narrow band of less saline waters are observed along the Inner-AB as well as a tongue east of 24°E (Figure 5.4c). This could suggest coastal upwelling or wind-mixing.

Summer-mean currents on the Inner-AB, east of Cape Agulhas are generally westwards (Figure 5.2e, Figure 5.4e). However, between Plettenberg Bay and Algoa Bay, the mean currents are very weak (less than $0.1 m.s^{-1}$) and average out, such that there is no dominant current direction. There is an increase in the magnitude of current to $0.1–0.2 m.s^{-1}$, west of Mossel Bay. These currents could transport less saline waters from further east, westwards along the coast and contribute to the lower salinity band observed at the coast (Figure 5.2c) rather than local wind mixing or upwelling that was suggested previously. Currents are weaker at the bottom (less than $0.1 m.s^{-1}$) but also generally, westwards.

In winter, east of Cape Agulhas, near-surface currents (Figure 5.2f) are eastwards and aligned to the coastline thus appearing to be driven by the strong seasonal westerly winds in the region. Bottom currents in this region (Figure 5.4f) are slower, less than $0.05 m.s^{-1}$ (see

Appendix for enlargement) and vary in direction to the 10m currents. Instead, the winter bottom currents are rotated offshore as compared to that at 10m (Figure 5.4f, see Appendix for enlargement). This suggests downwelling: easterly currents at 10m would cause onshore Ekman transport which is then compensated by offshore movement through the bottom levels.

Inner-AB: Cape Peninsula – Cape-Agulhas

Coastal wind-driven upwelling is present in summer in this region, west of Cape Agulhas (Figure 5.2a,c). Isotherms and isohalines upwell along the coast resulting in decreasing temperature (and salinity) towards the coast: from 18°C (35.5psu) to 14°C (35.15) on the WAB and from 18°C (35.5psu) to 10°C (34.95psu) off the Cape Peninsula coast (Figure 5.2a,c). The upwelling structure of the Inner-AB is still observed in the temperature and salinity structure at 50m (Figure 5.3a,c) by the sharp offshore gradients. At z1, west of Cape Agulhas, bottom temperatures on the Inner-AB are colder and fresher than above, ranging from 9–12°C and 34.65–34.85psu.

Associated with this summer upwelling are coastal jets (Figure 5.2e). The upwelling jet off the WAB is a mean of 0.3–0.4m.s^{-1} and flows northwestwards along the Inner-WAB following the topography, moving around the Cape Peninsula. Off the Cape Peninsula, the WAB jet joins the Good Hope Jet off the Cape Peninsula of summer mean 0.4–0.5m.s^{-1}. The Good Hope Jet and Inner-WAB coastal upwelling jet weaken with depth as observed at 50m (Figure 5.3e) and are less than 0.1m.s^{-1} Figure 5.4e). Close to the coast, bottom flow is onshore indicating strong upwelling.

The Inner-AB in winter is horizontally uniform and vertically well mixed as seen at 10m (Figure 5.2b,d) and at z1 (Figure 5.4b,d). Off the Cape Peninsula in winter, the Inner-AB is cool at 14–15°C and salinity is lower at 35.25–35.35psu (Figure 5.2b,d, Figure 5.4b,d). The inner WAB is also vertically uniform with winter temperatures of 15–16°C found at 10m (Figure 5.2d) and z1 (Figure 5.4d). Currents in winter on the inner WAB are weak, less than 0.1m.s^{-1} (Figure 5.2f, Figure 5.4f) and northwesterly. This mean direction is maintained despite westerly winds in winter compared to east of Cape Agulhas which shows wind-driven eastward flow. However, westerly wind stress in winter for the model is weaker over the WAB region compared to further east (Figure 2.4c). Remnants of the Good Hope Jet are still apparent in winter at 0.1–0.2m.s^{-1} at 10m (Figure 5.2f) but not along the bottom, where currents are less than 0.05m.s^{-1} (Figure 5.4f).

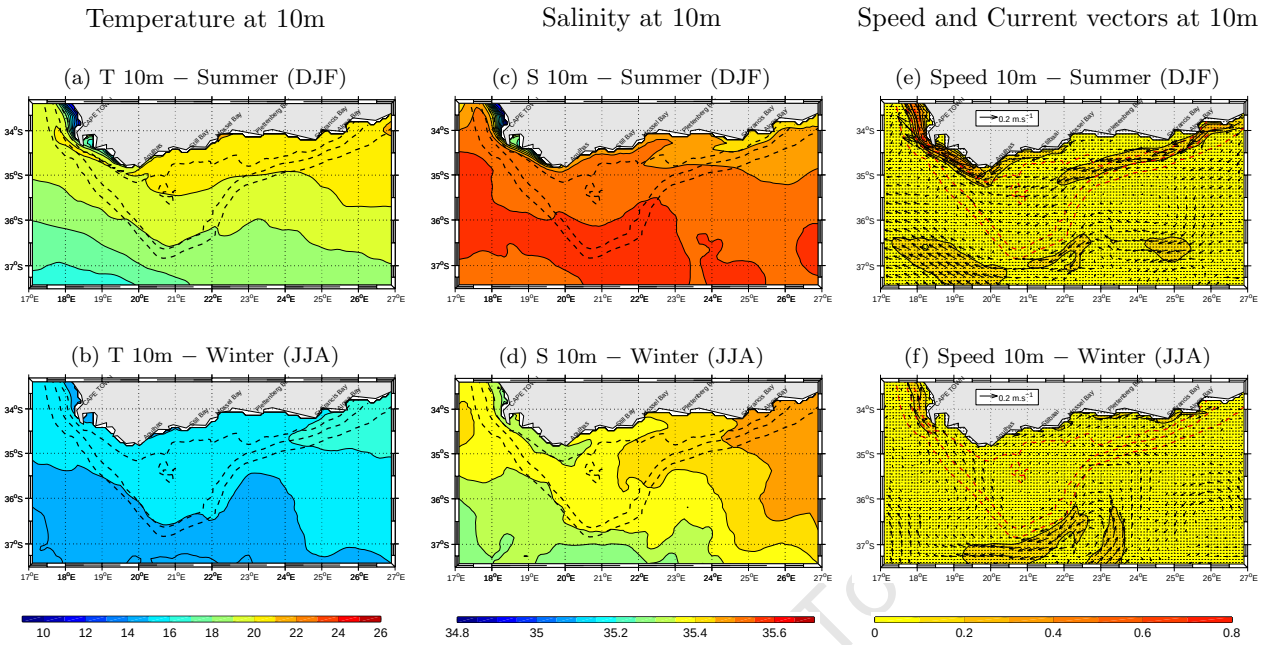

Figure 5.2: Seasonal mean structure (°C) of the Adjusted-AB at 10m without the Agulhas Current for summer and winter for: (a,b) temperature, (c,d) salinity and (e,f) current speed with overlaid current vectors.

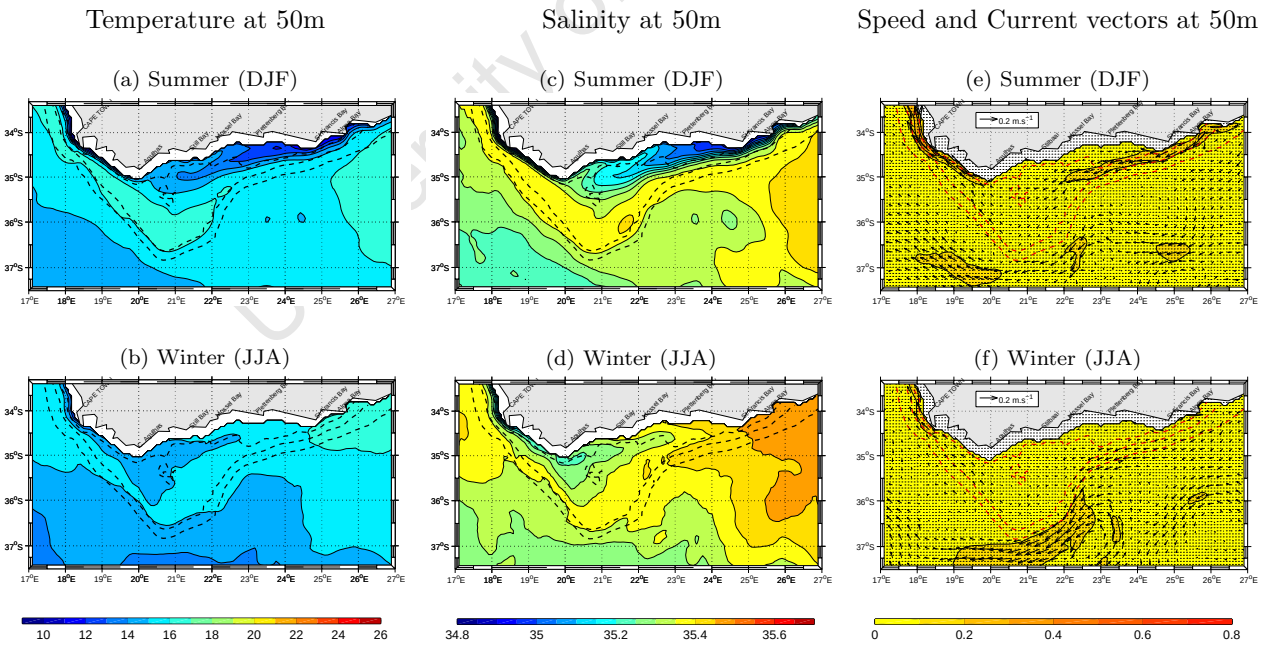

Figure 5.3: Seasonal mean structure (°C) of the Adjusted-AB at 50m without the Agulhas Current for summer and winter for: (a,b) temperature, (c,d) salinity and (e,f) current speed with overlaid current vectors.

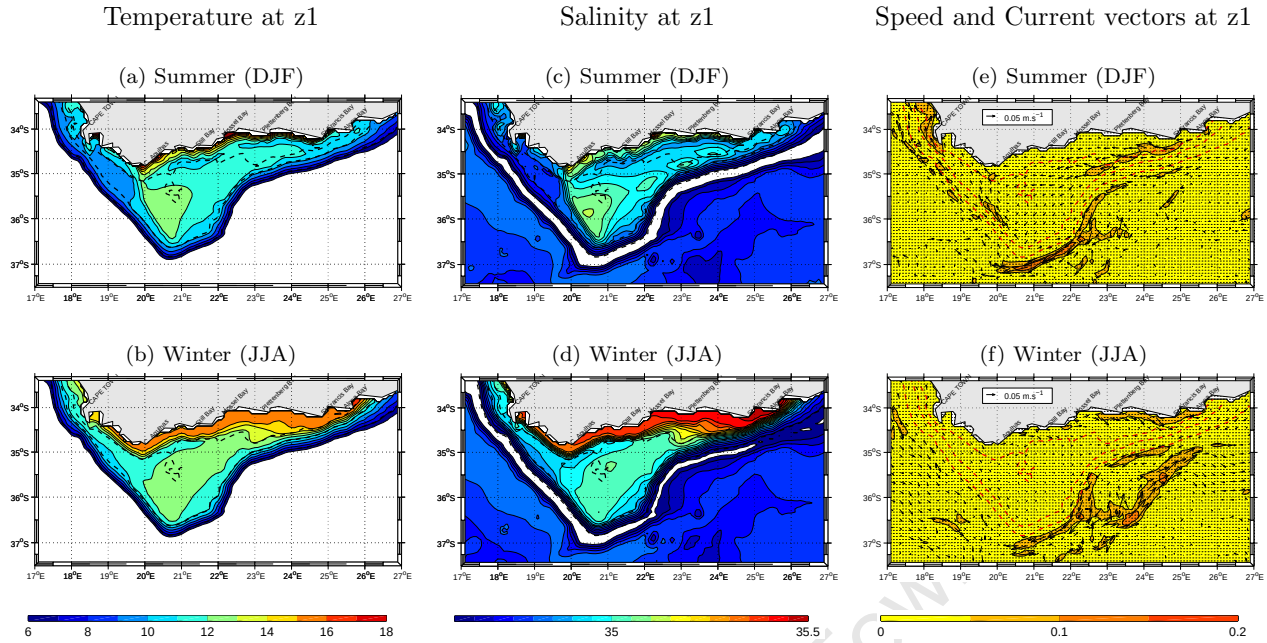

Figure 5.4: Seasonal mean structure (°C) of the Adjusted-AB at z1 without the Agulhas Current for summer and winter for: (a,b) temperature, (c,d) salinity and (e,f) current speed with overlaid current vectors.

Mid-AB and Outer-AB

The outstanding features of the Mid-AB and Outer-AB for the No Agulhas Experiment are: the near-zonal alignment of temperature and salinity contours observed at 10m (Figure 5.2a–d), with temperature decreasing polewards suggesting solar warming; and an alongslope surface jet on the EAB (which will be referred to as the "EAB jet".

General summer conditions for the Mid-AB and Outer-AB

In summer at 10m, the AB is warmer at the coast (20–21°C), cooling to the south to 18–19°C over the southern tip (Figure 5.2a), with the isotherms oriented zonally. The salinity (Figure 5.2c) is oriented similarly and ranges from 35.4–35.6psu. Summer waters at 50m are much cooler and fresher than above (11–18°C, 33.95–35.45psu) (Figure 5.2a,c). At z1, the bottom layer for the Mid-AB and Outer-AB within the 200m isobath ranges from 9–13°C, water colder than 9°C lies deeper than 200m (Figure 5.4a). Salinity along the bottom ranges from 34.5–35.15psu (Figure 5.4c). The WAB shows cold water of 9–10°C up to the 100m isobath. The EAB is slightly warmer. West of St Francis Bay (24.5–25°E), 10–11°C water upwells onto the shelf, crosses the 100m isobath and then moves westwards parallel to the coast. This water is bound inshore by the sharp thermal gradients associated with the Inner-

AB. The warmest bottom temperature is found Mid-AB in the region of 20–21°E (12°C and 35.0–35.15psu).

In general, without the AC, summer-mean currents over the AB (Figure 5.2e, Figure 5.3) are weak, less than 0.1m.s^{-1}. On the Outer-AB currents are oriented to the topography: east of the AB tip, the flow is southwestwards, aligned to the 200m isobath, while west of the tip, the flow is northwestwards. Mid-AB the flow is westwards. Bottom flow, between the 200 and 500m isobath, on the WAB is reverse / poleward (Figure 5.4e). Although weak mean flow is found at the tip of the AB, reverse flow on the EAB at this depth is also reversed (southwesterly), possibly a continuation of the deep poleward flow from the WAB.

In the region of the Agulhas Bight (23.5°E), limited cross-isobath flow is observed along the bottom in summer (Figure 5.4e). This flow crosses the 100m isobath and proceeds westwards.

General winter conditions for the Mid-AB and Outer-AB

In winter, conditions are horizontally uniform. Winter-mean waters at 10m range from 15—17°C (Figure 5.2b) and 35.3–35.5psu (Figure 5.2d). The EAB is vertically-well mixed with the same structure at 50m (Figure 5.3b, Figure 5.3d) as at 10m. The CAB and WAN are slightly cooler and fresher at 50m (4–15°C, 35.2–35.35psu). At the bottom, winter temperatures (Figure 5.4b) and salinities (Figure 5.4d) are colder and fresher (10–13°C, 34.8–35.1psu) than the upper layers, yet warmer than summer bottom conditions.

In winter, 10m and 50m currents in this region are weak (less than 0.1m.s^{-1}) yet variable (Figure 5.2f, Figure 5.3f). Mean-winter currents at 10m on the Mid-AB and Outer-AB show no dominant forcing. Mesoscale circulation patterns off the shelf may influence the Outer-EAB between the 200 and 500m isobath. Outer EAB currents are westwards, opposite to the currents within the 100m isobath, possibly due to oceanic influence. Mid-AB (20.5–22.5°E) shows no dominant current direction. For the WAB, the winter currents at 10m and 50m are similar to summer: northwesterly in direction. Bottom currents in winter (Figure 5.4f) are weaker than above (less than 0.05m.s^{-1}). On the WAB, flow is reversed, being southeasterly on the bottom as opposed to northwesterly at 10m and 50m. Between the 200m and 500m isobaths, the summer reverse flow on the WAB leading to the EAB is not evident. Bottom flow, between these isobaths, are southwesterly, corresponding with the oceanic flow.

EAB jet

Speeds at 10m (and to a limited extent at 50m), in summer (Figure 5.2e, Figure 5.3e) distinguish a jet of 0.1–0.2m.s^{-1} on the EAB between the 100 and 200m isobaths. This jet, is fastest where the shelf is narrow, in the region of Algoa Bay at 0.2–0.3m.s^{-1}. The jet appears to assist in distributing the colder, fresher waters further west across the AB, along the 100m isobath. At 10m, a lower salinity tongue is found in the region (Figure 5.2d). At 50m, temperature and salinity on the EAB (Figure 5.3b,d) is aligned to the 100m isobath, with the coldest and freshest waters (11–13°C, 34.95–35.05psu) constrained by the jet.

In winter, the jet is not present.

Summary

The horizontal description has shown that without the AC, the AB maintains a steady wind-driven Inner-AB while the Outer-AB has no distinguishing flow except for the EAB shelf jet. The summary is divided into the Inner, Mid and Outer AB.

Inner-AB

The Inner-AB in summer shows similar structure to that in the Reference Experiment with warm, saline near-surface waters east of Cape Agulhas. A band of lower salinity water along the coast between Cape Agulhas and Plettenberg Bay might suggest upwelling or local wind-mixing. Summer bottom temperatures on the Inner-AB are comparatively colder and fresher, suggesting a stable water column. In summer, near-surface and bottom currents east of Cape Agulhas are both westerly but weaker at the bottom, suggesting that coastal flow is wind-driven.

West of Cape Agulhas, near-surface waters are cold and fresh from wind-driven coastal upwelling in summer. West of Cape Agulhas, stronger coastal jets are found associated with wind-driven upwelling, at the bottom the currents are much weaker but display an onshore component, suggesting that upwelling along the bottom contributes towards replenishing surface coastal waters. However, off the Cape Peninsula, the Good Hope Jet appears to reach the bottom with slightly higher speeds than the surrounding region, directed similarly to the 10m flow.

In winter, the water column structure of the Inner-AB is vertically uniform. East of 21°E, 10m currents are eastwards possibly resulting in onshore Ekman flow which is compensated by downwelling along the bottom, as suggested by currents at the bottom. Despite westerly

wind stress, currents throughout the water column on the inner WAB are northwesterly and decrease in magnitude with depth. The Good Hope Jet is still apparent in winter although weaker than summer.

Outer-AB and Mid-AB

Despite the absence of the AC, near-surface summer waters on the Outer and Mid-AB are generally warm and saline. Temperature and salinity decrease with latitude. A well-stratified water column is suggested by colder and fresher waters at 50m and z1. The deeper layers of the WA B are colder and fresher than that of the EAB.

Without the AC, flow over the Outer- and Mid-AB in summer, is generally weak except for the jet on the EAB. Bottom poleward flow is found between the 200m and 500m isobaths on the WAB which may join the flow on the EAB at the same depths.

In winter, without the influence of the AC, 10m temperature and salinity on the Outer and Mid-AB are horizontally uniform. Vertically, the EAB is well-mixed with temperatures at 50m the same as above. Bottom temperatures are colder than shallower depths but warmer than summer. Winter-mean currents are weak (less than $0.1 m.s^{-1}$), the strongest flow is remnants of the Good Hope Jet. No dominant current pattern is found on the Outer and Mid-AB at 10m and 50m, the Outer-EAB currents are westwards, opposite to the currents within the 100m isobath. On the outer WAB currents at 10m and 50m are northwesterly in direction.

EAB jet

The EAB jet is observed at 10m and 50m in summer only. It is located and oriented between the 100m and 200m isobaths with mean speeds of $0.1–0.3 m.s^{-1}$, significantly weaker than the AC.

5.1.3 Vertical Structure of the Adjusted-AB: Summer vs. Winter

Figure 5.5 shows the vertical structure in the No Agulhas Experiment, for sections on the WAB, CAB and EAB. The location of these sections are shown in Figure 2.6 and are the same as used in the Reference Experiment.

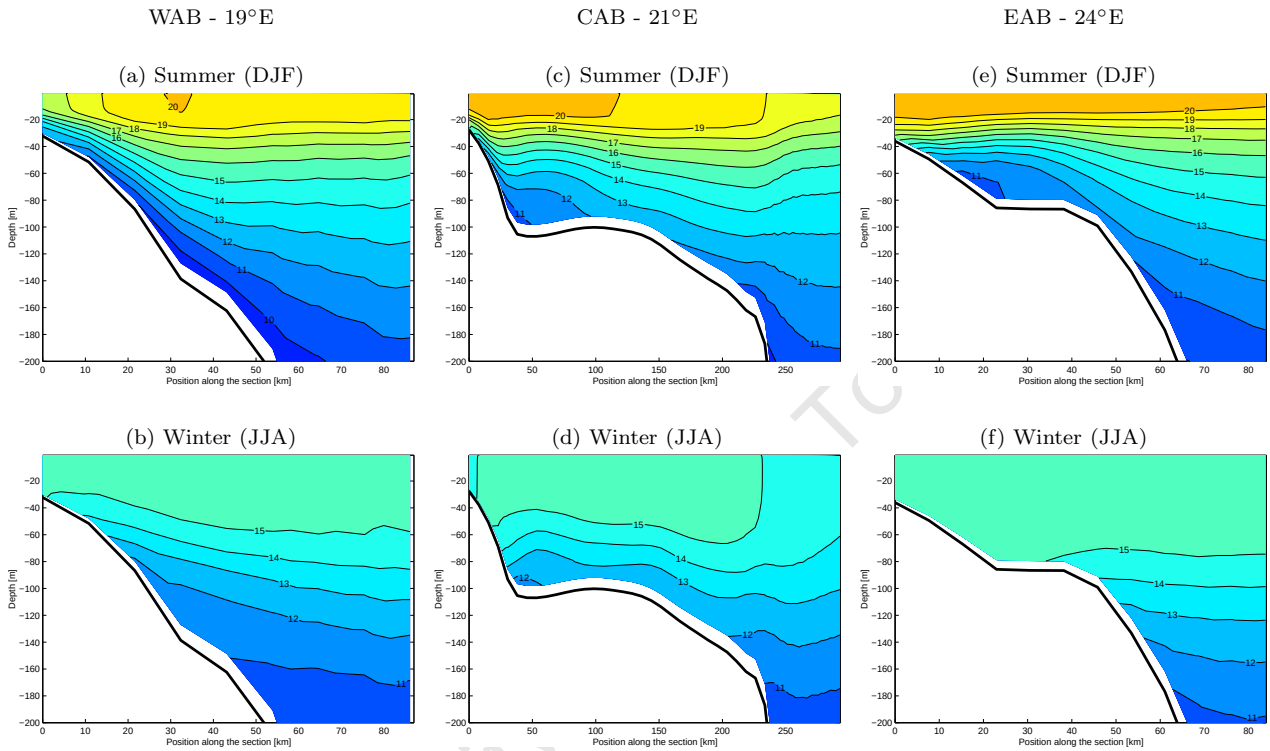

Figure 5.5: Seasonal mean vertical temperature structure (°C) up to 200m depth for the WAB (19°E) in (a) summer and (b) winter; the CAB (21°E) in (c) summer and (d) winter; and the EAB (24°E in (e) summer and (f) winter, without the Agulhas Current. Contour intervals are 1°C.

WAB

Figure 5.5(a,b) shows the vertical section representing the WAB. In summer (Figure 5.5a), the surface layer is warm and the water column appears stable and stratified. Isotherms are generally flat but within 45m of the coast and along the shelf bottom, isotherms are tilted upwards to the coast.

Outer-AB and Mid-AB

In summer (Figure 5.5a), a surface layer of 18–21°C water, approximately 30–40m thick, overlies cold waters. Below this surface layer, cold waters (9–11°C) upwell along the slope

and shelf bottom and upward toward the coast. These cold waters reach bottom depths of 50m but do not reach the coast.

Winter isotherms (Figure 5.5b) over the shelf and slope are relatively flat compared to summer (Figure 5.5a), where isotherms along the shelf bottom. The winter surface layer is horizontally uniform at 15–16°C and vertically well-mixed to 40–60m depth. The shelf bottom in winter is lined with waters of 11–15°C. Cold waters, less than 11°C, found below 150m. The slight tilting of isotherms on the shelf, within 50km of the coast, do not appear due to coastal wind-driven upwelling but could be attributed to the effect of northwestward currents as seen at 50m (Figure 5.3e).

Inner-AB

In summer (Figure 5.5b), wind-driven upwelling brings waters of 17–18°C to the surface at the coast.

In winter (Figure 5.5b), no upwelling is found at the coast; instead the surface layer is uniform at 15–16°C and 30m deep at the coast deepening offshore.

CAB

The CAB is represented by the vertical section at 21°E, this is shown in Figure 5.5(c,d). Three regions are distinguishable in this section in summer and winter: the oceanic waters located off the shelf; the shelf waters, which are stratified and relatively flat; and the coastal region.

Outer-AB

In summer (Figure 5.5c), oceanic waters off the CAB are slightly colder then over the adjacent AB in the upper 100m (13–19°C). Thus isotherms tilt downwards onto the shelf over the shelf-edge. Below 100m, 10–12°C waters upwell onto the shelf-edge.

Winter oceanic waters are cooler than on the AB, with a surface well-mixed layer of 14–15°C extending to a depth of 80m. The shelf-edge below 140m is similarly cold as summer at 10–12°C but this water does not reach as far up the shelf as summer.

Mid-AB

Between the shelf edge 100km offshore, the summer water column consists of flat isotherms with a warm upper mixed layer of 18–20°C of 30–40m depth, overlying waters of 11–18°C

(Figure 5.5c). Closer to the coast, within 100km, the surface layer is slightly warmer (20–21°C).

Below this upper layer, centered at 50km, is a doming of colder isotherms over water of 10–12°C. This cold water (30m thick) is not connected to bottom waters overlying the shelf of this section. Instead, summer bottom currents in the region (Figure 5.5e) are westerly, suggesting that the origin of this colder water is further east.

Winter surface waters over the shelf are 15–16°C and 50–60m thick (Figure 5.5d). Below this well-mixed surface layer, cooler waters of 12–15°C line the bottom of the AB. These are similar to general summer bottom temperatures.

As in summer, centered at 50km offshore, doming of cold waters are found below the surface layer, a thin (10m) layer of 11–12°C lies at the bottom, in the region of the 100m isobath. In the summer, the origin of these cold waters are from the east, however, the horizontal bottom currents (Figure 5.4f) in this region are easterly and the bottom temperature (Figure 5.4b) in this region, as seen in the horizontal, appears to be part of the WAB.

Inner-AB

In summer, within 30km of the coast, the upwelling of isotherms on the Inner-AB suggests wind-driven coastal upwelling (Figure 5.5c). However, in the seasonal mean, upwelling is not strong enough for the uptilted isotherms to breach the surface.

In winter (Figure 5.5d), the isotherms within 40km of the coast, downwell. Within 10km of the coast, the waters are uniform at 14–15°C to the bottom, down to 30m from winter mixing.

EAB

The vertical temperature sections representing summer and winter for the EAB (24°E) are shown in Figure 5.5(e,f). The summer compared to winter sections are notably different both in temperature and in structure.

Outer-AB

In summer (Figure 5.5e), a warm (18–21°C) surface layer of approximately 30m overlies the EAB section. Below this, isotherms upwell over the shelf edge bringing 11–12°C water onto the shelf bottom. This upwelling appears comparatively different to the doming under the AC in the Reference Experiment (Figure 4.6j). The incline of these isotherms could

possibly be due to the jet on the shelf edge (Figure 5.3e).

Winter temperatures for the EAB (Figure 5.5f), show a well-mixed upper layer of 15–16°C extending down to 70m depth. Below the upper layer, isotherms are flat with temperatures of 13–15°C found at the shelf edge. Water colder than 11°C lies below 180m. The uptilted isotherms seen in summer are not observed in winter, possibly as horizontal currents show that the EAB shelf-edge jet is not found in winter (Figure 5.3f).

Mid-AB

On the shelf, the isotherms are flat in summer (Figure 5.5e). Between 10–20km offshore, 10–11°C water is located on the shelf bottom, between 60 and 80km. This water does not upwell over the shelf edge but enters the AB further east as seen for the bottom temperature (Figure 5.4a).

In winter, the water column on the shelf is vertically uniform with the 15–16°C water mixed down to the bottom (Figure 5.5f).

Inner-AB

Coastal upwelling in summer is not found on the Inner-AB for this section (Figure 5.5e). Isotherms at the coast are flat and temperatures range from 16–17°C at the bottom to 20–21°C at the surface.

The inner EAB in winter, is vertically well-mixed to the bottom at 15–16°C, similar to the rest of the shelf in this section (Figure 5.5f).

Summary

General vertical structure

The vertical sections have shown that the AB is highly seasonal without the AC present. In summer, the AB is covered by a warm (18–21°C) surface layer of 20–40m while in winter, a deeper colder (15–16°C) surface layer develops, with depths exceeding 40m. Below the surface mixed-layer, the structure over the AB also shows marked differences between summer and winter.

Inner-AB

On the WAB, summer upwelling is observed with cold waters upwelled along the shelf bottom and the upwelling of isotherms at the surface. Evidence of weak summer upwelling is

shown by the uplift of isotherms up to the coast but not strong enough to breach the surface. On the EAB, no discernible upwelling is present, instead a highly stratified water column is found at the coast with a deep warm surface layer.

In winter, the Inner-AB is well mixed down to the bottom, Downwelling is suggested for the CAB.

Mid-AB

In summer, a warm surface layer overlies colder waters. However, these cold waters behave differently in each of the sections in summer. For the WAB, these cold waters upwell along the shelf bottom. The CAB and EAB show small domes of cold (10–12°C) water in this region. Bottom currents suggest that these waters are advected from further east.

In winter, the Mid-AB shows a cold deep surface layer. It deepens from west to east, with the EAB vertically uniform to the bottom. The cold dome / patch on the CAB decreases in size and what remains appears to be linked to flow from the west.

Outer-AB

Summer, warm waters over the Outer-AB are an extension of that observed on the shelf. For the CAB, differences between the surface waters of the oceanic region and the outer shelf is observed, with the former region being colder. Below the surface layer, on the outer EAB in summer, isotherms tilt upward probably in response to the EAB shelf-edge jet.

Except for the CAB, where oceanic waters are colder in winter, the Outer-AB and adjacent oceanic region are vertically well-mixed to similar depths as that on the shelf. Outer EAB uptilted isotherms are not observed in winter.

5.1.4 Model Comparison: The vertical structure at 24°E

In Chapter 4, the CR was plotted at 20m, which was the depth for largest lateral extent of the CR in summer (Figure 4.2b,f). The No Agulhas Experiment, in comparison, does not show a comparable CR structure and therefore only the vertical sections will be compared. The vertical section for temperature, salt, and speed and density across 24°E is shown in summer for the No Agulhas Experiment (Figures 5.6d–f). Same vertical sections across 24°E for summer for the Reference Experiment is included for comparison(Figures 5.6a–c). No ridging of isotherms at this longitude for the No Agulhas Experiment was observed in winter (Figure

5.5) thus this season has not been included in this analysis but is shown in the Appendix. This also shows the vertical section through the EAB jet. The vertical temperature section has previously been discussed in context of the EAB. This section, focuses on the CR or the doming of cold water.

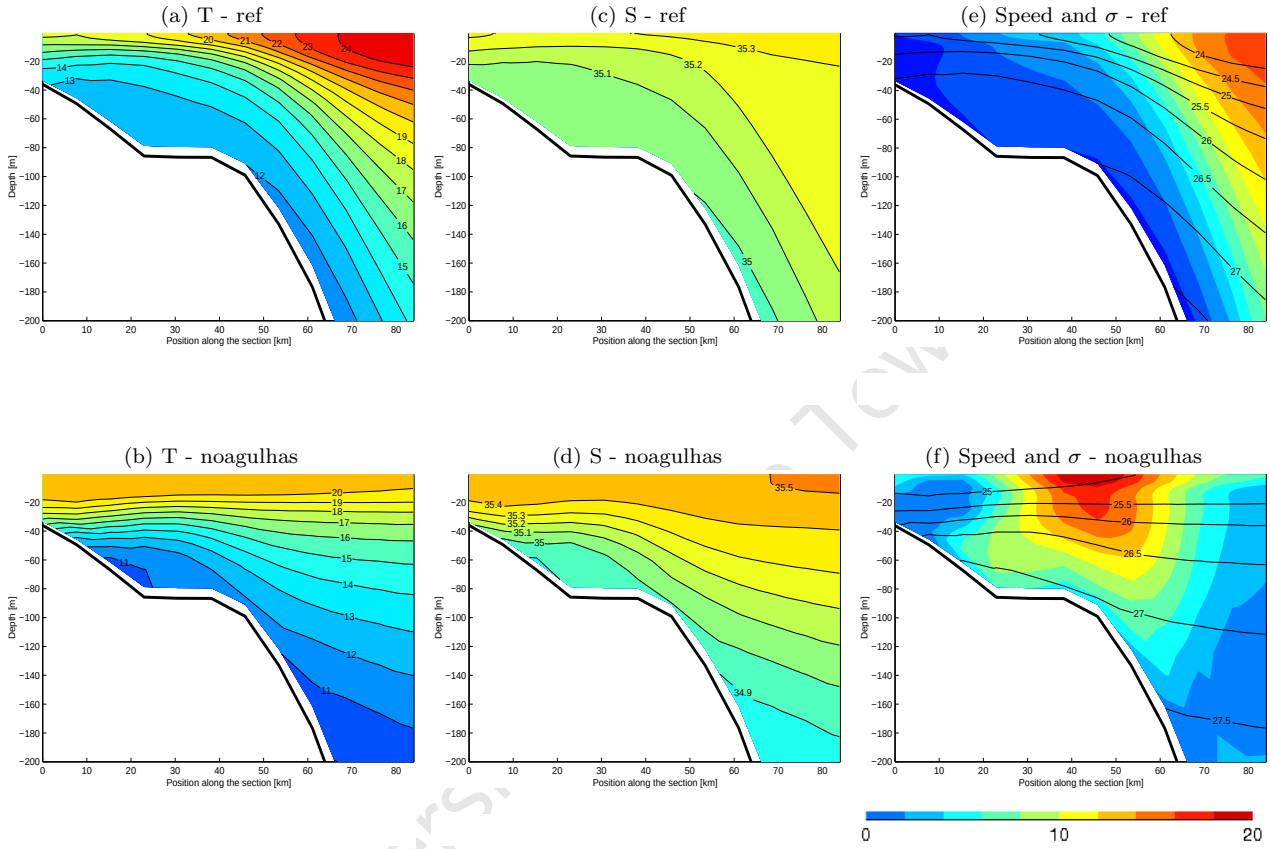

Figure 5.6: Comparison of the vertical sections at 24°E for the Reference and No Agulhas Experiment. Displayed are the summer (DJF) mean (a–b) temperature (°C), (c–d) salinity (psu) and (e–f) speed (cm.s^{-1}) with density (σ) contours (kg.m^{-3}) overlaid. Speed contour interval is 2cm.s^{-1}, density contours are 0.5kg.m^{-3}.

Vertical structure at 24°

Figures 5.6(d–f) shows the doming of isotherms, isohalines and isopycnals over the shelf edge at 24°E for the No Agulhas Experiment. In summer, it shows cool water of 10–12°C (34.8–35psu) lying along the bottom in a 30–40m thick layer. In summer, the water column is capped by warm upper layer. Below this layer, there is limited uplift of the contours over the shelf edge. The thermocline does not dome over these cold waters as observed in the Reference Experiment (Figure 5.6a).

Role of the EAB jet

The vertical temperature structure in the previous section suggested that the source of the coldest waters are further east, upwelled near Cape St Francis (Figure 5.4). Also suggested, was the influence of the EAB jet on the uplift of isotherm observed over the shelf edge. The vertical speed section, shows the influence of the EAB jet (Figure 5.6f). Centered roughly over the 100m isobath at 24°E, the jet is strongest at the surface in summer, exceeding 18cm.s^{-1}. The jet does reach throughout the water column, with weak bottom speeds of 4–6cm.s^{-1}. The jet does not appear strong enough to cause Ekman veering along the bottom (Figure 5.2e and Figure 5.4e). Instead, cross-isobath flow occurs to the east of this region where the shelf is narrower and the current slightly faster. Thus, the jet may influence the structure of isotherms but does not actively advect cool waters onto the shelf.

Isopycnal structure

Isopycnals at 24°E (Figure 5.6f), shows the EAB in the No Agulhas Experiment to consist of relatively flat contours. The Reference Experiment, on the other hand, showed large doming of the isopycnals and the 26.5 isopycnal was used to infer the location of the CR (Figure 5.6c). The oceanic structure in the two experiments are remarkably different. At 200m offshore, the 26.5 sigma contour in the No Agulhas Experiment is found at approximately 60m depth, and similar waters are found on the adjacent AB. In comparison, the Reference Experiment shows this contour at 140m, significant doming of these waters are required to reach shallower depths and to move this water onto the shelf. The AC, as in the Reference Experiment, depresses the offshore density structure such that the CR waters require an active method of reaching the AB, such as Ekman veering.

Summary

In the No Agulhas Experiment, cold water is present at the bottom of the AB from offshore. Cold water also enters this section along the bottom from further east. These waters are constrained below 40m) under a thick layer of warm water at the surface.

Although, the EAB jet uplifts the isotherms this effect is weak and little doming occurs at 24°E. Compared to the Reference Experiment, the current on the EAB is weak and doming of isopycnals is minimal for the Adjusted-AB.

The vertical density structure in this experiment is relatively flat. This suggest that the AC plays a large role in both the offshore structure and the observed doming of the CR.

5.2 Discussion

This chapter has described a simplified AB without the influence of the AC. In other words, the influence of a strong current (greater than 0.8m.s^{-1}), transporting warm saline waters along its shelf edge, is absent. In the No Agulhas Experiment, the SSH contours showed that the dam effectively reduced the effect of the the AC off the AB.

The Outer-AB

The Outer-AB without the AC

The AC, with its high SSH levels as seen in the Reference Experiment, was not discernible on the Outer-AB. Without the AC and the AC filament, waters on the Adjusted-AB and surrounding oceans are generally colder. Thus, colder waters than in the Reference Experiment are found along the bottom of the AB. In the vertical, the warm waters and the doming of isotherms along the slope and over the shelf edge of the AC are absent. Instead, the isotherms lie relatively flat across the shelf and slope. In general, the Adjusted-AB shelf showed horizontally uniform temperatures, with warm waters at 10m and cooling vertically through the water column. A warm upper-mixed layer, thicker than in the Reference Experiment, overlies the water column confining water colder than 16°C to depths below 40m. Noticeably absent, when compared to the Reference Experiment, is the cool, less saline tongue observed at 10m. Without the warming stabilising effects of the AC on the Outer-AB, the whole shelf is subject to wind mixing in winter. This is most noticeable for the EAB.

The EAB jet and WAB currents

The removal of the AC for the Adjusted-AB did not reduce all the currents on the Outer-AB. SSH contours on the EAB suggested flow along the 100m isobath which was found to be a jet-like flow with corresponding temperature and salinity structure. In the vertical, this flow corresponded to an uplift of isotherms below the thermocline. This "EAB jet", although significantly weaker than the AC at 0.1–0.3m.s^{-1}, advected colder less saline water below the thermocline from the east corner of the AB southwestwards across the AB, centered over the 100m isobath. The jet is stronger where the shelf is narrower, between 24.5–25°E. The origin of the EAB jet is not understood. It could possibly be attributed, by continuity, to the currents further west: strong coastal jets of the WAB and Good Hope Jet which flow along

similar isobaths.

Bottom currents suggest some Ekman veering occurs with cold waters moving up the shelf crossing the 100m isobath. This cross-isobath flow brings colder water further onto the slightly warmer, more saline AB, where it moves westwards constrained to the north by the structure of the Inner-AB.

Without the AC, the WAB still experiences northwesterly flow albeit to a smaller magnitude (less than 0.1m.s^{-1}). In the Reference Experiment, the currents on the outer WAB were attributed to the AC filaments on the shelf edge. This suggests, that without the AC filament, the Good Hope Jet may play a role in influencing flow on the WAB.

The Inner-AB

SSH contours confirm the Inner-AB to be wind-driven with similarly low SSH as in the Reference Experiment, particularly in the upwelling regions in summer and winter mixing in the region of Cape Agulhas. The Inner-AB, as well as displaying similarly low SSH level in summer and winter as the Reference Experiment, displays similar structure and currents, reinforcing the notion that it is sensitive to wind fluctuations. In summer, upwelling is comparable in the two experiments and current direction is easterly.

The Inner-AB: CAB and EAB

On the CAB, the surface is warmer and there is weak upwelling of isotherms at the coast. In the Reference Experiment, the coastal CAB showed flat isotherms. This shows that the winds used in these experiments are capable of causing weak upwelling and the lack of coastal upwelling in the Reference Experiment is due to other effects related to the AC. For the EAB, in the Reference Experiment, cool waters were available higher in the water column than in the No Agulhas Experiment, the AC may play a role in bringing cool waters to the upper layers near the coast. Thus event-scale upwelling, by relatively weak winds that are found on the AB, is possible.

The Inner-AB: WAB

Coastal upwelling on the WAB is similar to the Reference Experiment, although the bottom waters are colder. The WAB coastal jet in summer is of similar magnitude to that in the Reference Experiment (0.3–0.4m.s^{-1}). However, current speeds associated with the upwelling front off the Good Hope Jet are weaker in this experiment. In Chapter 4, the model

showed that the Good Hope Jet was not solely wind-driven but was also a continuation of the northwesterly flow on the outer WAB, the Good Hope Jet was still present in winter despite strong westerlies although weaker 0-3–0.4m.s^{-1}. In the No Agulhas Experiment, the northwesterly flow on the outer WAB is diminished yet the signature of the Good Hope Jet is still found in this experiment at 0.1–0.2m.s^{-1}. This could be due to the converging of the weak flow on the WAB onto the narrow shelf off the Cape Peninsula or from non-local effects further north, out of the domain.

The Cool Ridge

Influence of the EAB jet on the EAB cool tongue

The CR, as observed in the Reference Experiment, is not found in the No Agulhas Experiment. However, the EAB jet found along the length of the AB as well as localised Ekman veering is able to produce a perceptible cool tongue at 50m. The EAB jet caused cold waters below the surface layer to uplift, but the coldest waters (10–11°C) were sourced from further east. On the EAB, Ekman veering near St Francis Bay upwelled these waters which were then driven laterally westwards by currents on the EAB. The influence of this water is small in comparison to that observed in the Reference Experiment. The cold shelf-upwelled water lies deep in the water column, below 60m, capped by flat isotherms and a warm upper mixed layer. It is approximately 10km wide at 24°E. Thus, although a single source of cold water combined with weak westward flow may move cold water across the AB, a larger influence is required to produce the vertical doming associated with the CR as observed in the Reference Experiment. Thus, making cold nutrient-rich water available at shallow depths.

The role of oceanic density structure on the CR

Also to be considered, is the source of cool waters. In the previous experiment, the CR waters are pumped up the slope over a larger vertical distance. In the No Agulhas Experiment, similarly cold waters are already available at the bottom of the AB and the shelf edge, with the isopycnals shown to be relatively flat. Stronger currents are required to interact with the slope and more Ekman veering. The offshore density structure may play also a role in assisting this uplift. Thus allowing cool waters to upwell along the bottom, pushing the thermocline closer to the surface to be eroded by the winds. The density structure of the AC, causing vertical doming onto the shelf, contributes to the CR in addition to the AC speed, which affects the amount of Ekman veering.

Chapter 6

The effect of the Agulhas Current on the Agulhas Bank 2: Diagnosis

The Reference Experiment and the No Agulhas Experiment have shown that the CR on the EAB is primarily forced by the AC. The CR is determined by the vertical thermal structure imposed by the AC as well as the speed of the AC on the EAB which affects the cross-isobath advection by Ekman veering. Solar heating and the winds have also been excluded as drivers of the model CR for the Reference Experiment. Thus, the model CR results from a combination of heating and cooling by advection, particularly at depths of 50m and deeper. Transient features such as the onshore/offshore movement of the AC as well as the passage of eddies and plumes are reported to alter the thermal structure and circulation on the EAB, for example Swart and Largier (1987) showed the doming of cold water onto the EAB within a cold-core frontal eddy enclosed within a reverse plume. However, unless these features are long-lived, they will not be included in the calculated seasonal mean which was previously discussed.

To further discuss the heating and cooling of the AB, the temperature and velocity of the Reference Experiment and the No Agulhas Experiment are directly compared by exploring the temperature differences in the two experiments. This may help in elucidating the effect of the AC on the AB. To further investigate the heating and cooling by the AC, the heat flux advection terms of the EAB are calculated. Heating and cooling on the WAB (not shown) are not as significant to that on the EAB and has not been included. The horizontal and vertical heat advection terms are discussed in this chapter. This analysis was performed at depths where the total heat budget in the region is balanced by only the advection terms and not wind-mixing and solar warming, etc. These depths are 50m, 100, and 200m. The annual

mean advection terms were divided into their mean and time-varying (eddy) components. Three advection terms dominated the advection balance and are discussed in this chapter: the horizontal mean advection, vertical mean advection and horizontal eddy advection terms. The vertical eddy term did not show a significant contribution to the total budget and therefore has not been included.

This chapter explores the differences in the temperature structure between the Reference Experiment and the No Agulhas Experiment. By comparing these two experiments, the effect of the AC on the AB can be further discussed. Furthermore, the heat flux advection terms are studied to investigate the contribution of cooling and warming on the EAB in the Reference Experiment.

6.1 Model Results: Model Comparison

6.1.1 Horizontal temperature difference

Figure 6.1 presents the temperature difference between the No Agulhas Experiment (noagulhas) and the Reference Experiment (ref). The temperature obtained in the No Agulhas Experiment is subtracted from the Reference Experiment (T_{diff} = T_{ref} - $T_{noagulhas}$). The difference between these two experiments provides a quantification of the influence of the AC. Red colours on the colour bar indicate that temperatures in the Reference Experiment are warmer than in the No Agulhas Experiment, i.e. the AC and its associated processes warm the region. In contrast, blue colours indicate that the AC cools the region.

Oceanic region: warming by the AC

Difference maps for 10m, 50m and z1 in summer (Figures 6.1a,c,e), show the marked warming of the region by the AC. Figure 6.1(a–d) shows a temperature difference of up to 7°C off the AB shelf.

The oceanic temperature difference between the Reference Experiment and No Agulhas Experiment shows a greater difference at 50m than 10m (Figures 6.1a–d). The contribution of solar warming in the No Agulhas Experiment, warms the surface waters in the absence of the AC (Figure 5.2a,b), thus accounting for the smaller temperature difference closer to the surface. In general, bottom temperatures (Figure 6.1e,f) deeper than the 500m isobath are relatively similar in both experiments.

On the Outer-AB, between the 200m and 500m isobaths, warming of 2–4°C is shown in

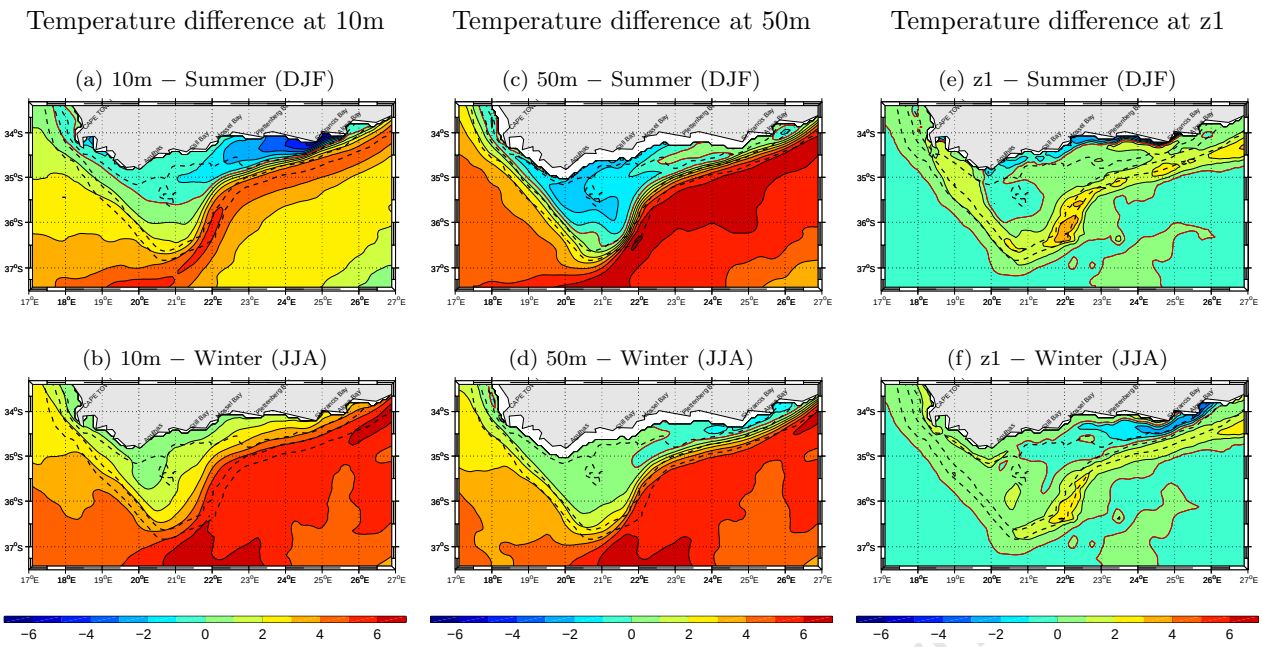

Figure 6.1: Temperature difference (°C) between the Reference and No Agulhas Experiment (T_{diff} = T_{ref} - $T_{noagulhas}$) at: 10m in (a) summer and (b) winter; 50m in (c) summer and (d) winter; and z1 in (e) summer and (f) winter. Contour interval 1°C. Red line indicates the 0°C contour. Positive / negative values (red / blue) indicate that the Reference Experiment is warmer / cooler than the No Agulhas Experiment.

regions directly affected by the AC. Without the AC, waters on the slope and off the shelf were generally colder (Figure 5.4a–b).

Effect of the AC on the outer EAB

The AC also appears to contribute to warming the Outer-AB. Difference maps for 10m, 50m (Figures 6.1a–d), show warming corresponding to the position of the AC and the AC filament. The AC appears to influences the EAB shelf up to approximately the 100m isobath.

There is little indication on the EAB slope of the cooling by Ekman veering due to the AC for the Outer-AB at 50m and the bottom (Figures 6.1c–f). However, cooling can be observed on the AB shelf, generally, within the 100m isobath.

EAB: 10m summer cooling and winter warming by the AC

On the shelf, temperatures are cooler at 10m and 50m in summer (Figure 6.1a,c) with the presence of the AC. At 10m in summer (Figure 6.1a), the similarity of the temperature difference structure with the observed mean temperature structure at 10m of the Reference Experiment (Figure 4.2) is observed. Cooling on the EAB in summer (Figure 6.1a) occurs in the tongue indicated by a temperature difference of 1–6°C. This coincides with the position of the cool tongue/CR observed at 10m in summer for the Reference Experiment (Figure

4.2b).

The tongue feature, indicating cooling in summer, is not found in winter at 10m (Figure 6.1b). Thus, the general effect of the AC serves to warm the upper water column in winter.

EAB: cooling by the AC at 50m

At 50m in summer (Figure 6.1c), temperature difference on the EAB is small (less than 1°C). Summer-mean temperatures are comparable at this depth, both experiments show similarly cold water lying aligned to the 100m isobath.

In winter (Figure 6.1d), 50m temperatures in the CR region show a difference of up to 2°C, showing that the CR cools this region in winter. Evidence of the CR from the Reference Experiment, can be seen as the tongue feature in the 50m temperature difference map between 22–23°E.

EAB: Bottom temperature differences

Along z1 (Figure 6.1e), summer temperatures appear warmer on the Inner-AB between Plettenberg and St Francis Bay. This is possibly due to slope waters in this region being warmer in the Reference Experiment. Thus Ekman veering of slope waters introduces warmer waters onto the shelf in this region.

In winter (Figure 6.1f), the CR region is 1–3°C cooler at the bottom with the AC present. Vertical winter mixing in the No Agulhas Experiment is to the bottom on the EAB (Figure 5.5e) which increases the temperature along the bottom as compared to the Reference Experiment in which cool water still upwells onto the shelf edge in winter, decreasing the temperature.

Mid-AB

The Mid-AB shows slightly cooler temperatures in summer (Figure 6.1a,c,d) in the Reference Experiment compared to the No Agulhas Experiment. Generally, temperatures in these regions vary by less than 1°C as this region is away from the Outer-AB. The largest influences are solar warming in summer and winter wind-mixing which should produce a similar water column in both experiments. However, summer temperature differences at 50m (Figure 6.1c), show this region to be 1–3°C cooler. Since flow on the AB in summer is westwards in both experiments, this cooling is attributed to the conditions to the east, on the EAB which at 10m and 50m are much cooler for the Reference Experiment. In the Reference Experiment,

Ekman veering on the EAB is greater and westward shelf currents slightly larger thus allowing cool water to uplift higher in the water column and move further west across the AB. Thus the effects of the AC reaches far across the AB.

Inner-AB: EAB

As with the Mid-AB, the inner EAB at 10m and the z1 in summer is cooler in the Reference Experiment (Figure 6.1a,e). At 10m (Figure 6.1a), away from the CR, the Reference Inner-AB is less than 1°C cooler.

Summer bottom temperatures on the Inner-AB, east of Cape Agulhas, are cooler by up to 3°C with the presence of the AC (Figure 6.1e). This is contrary to Chapter 4, in which the Inner-AB was prescribed to be dominated by wind effects and not the AC. This cooling can be attributed to the increased Ekman veering in the Reference Experiment, not only does the cool upwelled water move further west, it moves closer to the coast where eastward coastal currents would distribute this water.

Inner-AB: WAB

On the coastal WAB at 10m (Figure 6.1a), temperatures in the Reference Experiment are less than 1°C cooler. However, between 18.5–19°E, at the coast at 10m is 1–3°C cooler with the AC present. This is probably due to the influence of the AC filament on the WAB (Figure 4.6b) which helps tilt the isotherms upwards towards the coast as compared to the flat isotherms of the No Agulhas Experiment (Figure 5.5a), making upwelling of isotherms at the coast easier in the Reference Experiment.

Temperatures at the bottom (Figure 6.1e) are up to 2°C warmer in summer in the Reference Experiment. In Chapter 5, the No Agulhas Experiment showed that without the AC filament bringing warm water to the WAB region, colder waters are found higher in the water column, particularly along the bottom in summer. Thus, warmer bottom waters are found in the Reference Experiment than the No Agulhas Experiment. Warmer bottom waters contrast to the colder waters found at 10m and 50m. If waters that upwell in this region are sourced from the bottom, a similarly warmer signal would be observed for the shallower depths. This suggests that waters that upwell to the surface in this region, are sourced from mid-depth / the interior of the water column and not from the bottom.

In winter at 10m and z1 (Figure 6.1b,f), inner WAB temperatures are similar and differ by less than 1°C.

Summary

The AC warms the oceanic region adjacent to the AB and the Outer-AB, both in summer and winter. The effect of the CR and Ekman veering due to the AC is observed on the AB. It is observed as cooler temperatures on the EAB in summer, at 50m over the Mid-AB in summer and in winter along the EAB at 50m and z1. Bottom temperatures on the Inner-AB in summer, east of Cape Agulhas, are also cooler with the AC present.

Upwelled waters on the WAB are sourced not from the bottom but higher up in the water column. The structure of the AC filament off the WAB appears to influence coastal upwelling by altering the vertical structure. Thus the upwelling response to winds in summer is greater with the presence of the AC.

6.1.2 Vertical temperature difference

Figure 6.2 shows the temperature difference between the Reference and No Agulhas Experiment for the vertical sections across the EAB, CAB and WAB. The locations of these sections were shown in Figure 2.6. The positive (red) values indicate that temperature is warmer in the Reference Experiment, i.e. the AC contributes to the warming; while negative (blue) values indicates the temperature is cooler in the Reference Experiment.

WAB

Oceanic region

In the horizontal temperature difference maps (Figure 6.1), the warming of the Outer-AB by the AC filament was observed. In the vertical (Figure 6.2a–b), this corresponds to warming of the adjacent oceanic region of 1–4°C, extending throughout the water column. In Chapter 4, the AC filament was described to be a shallow feature in summer with deeper warming along the Outer-AB as an extension of the effect of the AC on the outer EAB.

WAB shelf

Cooling of the WAB was observed at 50m in the horizontal in summer (Figure 6.1c). In the vertical, this summer cooling (Figure 6.2a–b) extends from the surface at the coast to 60m deep at 45km offshore. Below this, the warmer bottom waters observed in the horizontal (Figure 6.1a), appears to be part of the warmer offshore waters. Thus suggesting that because the offshore waters are warmer due to the AC, warmer waters upwell along the bottom.

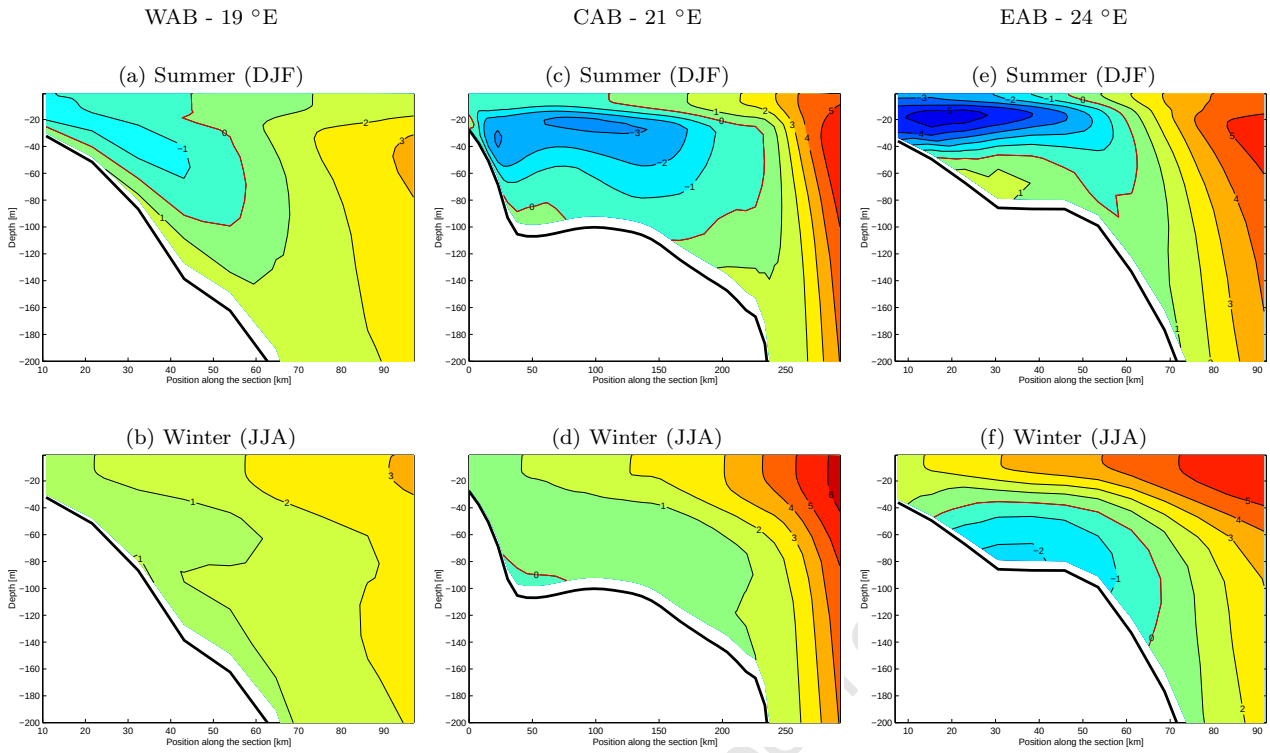

Figure 6.2: Vertical temperature difference (°C) between the Reference and No Agulhas Experiment (T_{diff} = T_{ref} - $T_{noagulhas}$) up to 200m depth for: the WAB (19 °E) in (a) summer and (b) winter; the CAB (21 °E) in (c) summer and (d) winter; and the EAB (24 °E) in (e) summer and (f) winter. Contour interval 1°C. Red line indicates the 0°C contour. Positive / negative values (red / blue) indicate that the Reference Experiment is warmer / cooler than the No Agulhas Experiment.

In winter (Figure 6.2b), vertical mixing at the surface confining cold waters to deeper in the water column is comparable in the two experiments, thus larger temperature differences are confined off the shelf where the AC warms the region, even in winter.

CAB

Oceanic region

In summer across the CAB (Figure 6.2c), the effect of the AC can be observed. Warming off the shelf, increases with offshore distance from the shelf break showing up to a 6–7°C difference approximately 300km offshore. Warming of the oceanic region by the AC is also found in winter (Figure 6.2d). In winter, due to surface cooling and deeper mixing from a weakly stratified water column, the temperature difference in the No Agulhas Experiment is greater in winter than summer.

CAB shelf

Summer cooling at mid-depth in the water column, similar to the WAB, is present for the CAB section which shows cooling up to 3–4°C (Figure 6.2c). The AB with the presence of the AC, is cooler even over the widest part of the shelf and away from direct AC forcing. Surface and bottom waters are comparable in temperature for the two experiments. At the shelf edge, the 1–2°C temperature difference is due to the effect of warmer AC waters from offshore in the Reference Experiment.

At the coast and over the shelf, where deep winter mixing occurs in both experiments, CAB waters are of comparable temperatures, generally less than 1°C different (Figure 6.2c).

EAB

Oceanic region

The vertical sections across the EAB shown in Figure 6.2(e–f), show the influence of the AC, warming the oceanic region off the EAB to depths greater than 200m. As described in the horizontal, the greater warming occurs below the surface by as much as 5–6°C in the summer section (Figure 6.2e).

In winter, the AC warms the oceanic region by up to 5–6°C as well as surface waters (in the upper 20m) on the adjacent shelf by up to 3–4°C (Figure 6.2f).

EAB shelf

Colder summer temperatures, with the presence of the Agulhas Current, are observed at the coast and upper 40–50m along the EAB section by up to 5–6°C (Figure 6.2e). This cooling was attributed to the CR in the Reference Experiment, as seen in the horizontal. The CR vertically cools the water column to shallow depths on the EAB. Summer bottom temperatures are comparable for both experiments. The structure of the -1°C difference contour coinciding with the 11°C isotherm of the No Agulhas Experiment in the summer mean vertical section (Figure 5.5e), suggests that the colder waters of the No Agulhas Experiment are due to the EAB jet which transports cold water from further east through this section at 24°E.

In winter (Figure 6.2f), the cooling on the shelf by up to 3°C is aligned to the bottom. In the No Agulhas Experiment, the EAB jet is not present and the water column over the shelf is vertically-uniform. Cooling in this region thus reflects the influence of the CR from the Reference Experiment which remains deep in the water column and does not progress closer to the coast as in summer.

Summary

In the vertical, the AC warms the oceanic regions adjacent to the EAB and the CAB as well as the WAB to a lesser extent.

Despite the apparent influence of the AC to warm, the presence of the AC cools the AB shelf in summer. Since both models have cold bottom waters, the effect of the AC in cooling the shelf is most noticeable at mid-depth in the water column.

Cooling by the AC, in the form of the CR, is prominent for the upper layers of the EAB in summer as well as at the bottom on the outer EAB in winter.

6.1.3 Thermocline depth difference

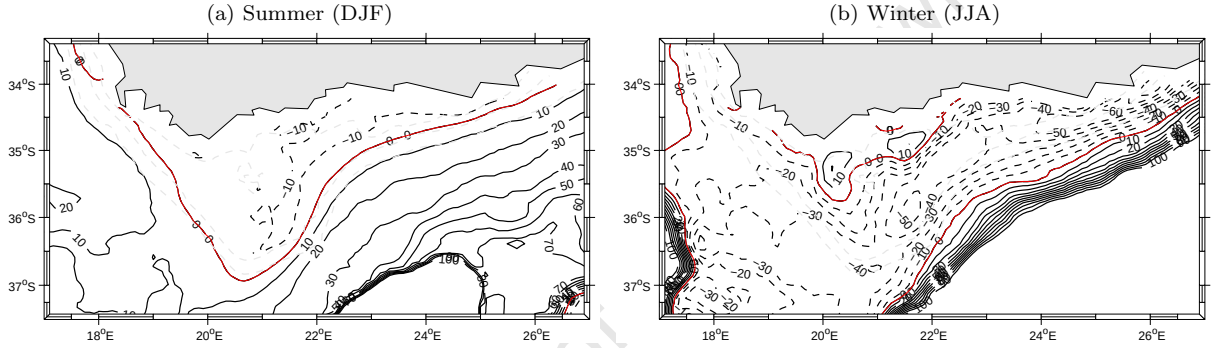

Figure 6.3: Seasonal mean thermocline depth difference (m) for (a) summer and (b) winter between the Reference and No Agulhas Experiment (depth_{diff} = depth_{ref} - $\text{depth}_{noagulhas}$). Contour intervals are 10m apart, red line indicates 0m. Positive (negative) values indicate that the thermocline is deeper (shallower) with the AC present and are shown as solid (dashed) lines.

Figure 6.3 shows the difference in depth of the thermocline between the No Agulhas and Reference Experiment. As in the Reference Experiment, the thermocline depth for each experiment was calculated individually as the greatest vertical temperature gradient and then differenced.

Summer thermocline difference

Figure 6.3(a) shows the difference in thermocline depth in summer. Summer thermocline depth difference indicates that thermocline over the Outer-AB and surrounding oceans are deeper with the AC present. Despite the thick warm surface layer overlying the AB of the No Agulhas Experiment, the thermocline is deeper in the Reference Experiment. The AC, in the previous section (Figure 6.2) warms the oceanic region through the depth of the shown

section, 200m, and serves to deepen the thermocline.

On the AB shelf in summer (Figure 6.3a), the thermocline in the Reference Experiment is 10m shallower on the EAB. This can be attributed to the cooling by Ekman veering / the CR in the Reference Experiment which uplifts the thermocline. The rest of the AB shows comparable thermocline depth.

Winter thermocline difference

In winter (Figure 6.3b), a marked difference in thermocline level between the two experiments is apparent. The oceanic region adjacent to the EAB shows similar differences to summer, marked by the deepening associated with the AC. These contours coincide with the offshore position of the AC in the Reference Experiment which lie offshore the 500m isobath. The Outer-AB and South Atlantic display a shallower thermocline in winter as compared to summer.

The influence of the AC on the outer WAB in winter is not as marked as summer but, as seen in the vertical temperature difference (Figure 6.2b), still contributes to warming this region and influencing the thermocline depth.

On the outer EAB, large differences in thermocline depth of up to 50m are shown. The large values observed on the EAB are due to the uniform water column in the No Agulhas Experiment in winter (Figure 5.5f) which contrasts to a comparatively shallower thermocline in the Reference EAB in winter. The EAB of the Reference Experiment showed a water column in which warm surface waters of the AC overlies cool CR waters (Figure 4.6f). The Reference Experiment thermocline for the Outer-AB remains shallower than that of the No Agulhas Experiment. Although the No Agulhas Experiment mixes down to deeper levels in winter, vertical mixing in the Reference Experiment is tempered by the influence of the AC.

On the Mid-AB, similar thermocline depths are found in winter for the two experiments. However, the thermocline in winter is 10m deeper in the Reference Experiment for the two regions which show the deepest mean winter mixing (Figure 4.5c). Although, the No Agulhas Experiment has shown deeper vertical mixing than the Reference Experiment, these two regions are deeper with the AC. It appears that although the thermocline destabilises and surface waters may mix in the Reference Experiment, cool bottom waters from further east continue to advect into the region, thus the maximum vertical temperature gradient lies deeper in the water column.

Summary

The AC serves to deepen the thermocline off the shelf by the movement of warm water over large depths, both in summer and winter.

In summer, the EAB shows a shallower thermocline as the effect of the CR in uplifting the thermocline is larger than the effect of the cool waters transported by the EAB jet in the No Agulhas Experiment.

In winter, the effect of the AC on the shelf is to limit the destabilisation of the thermocline and the depth to which mixing occurs.

In winter, the two regions of deepest mixing as seen in the Reference Experiment, appears to be due to the cool bottom waters from further east.

6.2 Model Results: Heat Equation Advection Terms

Figure 6.4 shows the annual-mean contribution of the horizontal and vertical heat advection from the mean component as well as the horizontal eddy advection term for the Reference Experiment. Depths shown are depths generally below the thermocline: 50m, 100, and 200m. These depths are below the surface mixed layer, where the equation of heat is mostly balanced by advection terms (i.e. where vertical mixing effects or short wave penetration are less important). The vertical eddy term did not show a significant contribution to the budget and therefore has not been included. Negative values indicate cooling while positive values indicate warming. The colour bar has been adjusted to show only the largest contributions to heating and cooling over the AB. At 500m the effect is not as marked (not shown).

Contribution of mean horizontal advection

Figure 6.4(a–c) shows the contribution of the horizontal advection by the mean flow in the heat equation at 50m, 100, and 200m. In the horizontal, the most significant warming by advection occurs east of 23.5°E and at the tip of the AB, at depths generally below the thermocline: 50m, 100, and 200m. This shows that the warming by the AC, observed in the vertical temperature difference in the upper 200m, is caused by the lateral advection of warm waters by the mean AC. Notably, at 26°E, 34.5°S, a strong mean flow (indicated by the streamlines) crosses a mean gradient of temperature, resulting in a large positive mean

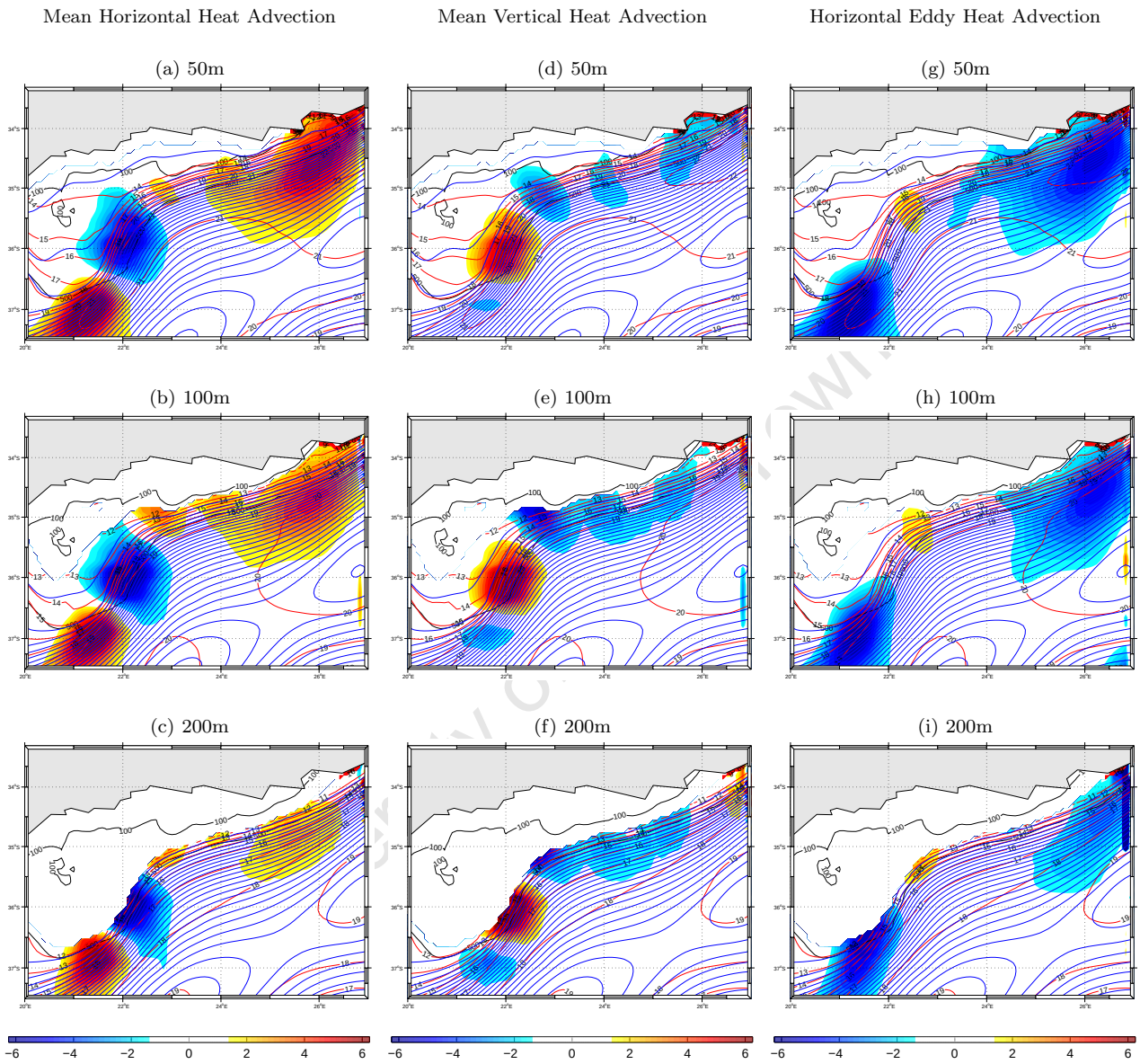

Figure 6.4: Annual mean heat advection terms (1x10^6 °C.s^{-1}) (a–c) horizontal mean ($\overline{u}\overline{T_x}$ + $\overline{v}\overline{T_y}$), (d–f) vertical mean ($\overline{w}\overline{T_z}$) and (g–i) horizontal eddy ($\overline{u'T'_x}+\overline{v'T'_y}$) terms for the EAB in the Reference Experiment. Red indicates warming, blue indicates cooling. Also displayed are the 100m and 500m isobaths (black), the streamfunction (blue) and isotherms (red).

horizontal advection term.

In the southern region of the Agulhas Bight (22°E, 36°S), the horizontal mean advection causes marked cooling. Even though, it was previously shown that, the AB is warmer with the AC as opposed to without, this represents the advection of waters within the Reference Experiment. Cooling occurs as the AC laterally advects cooler water from the shelf (as shown by the isotherms in red) away from the shelf along the path by the blue streamlines. The effect is diminished deeper in the water column as the offshelf temperature gradient decreases.

Contribution of mean vertical advection

Figure 6.4(d–f) shows the vertical mean contribution to heating and cooling the AB. East of 22°E along the Outer-AB, cooling occurs by the vertical advection of waters. At 200m (Figure 6.4f), the largest amount of cooling occurs. Higher in the water column the cooling moves closer inshore and decreases in magnitude as well as areas affected, at 50m marked cooling is found up to the 100m isobath (Figure 6.4d). This is consistent with the Ekman veering along the EAB shelf edge described in the Reference Experiment (Chapter 4), in which colder waters from depth move up the shelf by the interaction of the AC with the slope bottom.

Around the Agulhas Bight (22°E, 36°S), the cooling observed by the mean horizontal advection is balanced out by warming by the vertical advection of waters. Warming is strongest at 200m (Figure 6.4f). In this region, mean currents are parallel to the topography throughout the year (Figure 4.4i–l), in contrast to north of the region where Ekman veering occurs. Downwelling could produce vertical advection of warmer waters into the cooler waters.

Contribution of horizontal eddy advection

Figure 6.4(g–i) shows the contribution of heating and cooling by the horizontal eddy term or time varying motions. Marked results were due to variations in the horizontal eddy terms and not the vertical eddy term (not shown). Cooling east of 23°E and at the tip of the AB, by the horizontal eddy term balances out the warming by the mean horizontal advection term. The sporadic offshore movement of the AC is thought to produce divergence-driven upwelling, however, marked vertical cooling by the eddy term is not found. Rather, cooling occurs by horizontal advection, suggesting that offshore movement of the AC might be accompanied by the lateral offshore advection of cool shelf waters or, in the case of eddies, cooling is by the

horizontal movement of eddies as opposed to upwelling at the edges or center of the eddy.

Warming at the Agulhas Bight balances out the cooling observed by the mean vertical component, this probably relates to the movement the AC.

Summary

At depths between 50m and 200m, the total heat budget is almost totally balanced by three terms: advection by the mean in the horizontal, by the mean in the vertical and by the time-varying flow in the horizontal. Marked warming and cooling occur on the EAB, around the Agulhas Bight and the southern tip of the AB.

As a deep warm current, the AC laterally advects warm tropical water onto the edge of the EAB and adjacent ocean as seen in the upper 200m. This is balanced by the mean vertical motion by Ekman veering caused by the mean position of the AC and horizontal motion by transient flows. Horizontal transport of cooler waters associated with eddies and the horizontal movement of cold shelf waters were proposed as physical causes.

In the region of the Agulhas Bight, the AC overshoots onto the AB and turns polewards laterally moving the cool shelf water polewards or transporting the heat away from the AB. A slight warming is found north of the Bight where warm AC moves laterally in the mean as well as by the eddy component, this onshore motion contributes to warming the region further. This is balanced by cooling by the vertical mean component by Ekman veering. South of the Agulhas Bight, where the AC turn polewards lateral cooling by the mean is balanced by vertical heating in the mean.

At the tip of the AB, horizontal mean heating is balanced by cooling by the horizontal eddy term as well as a smaller contribution to cooling by the vertical mean. The mean position of the AC warms this tip of the AB, while movements of the AC or the passage of eddies and meanders cool the tip.

6.3 Discussion

In Chapter 4, the importance of the AC on the dynamics and structure of the AB was highlighted. Chapter 5 has shown that the AB without the AC is a cold shelf with very little current structure. This chapter has shown that the AC is responsible for much of the thermal structure and circulation on the AB.

Warming by the AC

In the horizontal, the AC is important for heating the slope (throughout the water column, down to the bottom) and surrounding oceans of the AB in both summer and winter. Temperature differences between the oceanic region adjacent to the AB with and without the AC are as much as 7°C. The largest contributions to heating and cooling are due to the advection of waters into the region at 50m and deeper. The most significant warming to the region is due to the lateral advection of the AC waters which are present in the mean. These warm waters deepen the thermocline off the AB.

Cooling by the AC

Although the AC primarily warms the Outer-AB and surrounding oceans, the presence of the AC shows the AB in the model to be cooler by up to 6°C, particularly at 10m and 50m in summer. This cooling is not overly apparent in the temperature difference at 50m and z1 on the EAB due to the cold bottom waters in both experiments in summer which are present by different processes (the No Agulhas Experiment Experiment by colder surrounding waters and limited Ekman veering and the Reference Experiment by active Ekman veering of slope waters along most of the EAB).

The cooling by the AC is clearly observed in winter. While the EAB of the No Agulhas Experiment in winter is vertically uniform from winter mixing, the Reference Experiment still experiences cooling from Ekman veering under the AC. The waters that cool the EAB come from deeper in the water column and are advected into the regions at 50m and deeper. A large contribution of cooling is the vertical advection of cool waters along most of the EAB due to the mean position of the AC.

In the Reference Experiment, Ekman veering was found on the slope in the seasonal means throughout the year but to varying extents. The amount of cool water on the EAB also varied seasonally, maximum in summer and minimum in winter. Thus, mean cooling in

the vertical of the EAB appears to be driven by Ekman veering under the AC by the mean position of the AC on the slope. Cooling on the EAB balances out the warming by the AC due to lateral advection of transient time varying features such as eddies and meanders of the AC. Vertical advection in these eddy processes may possibly contribute to cooling but, in the overall mean, their role is not a dominant one. Although vertical and horizontal eddy advection cools the AB at 50m and deeper, the tongue is also observed at 10m. The dominant contribution to cooling at 10m is not balanced by advection alone. Additional processes such as surface heating and vertical mixing must be considered to bring the waters to shallower depths. The combination of warming from the AC and cooling from Ekman veering, shows a shallower thermocline with the AC present as opposed to without it.

Indirect cooling by the AC

In the Reference Experiment, the influences of the AC were mainly ascribed to the Outer-AB. The influence of the AC on the CR and cooling the Outer-AB has been discussed above. The Mid-AB was characterised as a transitional region between the upwelling zone of the Inner-AB, determined by seasonal surface forcing with the additional influence of westward-moving cold waters upwelled in the Agulhas Bight. In this chapter's comparison, the AC was shown to indirectly affect the rest of the AB. Horizontal temperature difference maps show that bottom temperatures in summer of the Inner-AB east of Cape Agulhas as well as Mid-AB in summer at 50m to be cooler with the presence of the AC. In the vertical this was observed as cooler temperatures for the mid to upper water column for the WAB, CAB and EAB in summer for the Reference Experiment.

For the WAB, upwelling appeared similar in both the Reference and No Agulhas Experiment. In Chapter 5 (No Agulhas), it was noted that the bottom waters are cooler without the AC. However, this chapter has shown that, the mid to upper water column is cooler with the AC present. The colder bottom waters of the No Agulhas Experiment do not influence the waters that upwell to the surface at the coast. Instead, these waters are derived from shallower waters. Cooling by the AC is possibly due to the AC filament which depresses the isotherms offshore the WAB, possibly assisting in increasing the slope of isotherms in the upper layers across the WAB, preconditioning the shelf for further upwelling by equatorward winds.

For the Mid-AB, cool waters from further east particularly at mid-water column level adjusts the vertical structure. With stronger Ekman veering due to the AC in the Reference

Experiment, cool waters are available at shallow depths in the water column. These waters are then transported westwards with the mean westwards currents on the AB, cooling the mid to upper water column on the Mid-AB.

Summary

The AC is a major transporter of heat and salinity from the Indian Ocean to the Atlantic Ocean, around the AB. This chapter has shown that, in addition to determining the structure on the Outer-AB, the AC also affects the structure over the rest of the AB.

Chapter 7

Synthesis

This thesis has investigated the seasonal variability of the structure and circulation on the Agulhas Bank and the forcing of the cool ridge using output from a regional ocean model. In the literature review, it was shown that the Agulhas Bank is a dynamic region with various forcings and many interacting oceanic processes. However, the studies used to describe the Agulhas Bank in Chapter 1 (for example: Largier and Swart, 1987; Boyd and Shillington, 1994), used data of poor spatial and temporal resolution. This was insufficient to adequately describe the structure and circulation over the whole Agulhas Bank. Thus, the numerical ocean model, ROMS (Regional Ocean Modeling System), was used, which incorporated a one-way nested fine grid in a coarse-resolution parent model. Two experiments were performed: a climatological study of the Agulhas Bank (the Reference Experiment) and an Adjusted-Agulhas Bank model, with the Agulhas Current removed (the No Agulhas Experiment).

7.1 Summary of important results

The large-scale parent model, SAfE, was shown to be stable and the EKE was within expected bounds. The model produces a reasonable approximation of the oceanic features in the region and the main features of the Agulhas Current were resolved in the parent model. The parent model was too coarse to resolve the features on the Agulhas Bank but may be considered adequate to force the higher resolution child model of the Agulhas Bank.

In the Reference Experiment (Chapter 4), the position and strength of the Agulhas Current in the child model showed seasonal fluctuations, not only in temperature but in its position and strength as it passes the Agulhas Bank. The Agulhas Current is faster in spring

and summer whilst in winter, the Agulhas Current is slower and its core is located further away from the slope.

The Agulhas Bank displayed marked seasonal changes. The Agulhas Current is the main contributor to the structure and circulation on the Outer-Agulhas Bank. Seasonal changes in the position and strength by the Agulhas Current are manifested in the temperature, salinity and current structure of the Outer-Agulhas Bank. Changes in the seasonal wind field and solar insolation are reflected in the structure and currents of the Inner-Agulhas Bank and the transitional Mid-Agulhas Bank.

The Reference Experiment was able to simulate the cool ridge on the East Agulhas Bank. The Agulhas Current was determined to be the primary driver of the model cool ridge via Ekman veering along the East Agulhas Bank. Sources of cool water onto the Agulhas Bank bottom were from three main regions: the East Agulhas Bank slope (which contributes to the cool ridge signature); the Agulhas Bight and the West Agulhas Bank.

In the No Agulhas Experiment (Chapter 5), the currents on the Agulhas Bank were comparatively slow without the Agulhas Current. Wind-driven currents associated with upwelling, such as the Good Hope Jet and West Agulhas Bank coastal jet, were still present. These appeared to generate a jet on the East Agulhas Bank at similar depths.

The Good Hope Jet receives little influence from the Agulhas Current. Northwestward flow on the outer West Agulhas Bank provides only a small contribution to the Good Hope Jet.

Without the Agulhas Current, the cool ridge was not apparent. Thus, the No Agulhas Experiment addresses a central question of this thesis on what drives the cool ridge. This reinforces the Agulhas Current-driven nature of the feature as discussed in detail in Chapter 4. Without, the Agulhas Current, Ekman veering and the movement of cold waters across the shelf is limited. The uplift of isotherms required to create the doming of the thermocline is restricted without the Agulhas Current present. This suggests, that in addition to the speed of the Agulhas Current, the structure of the Agulhas Current on the East Agulhas Bank shelf edge also plays a role. The uplifted isotherms on the shelf edge possibly aids in enhancing or preconditioning the shelf for upwelling over the shelf edge.

Differences in the temperature of up to 7° for the oceanic region adjacent to the Agulhas Bank demonstrate the contribution of heat by the Agulhas Current.

The Agulhas Current indirectly cools the Agulhas Bank. Temperature differences in Chapter 6 showed that, although the Outer-Agulhas Bank is directly forced by the Agulhas Current as discussed in Chapter 4, the Mid-Agulhas Bank and Inner-Agulhas Bank are indirectly forced by the Agulhas Current. Cooling to shallow depths on the East Agulhas Bank, combined with the westward advection of waters, results in cooling over most of the Agulhas Bank, particularly in the mid to upper water column.

The Agulhas Current, thus, moderates the thermocline depth and contributes to the two-layer structure by warming the surface (particularly in winter) while feeding the cool ridge and cool bottom waters across the Agulhas Bank.

The contribution of advection to heating and cooling the East Agulhas Bank, with implications for the cool ridge, was discussed in Chapter 6. Vertical cooling by Ekman veering, is a process driven by the mean Agulhas Current and accounts for the role of the Agulhas Current in forming the cool ridge. The contribution by horizontal advection associated with transient features, such as eddies and the offshore movement of the Agulhas Current, also cooled the East Agulhas Bank but by the lateral movement of waters.

7.2 Discussion of key questions

The following addresses the questions posed in Section 1.7:

What is the effect of the Agulhas Current on the Agulhas Bank?

The Agulhas Current and an Agulhas Current filament warms the oceanic region off the Agulhas Bank and the Outer-Agulhas Bank at the surface. Warming by the Agulhas Current on the East Agulhas Bank occurs by the horizontal advection of waters in the mean.

Below the thermocline, Ekman veering occurs from the interaction of the Agulhas Current and the East Agulhas Bank shelf edge up to and including the Agulhas Bight. This vertical motion is found in the mean due to the mean position of the Agulhas Current. This forces colder water from the slope, up across the 100m isobath, vertically reaching shallower depths. The cold bottom waters caused the vertical ridging of the thermocline responsible for the

observed cold tongue, the cool ridge. Due to this, upper layers of the East Agulhas Bank are cooler. Due to seasonal changes in the position of the Agulhas Current in the model, the vertical and horizontal extent of these cold waters and the depth these waters originate varies seasonally. The vertical isopycnal structure of the Agulhas Current off the East Agulhas Bank may assist in priming the shelf edge for the upwelling of cold waters.

Additional cooling to the East Agulhas Bank, may occur by transient features, such as eddies or the lateral movement of the Agulhas Current. However, this is due to horizontal advection: possibly, the lateral movement of cold waters within the eddy or cold shelf waters and not by upwelling associated with these transient features.

Current shear with the slower adjacent Agulhas Bank flow enhances the current speed and influences the current direction on the Outer-Agulhas Bank. The prevailing currents over the East Agulhas Bank, which are predominantly southwest to westward moves the cold upwelled bottom waters across the Agulhas Bank. These currents transport cold sub-thermocline waters from the East Agulhas Bank across the Agulhas Bank which in turn affects the Inner-Agulhas Bank and Mid-Agulhas Bank.

On the West Agulhas Bank, the presence of the Agulhas Current filament alters the vertical structure, resulting in an uplift of isotherms in the upper water column thus enhancing upwelling on the inner West Agulhas Bank. In addition, westward flow on the outer West Agulhas Bank feeds into and enhances the Good Hope Jet.

What is the nature of the seasonality of the shelf ocean on the Agulhas Bank?

A full description of the seasonal conditions on the Agulhas Bank was provided in Chapter 4. As discussed in the previous question, the Agulhas Current plays a large role in the seasonal structure and circulation of the Agulhas Bank.

The water column is indeed a two-layer system as described in the literature (Eagle and Orren, 1985) and is dominated by the influence of the Agulhas Current. Warming at the surface is by seasonal insolation and the Agulhas Current. Cooling at the bottom is due to the vertical advection of cold waters onto the East Agulhas Bank under the Agulhas Current, followed by the lateral movement of these waters across the Agulhas Bank.

In winter, when the thermocline destabilises due to decreased solar insolation and enhanced local wind-mixing, the Agulhas Current moderates the thermocline by warming surface waters and the advection of cold bottom waters (although much weaker than summer).

Without the Agulhas Current, vertical mixing in winter would continue to greater depths, particularly on the East Agulhas Bank.

What processes affect the formation of the cool ridge?

Ekman veering by the Agulhas Current on the East Agulhas Bank shelf edge appears to be the primary mechanism that forms the cool ridge. Ekman veering is enhanced when the Agulhas Current is faster, as seen in summer. It is also enhanced by the vertical uplift of isotherms due to the position of the Agulhas Current on the shelf edge. Thus, both speed and the proximity of the Agulhas Current affect the cool ridge.

The upwelling of cold water along the bottom pushes up the thermocline from the bottom. Thus, the doming of the thermocline and isotherms are observed where Ekman veering occurs.

Without the Agulhas Current steadily forcing cold water onto the shelf, cold waters are still found on the bottom of the Agulhas Bank, particularly on the East Agulhas Bank. Limited uplift of isotherms may occur due to the East Agulhas Bank jet. However, these waters are separated from shallower depths by a relatively thick, warm, surface layer. Without the Agulhas Current the necessary doming to bring cold water to shallow depths does not occur. In Chapter 1, the premise used to define the cool ridge was these waters need to be made available higher up the water column to increase productivity. Thus, without the Agulhas Current, this criteria is not met.

The primary mechanism in driving the cool ridge is the Agulhas Current. However, the expression of the cool ridge in the model is limited, as the model lacks high frequency variability such as by the rapidly varying winds on the Agulhas Bank. The effect of the wind would be to alter the expression of the cool ridge at or near the surface. Without the primary mechanism of placing the cold waters at shallow depths, the cool ridge cannot form.

What is the seasonal behaviour and fate of the cool ridge?

As discussed previously, the seasonal behaviour of the cool ridge depends on the position and speed of the Agulhas Current. In general, the main cool ridge structure is subsurface. The cool ridge has its largest horizontal dimension in summer, where it reaches far across the East Agulhas Bank and to depths as shallow as 10m. In winter, it is smaller (confined to the shelf edge) and deeper as the Agulhas Current is further off shelf and current speeds on the slope are slower.

The cool ridge provides cold water for the Agulhas Bank and ultimately affects the struc-

ture over the Agulhas Bank. The cold waters within the cool ridge are lifted to shallow depths. These waters move westwards with the prevailing currents and cool the rest of the Agulhas Bank, particularly in the mid to upper water column. This enhances the thermocline over a larger region of the Agulhas Bank then just the Outer-Agulhas Bank.

7.3 Outlook

The primary forcing mechanism of the cool ridge (which is the Agulhas Current) has been discussed above. The role that the surface conditions play in adjusting the expression of the cool ridge, was not directly addressed. The resolution of coastal features, particularly the upwelling in this model have been poor due to the climatological forcing used in this model. Coastal upwelling in the region is a short-lived event and interaction between coastal upwelling, winds and the cool ridge would have to be explored on an event-scale scale basis. High spatio-temporal resolution winds are needed to resolve the effects of a coastline which has many bays and headlands.

In this study, the importance of the bottom boundary layer to shelf-edge upwelling between the Agulhas Current and slope was shown. Further studies should investigate the sensitivity of the model results to different bottom boundary parameterizations. However, *in situ* bottom measurements are also needed to improve understanding of the bottom boundary layer (bbl) as well as improve the model configuration. For example, Trowbridge and Lentz (1998) studied the bbl of the northern Californian shelf using moorings. However, being an eastern boundary region with comparatively weaker currents than that of the Agulhas Current, sampling may have posed less of a challenge. Previous analysis of the bbl of the Agulhas Current include ship-board hydrosonde measurements as well as a single mooring off Natal for August 1975 (Schumann, 1986). Measurements were taken where the shelf is 10km wide and the water depth about 50m. The data suggested that the currents displayed Ekman veering and the thickness of the bbl was recorded as between 29 and 34m. However, this analysis was subject to errors such as sampling technique and the vertical resolution of the measurements. For example, on days of rough weather near-bottom measurements were not obtained. In such shallow water depths, the behaviour of the surface Ekman layers adds complications to determining the behaviour of the bbl.

In Roy et al. (2007), a shift in anchovy spawning was shown on the Agulhas Bank, from the West Agulhas Bank to the Central Agulhas Bank and East Agulhas Bank, which was ascribed

to environmental changes: cooler waters due to more wind-induced upwelling. Rouault et al. (2008) have shown that the Agulhas Current has warmed during the last 20 years. The results from this thesis have shown that the Agulhas Current plays a large role on the dynamics of the Agulhas Bank. Thus, large-scale changes in the Agulhas Current will affect the Agulhas Bank dynamics. It is possible that with an increase in flow of the Agulhas Current (Rouault et al., 2008), increased Ekman veering may occur. Thus, increased volumes of cool water would be made available to the Inner-Agulhas Bank, as well as the rest of the Agulhas Bank, to support fish spawning. An ocean model study for the Agulhas Bank using more realistic, higher temporal resolution forcing can assist in this investigation. Furthermore, such a model study could provide key locations for *in situ* monitoring. However, the model can only allude to the changes in the physical environment on the Agulhas Bank, but do not address the biological aspects of this problem.

Bibliography

Bang, N. D. (1970). Dynamic interpretations of a detailed surface temperature chart of the Agulhas Current retroflexion and fragmentation area. *South African Geographic Journal*, 52:67–76.

Bang, N. D. and Andrews, W. R. H. (1974). Direct current measurements of a shelf edge frontal jet in the southern Benguela system. *Journal of Marine Research*, 32(3):405–417.

Barnier, B., Marchesiello, P., Pimenta de Miranda, A., and Molines, J. M. (1998). A sigma-coordinate primitive equation model for studying the South Atlantic. Part I: model configuration with error estimates. *Deep-Sea Research*, 45:543–572.

Barnier, B., Siefridt, L., and Marchesiello, P. (1995). Thermal forcing for a global ocean circulation model using a three-year climatology of ECMWF analyses. *Journal of Marine Systems*, 6(4):363–380.

Beal, L. M. and Bryden, H. L. (1999). The velocity and vorticity structure of the Agulhas Current at 32^{o}S. *Journal of Geophysical Research*, 104:5151–5176.

Beckley, L. E. (1983). Sea-surface temperature variabilty around Cape Recife, South Africa. *South African Journal of Science*, 79:436–438.

Beckley, L. E. (1988). Spatial and temporal variability in sea temperature in Algoa Bay, South Africa. *South African Journal of Science*, 84(1):67–69.

Ben-Avraham, Z., Hartnady, C. J. H., and Kitchin, K. A. (1997). Structure and tectonics of the agulhas-falkland fracture zone. *Tectonophysics*, 282:83–96.

Berger, M. and Oliger, J. (1984). Adaptive mesh refinement for hyperbolic partial differential equations. *Journal of Computational Physics*, 53:484–512.

Biastoch, A. and Krauss, W. (1999). The role of mesoscale eddies in the source regions of the Agulhas Current. *Journal of Physical Oceanography*, 29:2303–2317.

Biastoch, A., Reason, C. J. C., Lutjeharms, J. R. E., and Boebel, O. (1999). The importance of flow in the Mozambique Channel to seasonality in the greater Agulhas system. *Geophysical Research Letters*, 26(21):33221–3324.

Blanke, B., Roy, C., Penven, P., Speich, S., McWilliams, J., and Nelson, G. (2002). Linking wind and interannual upwelling variability in a regional model of the southern Benguela. *Geophysical Research Letters*, 29(24).

Blanke, B., Speich, S., Bentamy, A., Roy, C., and Sow, B. (2005). Modeling the structure and variability of the southern Bengeula upwelling using QuikSCAT wind forcing. *Journal of Geophysical Research*, 110(C07018):10.1029/2004JC002529.

Blanton, J. O., Atkinson, L. P., Pietrafesa, L. J., and Lee, T. N. (1981). The intrusion of Gulf Stream water across the continental shef due to topographically-induced upwelling. *Deep-Sea Research*, 28:393–405.

Blayo, E. and Debreu, L. (1999). Adaptive mesh refinement for finite–difference ocean models: first experiments. *Journal of Physical Oceanography*, 29:1239–1250.

Boyd, A. J. and Nelson, G. (1998). Variability of the Benguela Current off the Cape Peninsula, South Africa. *South African Journal of Marine Science*, 19:15–39.

Boyd, A. J. and Oberholster, G. P. J. (1994). Currents off the West and South coasts of South Africa. *SA Shipping News and Fishing Industry Review*, Sept/Oct:26–28.

Boyd, A. J. and Shillington, F. A. (1994). Physical forcing and circulation patterns on the Agulhas Bank. *South African Journal of Science*, 90(3):114–122.

Boyd, A. J., Taunton-Clark, J., and Oberholster, G. P. J. (1992). Spatial features of the near-surface and mid-water circulation patterns off western and southern South Africa and their role in the life histories of various commercially fished species. *South African Journal of Marine Science*, 12:189–206.

Boyd, A. J., Tromp, B. B. S., and Horstman, D. A. (1985). The hydrology off the South African south-western coast between Cape Point and Danger Point in 1975. *South African Journal of Marine Science*, 3:145–168.

Brink, K. H. and Shearman, R. K. (2006). Bottom boundary layer flow and salt injection from the continental shelf to slope. *Geophysical Research Letters*, 33(L13608).

Bryden, H. L. and Beal, L. M. (2001). Role of the Agulhas Current in Indian Ocean circulation and associated heat and freshwater fluxes. *Deep-Sea Research I*, 48:1821–1845.

Bryden, H. L., Beal, L. M., and Duncan, L. M. (2005). Structure and transport of the Agulhas Current and its temporal variability. *Journal of Oceanography*, 61:479–492.

Chapman, P. and Largier, J. L. (1989). On the origin of Agulhas Bank bottom water. *South African Journal of Science*, 85(8):515–519.

Conkright, M. E., Locarnini, R. A., Garcia, H. E., O'Brien, Boyer, T. P., Stephens, C., and Antonov, J. I. (2002). World Ocean Atlas 2001: Objective analyses, data statistics, and figures, CD-ROM documentation. Technical Report 17, National Oceanographic Data Center, Silver Spring, Md.

Cushman-Roisin, B. and Malai, V. (1997). Bottom ekman pumping with Stress-Dependent eddy viscosity. *Journal of Physical Oceanography*, 27(9):1967–1975.

Da Silva, A. M., Young, C. C., and Levitus, S. (1994). Atlas of surface marine data 1994, vol. 1, Algorithms and Procedures. Technical report, NOAA, Silver Spring, Md.

de Ruijter, W. P. M., Biastoch, A., Drijfhout, S. S., Lutjeharms, J. R. E., Matano, R. P., Pichevin, T., van Leeuwen, P. J., and Weijer, W. (1999). Indian-Atlantic interocean exchange: Dynamics, estimation and impact. *Journal of Geophysical Research*, 104(C9):20,885–20,910.

Demarcq, H., Barlow, R., and Hutchings, L. (2007). Application of a cholorphyll index derived from satellite data to investigate the variability of phytoplankton in the Benguela ecosystem. *African Journal of Marine Science*, 29(2):271–282.

Demarcq, H., Barlow, R. G., and Shillington, F. A. (2003). Climatology and variability of sea surface temperature and surface chlorophyll in the Benguela and Agulhas ecosystems as observed by satellite imagery. *African Journal of Marine Science*, 25:363–372.

Dingle, R. V. and Scrutton, R. A. (1974). Continental break-up and the development of post-Palaeozoic sedimentary basins around Southern Africa. *Geological Society Amer. Bull*, 85:1467–1474.

Ducet, N., Le Traon, P. Y., and Reverdin, G. (2000). Global high-resolution mapping of ocean circulation from topex/poseidon and ers-1 and -2. *Journal of Geophysical Research*, 105:19477–19498.

Durski, S. M., Glenn, S. M., and Haidvogel, D. B. (2004). Vertical mixing schemes in the coastal ocean: Comparison of the level 2.5 Mellor-Yamada scheme with an enhanced version of the K profile parameterization. *Journal of Geophysical Research*, 109(C01015):10.1029/2002JC001702.

Eagle, G. A. and Orren, M. J. (1985). A seasonal investigation of the nutrients and dissolved oxygen in the water column along two lines of stations south and west of South Africa. Technical report, Council for Scientific and Industrial Research.

Flather, R. A. (1976). A tidal model of the northwest European continental shelf. *Memoires de la Societe Royale des Science de Liége*, 10:141–164.

Garzoli, S. L. and Gordon, A. L. (1996). Origins and variability of the Benguela Current. *Journal of Geophysical Research*, 101:897–906.

Gill, A. E. and Schumann, E. H. (1979). Topographically induced changes in the structure of an inertial coastal jet: application to the Agulhas Current. *Journal of Physical Oceanography*, 9:975–991.

Goschen, W. S. and Schumann, E. H. (1988). Ocean current and temperature structures in Algoa Bay and beyond in November 1986. *South African Journal of Marine Science*, 7:101–116.

Goschen, W. S. and Schumann, E. H. (1995). Upwelling and the occurrence of cold water around Cape Recife, Algoa Bay, South Africa. *South African Journal of Marine Science*, 16:57–67.

Grundlingh, M. L. (1980). On the volume transport of the Agulhas Current. *Deep-Sea Research*, 27:557–563.

Grundlingh, M. L. (1983). On the course of the Agulhas Current. *South African Geographical Journal*, 65:49–57.

Haidvogel, D., Arango, H., Budgell, W., Cornuelle, B., Curchitser, E., Lorenzo, E. D., Fennel, K., Geyer, W., Hermann, A., Lanerolle, L., Levin, J., McWilliams, J., Miller, A., Moore, A., Powell, T., Shchepetkin, A., Sherwood, C., Signell, R., Warner, J., and Wilkin, J. (2008). Ocean forecasting in terrain-following coordinates: Formulation and skill assessment of the regional ocean modeling system. *Journal of Computational Physics*, 227(7):3595–3624.

Haidvogel, D. B. and Beckmann, A. (1999). *Numerical Ocean Circulation Modeling*. Imperial College press, London.

Hardman-Mountford, N. J., Richardson, A. J., Agenbas, J. J., Hagen, E., Nykjaer, L., Shillington, F. A., and Villicastin, C. (2003). Ocean climate of the South East Atlantic observed from satellite data and wind models. *Progress in Oceanography*, 59:181–221.

Hill, A. E., Hickey, B. M., Shillington, F. A., Strub, P. T., Brink, K. H., Barton, E. D., and C., T. A. (1998). Eastern Ocean boundaries coastal segment (E). In Robinson, A. R. and Brink, K. H., editors, *The Sea, Volume 11*, pages 29–67. John Wiley & Sons, Inc., New York.

Hunter, I. T. (1987). The weather of the Agulhas Bank and the Cape South Coast. Technical Report 634, CSIR, National Research Institute for Oceanology, Stellenbosch. 184pp.

Hutchings, L. (1994). The Agulhas Bank: A synthesis of available information and a brief comparison with other east-coast shelf regions. *South African Journal of Science*, 90(3):179–185.

Hutchings, L., Beckley, L. E., Griffiths, M. H., Roberts, M. J., Sundby, S., and van der Lingen, C. (2002). Spawning on the edge: spawning grounds and nursery areas around the southern African coastline. *Marine and Freshwater Research*, 53:307–318.

Jury, M. R. (1994). A review of the meteorolgy of the eastern Agulhas Bank. *South African Journal of Science*, 90(3):109–113.

Large, W. G., McWilliams, J. C., and Doney, S. C. (1994). Oceanic vertical mixing: a review and a model with a nonlocal boundary layer parameterization. *Reviews in Geophysics*, 32:363–403.

Largier, J. L., Chapman, P., Peterson, W. T., and Swart, V. P. (1992). The western Agulhas Bank: Circulation, stratification and ecology. *South African Journal of Marine Science*, 12:319–339.

Largier, J. L. and Swart, V. P. (1987). East-west variation in thermocline breakdown on the Agulhas Bank. *South African Journal of Marine Science*, 5:263–272.

Lutjeharms, J. R. E. (1981). Spatial scales and intensities of circulation in the ocean areas adjacent to South Africa. *Deep-Sea Research*, 28A(11):1289–1302.

Lutjeharms, J. R. E. (1996). *The South Atlantic: present and past circulation*, chapter The exchange of water between the South Indian and South Atlantic Oceans, pages 125–162. Springer-Verlag, Berlin.

Lutjeharms, J. R. E. (2006). *The Agulhas Current*. Springer.

Lutjeharms, J. R. E., Catzel, R., and Valentine, H. R. (1989). Eddies and other boundary phenomena of the Agulhas Current. *Continental Shelf Research*, 9(7):597–616.

Lutjeharms, J. R. E. and Cooper, J. (1996). Interbasin leakage through Agulhas Current filaments. *Deep-Sea Research I*, 43(2):213–238.

Lutjeharms, J. R. E., Cooper, J., and Roberts, M. (2000). Upwelling at the inshore edge of the Agulhas Current. *Continental Shelf Research*, 20(7):737–761.

Lutjeharms, J. R. E., Durgadoo, J. V., and Ansorge, I. J. (2007). Surface drift at the western edge of the Agulhas Bank. *South African Journal of Science*, 103:63–67.

Lutjeharms, J. R. E. and Meeuwis, J. M. (1987). The extent and variability of South-east Atlantic upwelling. *South African Journal of Marine Science*, 5:51–62.

Lutjeharms, J. R. E. and Meyer, A. A. (2008). On the origin and circulation of bottom waters on the Agulhas Bank, South Africa. *Continental Shelf Research*. Submitted.

Lutjeharms, J. R. E., Penven, P., and Roy, C. (2003). Modelling the shear edge eddies of the southern Agulhas Current. *Continental Shelf Research*, 23(11–13):1099–1115.

Lutjeharms, J. R. E. and Stockton, P. L. (1991). Aspects of the upwelling regime between Cape Point and Cape Agulhas, South Africa. *South African Journal of Marine Science*, 10:91–102.

Lutjeharms, J. R. E. and Webb, D. (1995). Modelling the Agulhas Current System with FRAM (Fine Resolution Antarctic Model). *Deep Sea Research I*, 42(4):523–551.

Marchesiello, P., McWilliams, J. C., and Shchepetkin, A. (2003). Equilibrium structure and dynamics of the California Current System. *Journal of Physical Oceanography*, 33:753–783.

Matano, R. P. and Beier, E. J. (2003). A kinematic analysis of the Indian/Atlantic interocean exchange. *Deep Sea Research II*, 50(1):229–249.

Matano, R. P., Beier, E. J., Strub, P. T., and Tokmakian, R. (2002). Large-scale forcing of the Agulhas Variability: The seasonal cycle. *Journal of Physical Oceanography*, 32:1228–1241.

Matano, R. P., Simionato, C. G., de Ruijter, W. P., van Leeuwen, P. J., Strub, P. T., Chelton, D. B., and Schlax, M. G. (1998). Seasonal variability in the Agulhas Retroflection region. *Geophysical Research Letters*, 25(23):4361–4364.

Nelson, G. (1985). *South African Ocean Colour and Upwelling Experiment*, chapter Notes on the physical oceanography of the Cape Peninsula upwelling system, pages 63–95. Sea Fisheries Research Institute, Cape Town.

Nelson, G., Boyd, A. J., Agenbag, J. J., and Duncombe Rae, C. M. (1998). An upwelling filament north-west of Cape Town, South Africa. *South African Journal of Marine Science*, 19:75–88.

Oke, P. R. and Middleton, J. H. (2001). Nutrient enrichment off port stephens: the role of the east Australian Current. *Continental Shelf Research*, 21:587 – 606.

Pearce, A. F. and Grundlingh, M. L. (1982). Is there seasonal variation in the Agulhas Current? *Journal of Marine Research*, 40:177–184.

Penven, P. (2000). *A numerical study of the Southern Benguela circulation with an application to fish recruitment*. PhD thesis, L'Universite de Bretagne Occidentale.

Penven, P., Chang, N., and Shillington, F. (2006a). Modelling the Agulhas Current using SAfE (Southern Africa experiment). *Geophysical Research Abstracts*, page Abstract 04225.

Penven, P., Debreu, L., Marchesiello, P., and McWilliams, J. C. (2006b). Evaluation and application of the ROMS 1-way embedding procedure to the central California upwelling system. *Ocean Modelling*, 12:157–187.

Penven, P., Echevin, V., Pasapera, J., and Tam, J. (2005). Average circulation, seasonal cycle and mesoscale dynamics of the Peru Current system: a modeling approach. *Journal of Geophysical Research*, 110(C10021):10.1029/2005JC002945.

Penven, P., Lutjeharms, J. R. E., and Florenchie, P. (2006c). Madagascar: A pacemaker for the Agulhas Current System. *Geophysical Research Letters*, 33.

Penven, P., Lutjeharms, J. R. E., Marchesiello, P., Roy, C., and Weeks, S. J. (2001a). Generation of cyclonic eddies by the Agulhas Current in the lee of the Agulhas Bank. *Geophysical Research Letters*, 28(6):1055–1058.

Penven, P., Marchesiello, P., Debreu, L., and Lefèvre, J. (2008). Software tools for pre- and post-processing of oceanic regional simulations. *Environmental Modelling & Software*, 23(5):660–662.

Penven, P., Roy, C., Brundrit, G. B., Colin de Verdiere, A., Freon, P., Johnson, A. S., Lutjeharms, J. R. E., and Shillington, F. A. (2001b). A regional hydrodynamic model of upwelling in the Southern Benguela. *South African Journal of Science*, 97:472–475.

Penven, P. and Tan, T. (2007). Romstools user's guide http://www.brest.ird.fr/roms_tools. Technical report, Institut de Recherche pour le Developpement, 213 rue Lafayette, Paris, France.

Perlin, A., Moum, J. N., Klymak, J. M., Levine, M. D., Boyd, T., and Kosro, P. M. (2007). Organization of stratification, turbulence, and veering in bottom ekman layers. *Journal of Geophysical Research*, 112(CO5S90):10.1029/2004JC002641.

Probyn, T. A., Mitchell-Innes, B. A., Brown, P. C., Hutchings, L., and Carter, R. A. (1994). A review of primary production and related processes on the Agulhas Bank. *South African Journal of Science*, 90:166–173.

Richardson, P. L. (2007). Agulhas leakage into the atlantic estimated with subsurface floats and surface drifters. *Deep-Sea Research I*, 54:1361–1389.

Risien, C. M., Reason, C. J. C., and Shillington, F. A. (2004). Variability in satellite winds over the Benguela upwelling system during 1999–2000. *Journal of Geophysical Research*, 109(CO3010).

Roberts, M. (2005). Chokka squid (Loligo vulgaris reynaudii) abundance linked to changes in South Africa's Agulhas Bank ecosystem during spawning and the early life cycle. *ICES Journal of Marine Science*, 62(1):33–55.

Rouault, M. and Lutjeharms, J. R. E. (2003). Estimation of sea-surface temperature around southern Africa from satellite-derived microwave observations. *South African Journal of Science*, 99:489–494.

Rouault, M., Penven, P., and Pohl, B. (2008). Warming in the Agulhas Current system since the 80's. *Nature Geoscience*.

Roughan, M. and Middleton, J. H. (2003). On the East Australian Current: Variability, encroachment and upwelling. *Journal of Geophysical Research*.

Roy, C., van der Lingen, C. D., Coetzee, J. C., and Lutjeharms, J. R. E. (2007). Abrupt environmental shift associated with changes in the distribution of Cape anchovy Engraulis encrasicolus spawners in the southern Benguela. *South African Journal of Marine Science*, 29(3):309–319.

Schumann, E. H. (1986). The bottom boundary layer inshore of the Agulhas Current off Natal in August, 1975. *South African Journal of Science*, 4:93–102.

Schumann, E. H. (1987). The coastal ocean off the east coast of South Africa. *Transactions of the Royal Society of South Africa*, 46:215–229.

Schumann, E. H. (1989). The propagation of air pressure and wind systems along the South African coast. *South African Journal of Science*, 85:382–385.

Schumann, E. H. (1992). Interannual wind variability on the South and East Coasts of South Africa. *Journal of Geophysical Research*, 97(D18):20,397 – 30, 403.

Schumann, E. H. (1999). Wind-driven mixed layer and coastal upwelling processes off the south coast of South Africa. *Journal of Marine Research*, 57:671–691.

Schumann, E. H. and Beekman, L. J. (1984). Ocean temperature structures on the Agulhas Bank. *Transactions of the Royal Society of South Africa*, 45(2):191–203.

Schumann, E. H. and Brink, K. H. (1990). Coastal trapped waves off the coast of South Africa: Generation, propagation and current structures. *Journal of Physical Oceanography*, 20:1206–1218.

Schumann, E. H., Cohen, A. L., and Jury, M. R. (1995). Coastal sea surface temperature variability along the south coast of South Africa and the relationship to regional and global climate. *Journal of Marine Research*, 53(2):231–248.

Schumann, E. H. and Martin, J. A. (1991). Climatological aspects of the coastal wind field at Cape Town, Port Elizabeth and Durban. *South African Geographical Journal*, 73:48–51.

Schumann, E. H., Perrins, L. A., and Hunter, I. T. (1982). Upwelling along the South Coast of the Cape Province, South Africa. *South African Journal of Science*, 78:238–242.

Schumann, E. H., Ross, G. J. B., and Goschen, W. S. (1988). Cold water events in Algoa Bay and along the Cape south coast, South Africa, in March/April 1987. *South African Journal of Science*, 84:579–584.

Schumann, E. H. and van Heerden, I. L. (1988). Observations of Agulhas Current frontal features south of Africa, October 1983. *Deep-Sea Research*, 35(8):1355–1362.

Shannon, L. V. (1966). Hydrology of the south and west coasts of South Africa. Technical Report 58, Investigational Report, Division Sea Fisheries, South Africa. 22 pp. + 30 pp. of figures.

Shannon, L. V. (1985). The Benguela Ecosystem. 1. Evolution of the Benguela, physical features and processes. *Oceanography and Marine Biology Annual Review*, 23:105–182.

Shannon, L. V. and Nelson, G. (1996). *The South Atlantic: Present & Past Circulation*, chapter The Benguela: Large Scale Features & Processes & System Variability, pages 163–210. Springer-Verlag, Berlin Heidelberg.

Shchepetkin, A. F. and McWilliams, J. C. (2003). A method for computing horizontal pressure-gradient force in an oceanic model with a non–aligned vertical coordinate. *Journal of Geophysical Research*, 108(C3):3090.

Shchepetkin, A. F. and McWilliams, J. C. (2005). The regional oceanic modeling system (ROMS): a split–explicit, free-surface, topography–following–coordinate oceanic model. *Ocean Modelling*, 9:347–404.

Shillington, F. A. (1998). *The Sea, Volume 11*, chapter The Benguela Upwelling System off Southwestern Africa, pages 583–604. John Wiley and Sons, Inc.

Shillington, F. A., Reason, C. J. C., Duncombe Rae, C. M., Florenchie, P., and Penven, P. (2006). *Benguela: Predicting a Large Marine Ecosystem*, chapter Large scale physical variability of the Benguela Current LME, pages 47–68. Elsevier, Amsterdam, The Netherlands.

Skogen, M. D. (1999). A biophysical model applied to the Benguela upwelling system. *South African Journal of Marine Science*, 21:235–249.

Smagorinsky, J. (1963). General circulation experiments with primitive equations. *Monthly Weather Review*, 91:99–164.

Smith, W. H. F. and Sandwell, D. T. (1997). Global seafloor topography from satellite altimetry and ship depth soundings. *Science*, 277:1957–1962.

Speich, S., Lutjeharms, J. R. E., Penven, P., and Blanke, B. (2006). Role of bathymetry in Agulhas Current configuration and behaviour. *Geophysical Research Letters*, 33(L23611).

Stramma, L. and Lutjeharms, J. R. E. (1997). The flow field of the subtropical gyre of the South Indian Ocean. *Journal of Geophysical Research*, 102(C3):5513–5530.

Swart, V. and Largier, J. L. (1987). Thermal structure of Agulhas Bank water. *South African Journal of Marine Science*, 5:243–254.

Trowbridge, J. H. and Lentz, S. J. (1998). Dynamics of the bottom boundary layer on the northern california shelf*. *Journal of Physical Oceanography*, 28(10):2075–2093.

Tyson, P. D. and Preston-Whyte, R. A. (2000). *The weather and climate of Southern Africa*. Oxford University Press.

Valentine, H. R., Lutjeharms, J. R. E., and Brundrit, G. B. (1993). The water mases and volumetry of the southern Agulhas Current region. *Deep Sea Research Part I*, 40(6):1285–1305.

Van Ballegooyen, R. C., Valentine, H. R., and Lutjeharms, J. R. E. (1991). Modelling of the Agulhas Current system. *South African Journal of Science*, 87(11/12):569–571.

van Foreest, D. and Brundrit, G. B. (1982). A two-mode numerical model with application to coastal upwelling. *Progress in Oceanography*, 11:329–392.

Verheye, H. M., Hutchings, L., Huggett, J. A., Carter, R. A., Peterson, W. T., and Painting, S. J. (1994). Community structure, distribution and trophic ecology of zooplankton on the Agulhas Bank with special reference to copepods. *South African Journal of Science*, 90:154–162.

Walker, N. D. (1986). Satellite observations of the Agulhas Current and episodic upwelling south of Africa. *Deep-Sea Research I*, 33(8A):1083–1106.

Appendix A: Extra Figures for Chapter 4

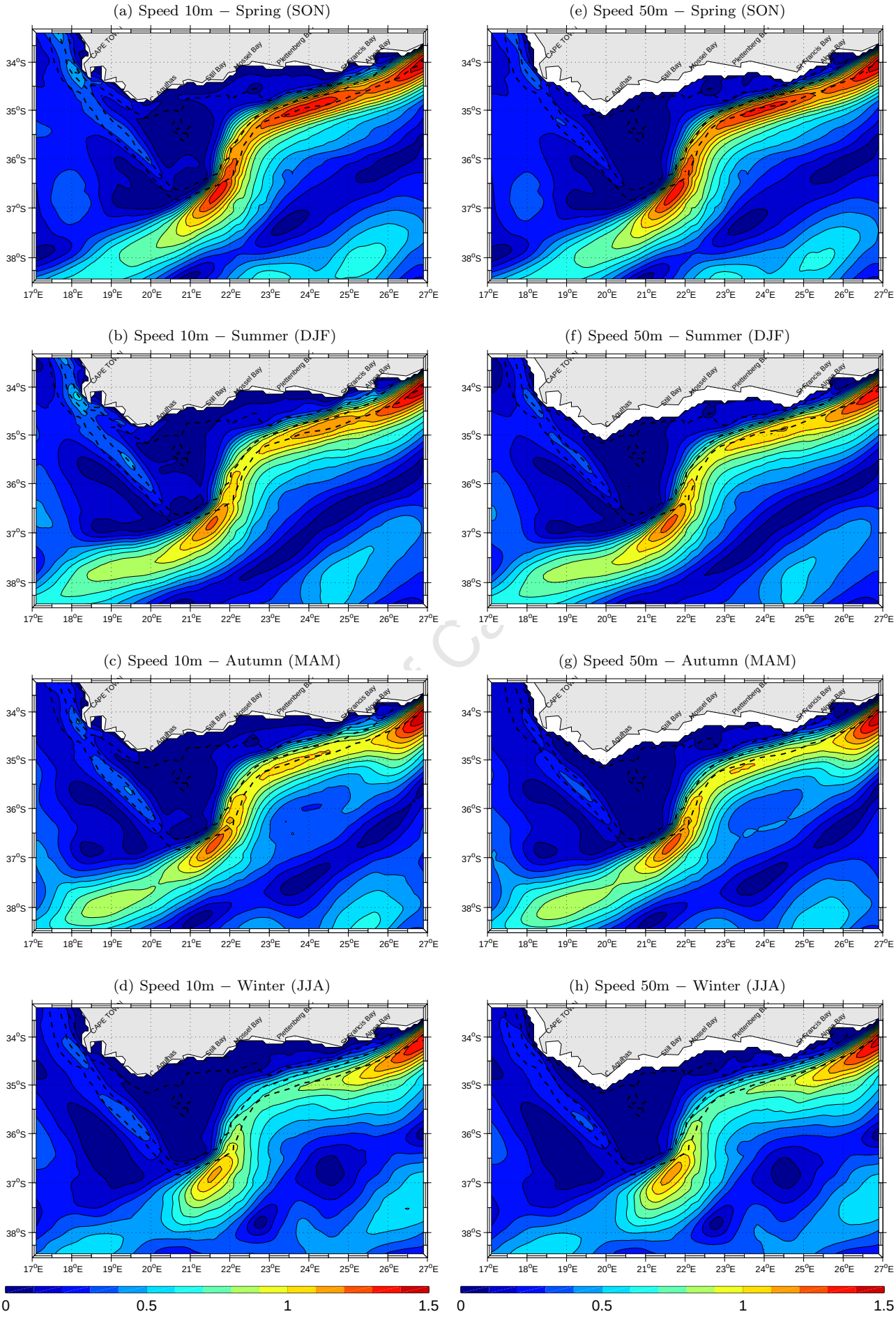

Figure A.1: Seasonally-averaged speed (m.s^{-1}) for the larger AB region at (a–d) 10m and (e–h) 50m.

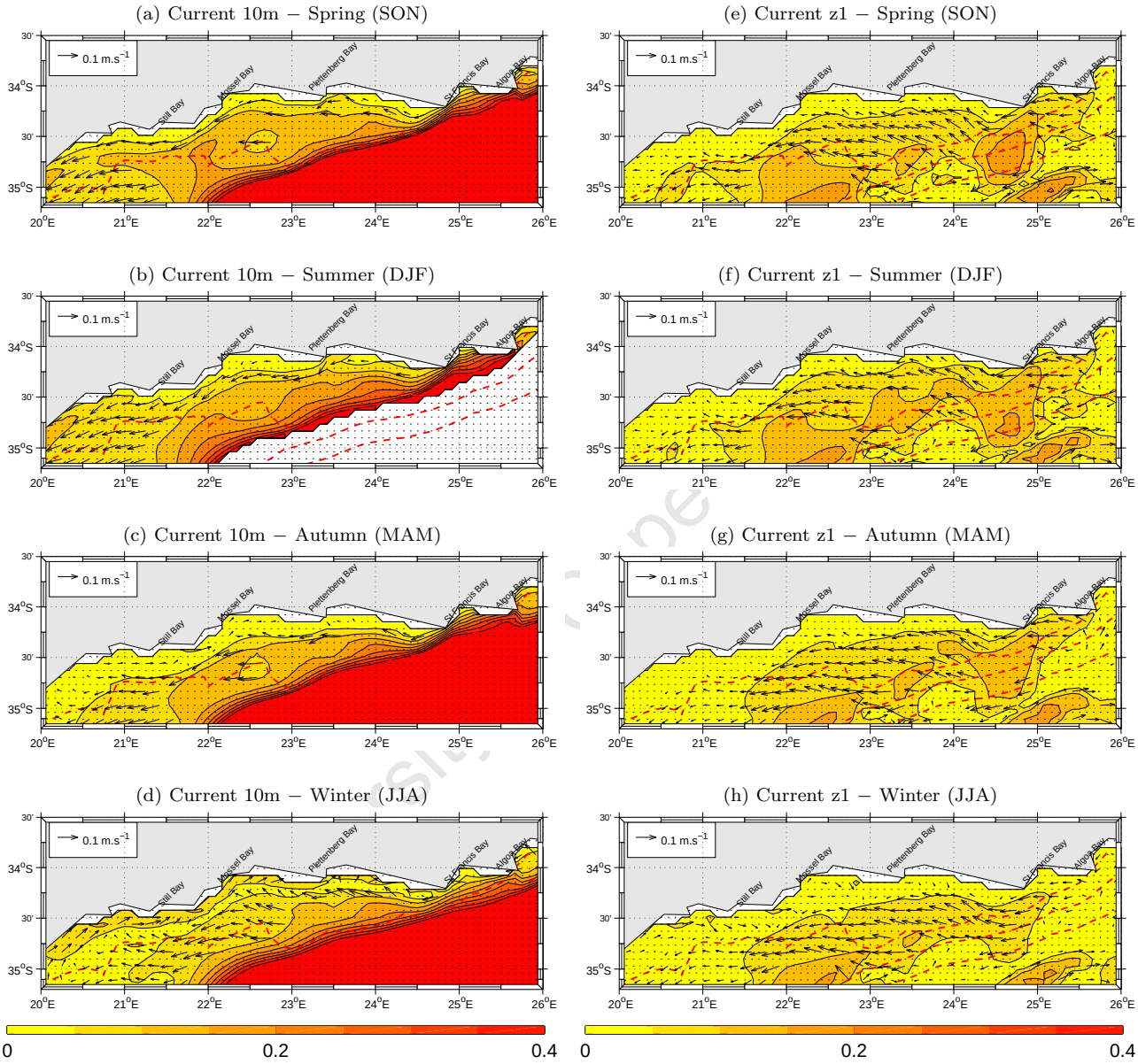

Figure A.2: Seasonally-averaged current vectors and speed (m.s^{-1}) for the model Inner-AB at (a–d) 10m and (e–h) z1, representing the bottom. Current vectors for speeds greater than 0.4m.s^{-1} have been removed for clarity.

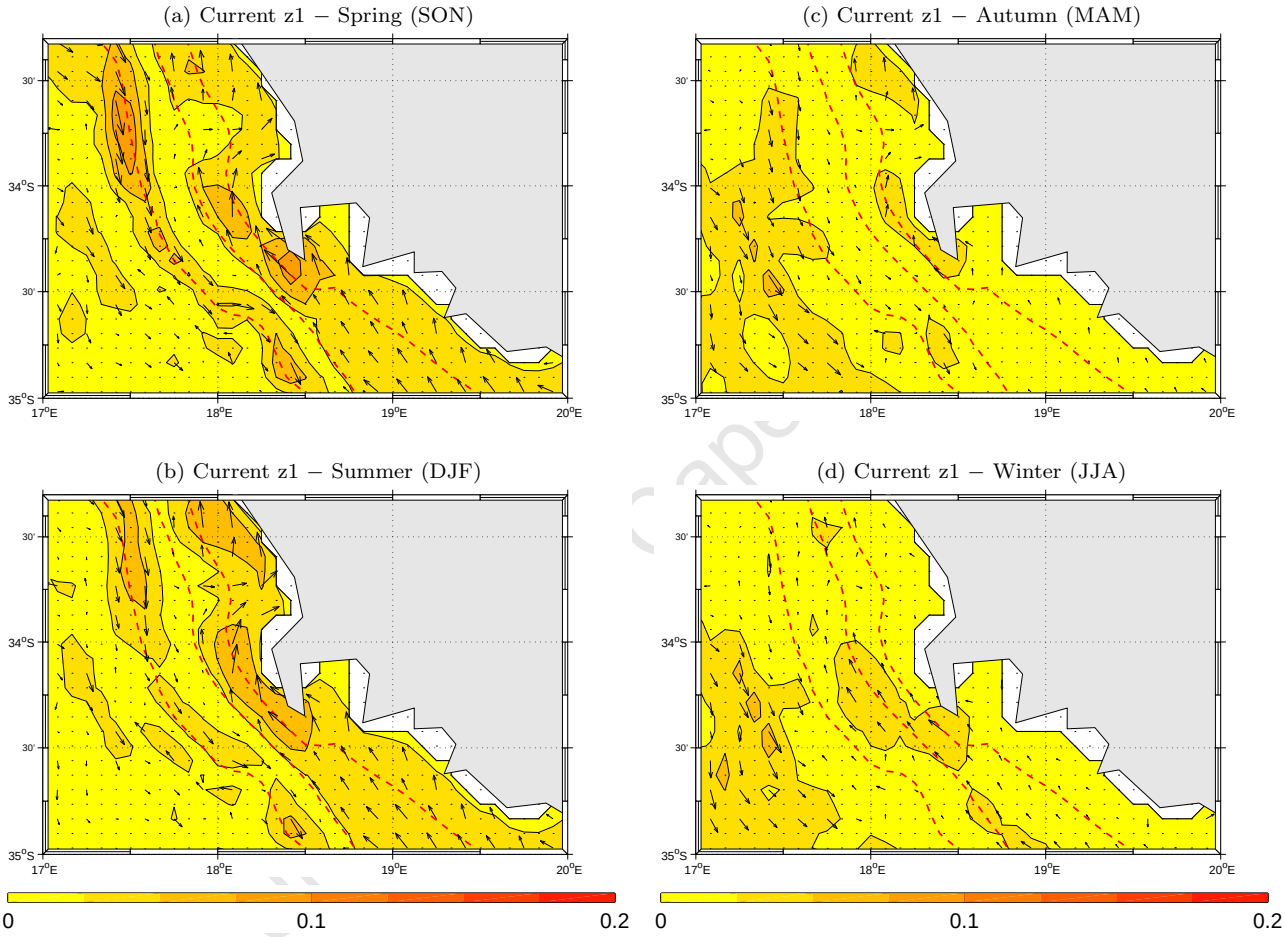

Figure A.3: Seasonally-averaged current vectors and speed (m.s^{-1}) at z1, representing the bottom of the Inner-AB for the Reference Experiment.

Appendix B: Extra Figures for Chapter 5

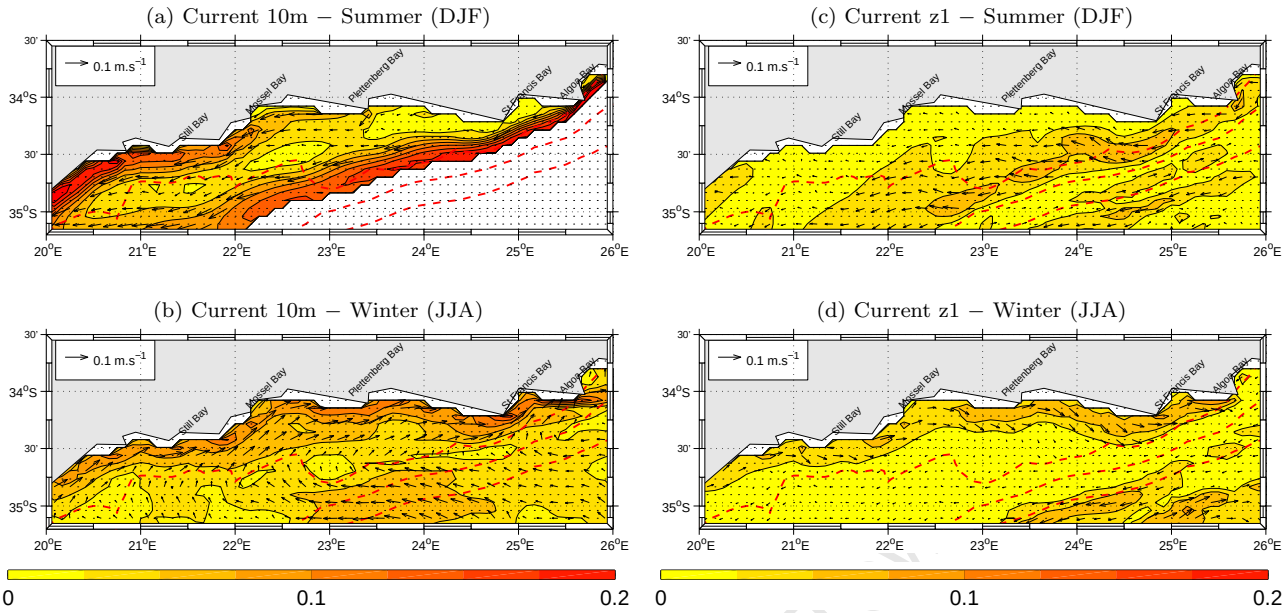

Figure B.1: Seasonally-averaged summer and winter current vectors and speed (m.s^{-1}) for the No Agulhas Experiment Inner-AB at (a–b) 10m and (c–d) z1, representing the bottom. Current vectors for speeds greater than 0.2m.s^{-1} have been removed for clarity.

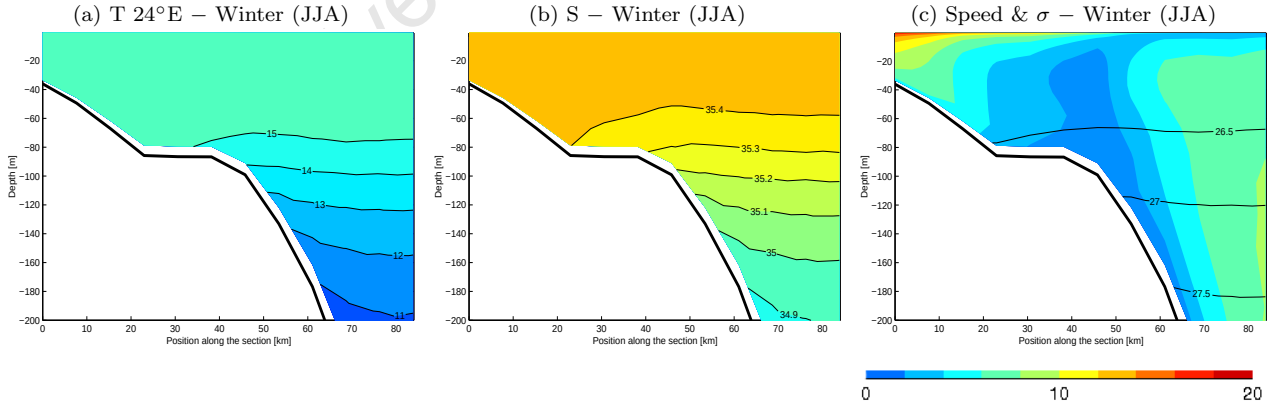

Figure B.2: Vertical sections at 24°E for the winter mean (a–d) temperature (°C), (e–h) salinity (psu) and (i–l) speed (cm.s^{-1}) with density (σ) contours (kg.m^{-3}) overlaid for the No Agulhas Experiment. Speed contour interval is 2cm.s^{-1}, density contours are 0.5kg.m^{-3}.